Harmonic Analysis and Effectiveness of Mitigation Techniques Applied to a Bipolar HVDC System

by

JIMMY MATABARO MUSHAGALA

Thesis submitted in fulfilment of the requirements for the degree

Master of Technology: Electrical Engineering, Power System

in the Faculty of Engineering

at the Cape Peninsula University of Technology

Supervisor: Prof. Gary Atkinson-Hope

Cape Town
09 March 2017

Declaration

I, Jimmy Matabaro Mushagala, declare that the contents of this thesis represent my own unaided work, and that the thesis has not previously been submitted for academic examination towards any qualification. Furthermore, it represents my own opinions and not necessarily those of the Cape Peninsula University of Technology.

Signed **Date**

For my Parents

I would like to thank you, you have always tried to understand my unusual choices, for your encouragement and because you have taught me to look beyond what I see. I am grateful for your contribution toward my education and for following from a distance the endeavours of my journey. To my sisters and brothers Bijoux, Deborah, Dina, Ada, Mervielle, Joe and Teddy, I am thankful for their support and patience they lent me in the past months and years and for making my life so much more worthwhile.

Preface

This thesis has taught me a great deal about HVDC power transmission and the available HVDC technologies found today. An HVDC bipolar transmission network was modelled and simulated. Results were recorded and an investigation on how harmonics generated by HVDC converters and transferred to the HVAC network could be effectively mitigated. I am left with a much better understanding on the simulation program DIgSILENT PowerFactory and how to approach the construction of an HVDC simulation model.

I have had a lot of help along the way in order for this thesis to be realized. I would like to thank my supervisor, Prof Gary Atkinson-hope, for helping me find an interesting topic that has increased my understanding on power systems and HVDC converter technology. His broad understanding on HVDC technology has introduced me to new and interesting perspectives.

Abstract

High Voltage Direct Current (HVDC) transmission is a safe and efficient technology designed to deliver large amounts of electrical power over long distances with minimal losses and at low costs. HVDC links require converters and filters at both terminal stations. The core component of the HVDC system is the power converter that connects the DC and AC systems together. The conversion from AC to DC, and vice versa, is achieved mainly through electronic switches called thyristors. The thyristor-based Line Commutated Converter (LCC) is a mature and trusted technology for HVDC transmission throughout the world.

HVDC converters are bidirectional and can function in either rectification (AC to DC) or inversion mode (DC to AC). This is achieved when the voltage polarity across the converter gets swapped by the controllers, because current cannot change its direction in thyristors.

In this thesis an analytical model of the HVDC converters is developed in the frequency domain by modelling it in DIgSILENT. The objective is to study the harmonics induced to the AC side from HVDC converters.

Therefore, it is important in the real world to understand the principles, what causes harmonics to be generated in HVDC and transferred to the HVAC system.

The objective of this thesis is to investigate the effectiveness of mitigation techniques used, on how they reduce harmonics by keeping these harmonic levels within specified values admissible by international standards (e.g. IEEE, etc).

The use of filters is one of the mitigation techniques used, and its purpose is to absorb harmonic currents on the HVAC side. Hence, they decrease the impact of the harmonics on the connected HVAC system, such as AC voltage distortion interference.

Moreover, other mitigation techniques are investigated, such as the role played by the converter transformers and the switching angle of converters on mitigating harmonics on the HVAC side.

An introductory overview of LCC HVDC is presented, covering usage, configurations and basic operating principles. A more detailed examination on the mitigation of harmonics generated by HVDC converters is covered. How to model the HVDC network in DIgSILENT is explained and different case study results are recorded and analysed as well. The contribution to research is a developed flowchart that shows how to assess the effectiveness of the harmonic mitigation techniques typically applied on bipolar HVDC systems using newly developed evaluation indices.

Conclusions and recommendations are provided. Appendices are included wherein specialised details are provided that can be useful to industry, especially for those needing to prepare a specification for a bipolar HVDC converter scheme, which includes harmonic mitigation techniques.

Acknowledgement

This work was conducted at the Centre of Power System Research Laboratory (CPSR) at Cape Peninsula University of Technology (CPUT) under the supervision of Prof Gary Atkinson-Hope. I would like to thank him very much for the opportunity he gave me to work in an excellent academic environment in the first place and for the scholarship he provided and his knowledge of HVDC especially that applied by the South Africa Power Utility, Eskom. His invaluable and thoughtful suggestions and guidance through the course of the thesis work was very pleasing.

I am really pleased to get a space here to thank Frank Kasangala who is an epitome of a good friend, very close and supportive as a friend, it is a pleasure to work with you and you really deserve all the gratitude.

My special thanks go to the Head of Department of Electrical Engineering Mr Ben Groenewald at the Cape Peninsula University of Technology for hosting me during my thesis period.

Lastly, I am deeply indebted to my family and all my friends for their support and advice.

Cape Town, South Africa: 09 Mar. 17

Jimmy Matabaro Mushagala

Dedication

This thesis is dedicated to the late Willem Stemmet of the Cape Peninsula University of Technology (CPUT) at the Department of Electrical Engineering, whom I knew during my studying period and has passed away. You have been a true inspiration to me, I salute you. I also, dedicate it to those who were forced to abandon their studies owing to life circumstances and to the many others for whom it is still not possible to fulfil their dream of starting or resuming tertiary education.
With the hope that in the future the doors of knowledge will be open to each and every one of you.

Table of Contents

List of Figures

List of Tables

List of Symbols

α	Rectifier ignition angle or delay angle
μ	Overlap angle
φ	It is an angle by which the fundamental frequency component of an alternating line current lags a line to neutral of the source voltage
ω	Overlap time taken by the current when it gets transfer from one phase to the next phase.
δ	Extinction angle
β	Inverter ignition angle
γ	Inverter extinction angle
$\mathfrak{R}$	Reluctance
γ_o	Inverter extinction angle minimum required value
Y-Δ	Star to delta winding coupling
Y-Y	Star to star winding coupling

Glossary

AC	Alternating Current
BPHVDC	Bipolar High Voltage Direct Current
CEA	Constant Extinction Angle
CSC	Current Source Converter
DC	Direct Current
DPF	Displacement Power Factor
ESCR	Effective Short Circuit Ratio
FFT	Fast Fourier Transformer
HD	Individual Harmonic Distortion
HLF	Harmonic Load flow
HVAC	High Voltage Alternating Current
HVDC	High Voltage Direct Current
IHA	Iterative Harmonic Analysis
LCC	Line-Commutated Converter
PI	Proportional Integral
pu	per unit
rms	root mean square
SCADA	Supervisory Control and Data Acquisition
SCL	Short Circuit Level
SCR	Short Circuit Ratio
TDD	Total Demand Distortion
THD	Total Harmonic Distortion

Chapter One:

1 Project Description

This chapter describes the background of the thesis and motivation related to the research. The objective of the thesis, main contributions of the work and the outline of the thesis are also presented. Finally, the project publications are listed.

1.1 Introduction

With the increased de-regulation of the power markets world-wide, the needs of the consumers are becoming more and more important. Power quality, particularly harmonic distortion, is a growing concern of consumers and power utilities due to the increasing number of power conversion devices at both transmission and industrial levels. To the ordinary consumer, harmonics are normally only noticeable as annoying buzzing, telecommunication interference or small appliance malfunction. However, they have a major indirect effect resulting from their impact on power system operation. Harmonics within power systems result in increased heating in system components which results in a shortening of their expected lifespan. They can also result in the malfunction of system protection, inaccurate powerflow metering and faults due to insulation breakdown. There are also instances where excessive harmonic levels have resulted in high voltage direct current (HVDC) installations shutting down due to control malfunctions. Therefore, the majority of new converter installations will require filtering banks to minimise their impact and existing filtered installations may need to be upgraded. However, to design systems with adequate harmonic power quality, simulation tools are required that can quickly and accurately perform multiple system contingency studies to determine the harmonic profiles at the Point of Common Coupling (PCC) and other busbars.

1.2 Theoretical Background

The semiconductor devices in the converter stations of a HVDC system are usually non-linear power electronic devices. A large amount of harmonic currents will be produced and injected into the high voltage alternating current (HVAC) power system when a HVDC system is connected, even when the supply voltage waveform on the HVAC side is a sinusoidal wave at fundamental frequency. These currents cause voltage distortion at busbars associated with the HVAC and HVDC system. The harmonics that come from the HVDC will increase losses, thermal stress of equipment, reduce equipment life, interfere with

communications, metering, protection and control devices causing them not to work properly and in some cases, it can even lead to the collapse of the system.
Harmonics are electric voltages and currents that appear in an electric power system as a result of non-linear electric loads. Harmonic frequencies in the power grid are a frequent cause of power quality problems. Harmonic components should be reduced as much as possible.

These are two types of harmonics in electrical power systems, namely current and voltage harmonics, which cause their resultant waveforms to be distorted, respectively. There are also another two types of harmonics; characteristic and non-characteristic harmonics and these depend on whether or not a system is symmetrical, balanced or not. These harmonic effects require special consideration specifically when designing new HVDC systems or evaluating existing or expanding networks. These distorted voltage and current waveforms affect the true and reactive powers present in the system.

There are various methods to analyse harmonics in a Line Commutated Converter (LCC) HVDC system. For example: the symmetrical component method and harmonic mapping. But each of the methods has limitations. However, the most common methods are harmonic penetration studies and the harmonic resonance method that uses frequency scanning versus impedance response and together they are commonly called harmonic analysis.

The most common methods for the reduction of harmonics are filters and transformer connections (e.g. star to delta and star to star). In integrated HVAC/HVDC systems it is common nowadays to find monopolar and bipolar LCC HVDC systems. For large systems where bi-directional flow of power is required, it is common practise to use bipolar HVDC systems. However, such systems cause unacceptable harmonic distortions and it is for this reason that the work in this thesis focuses on harmonic analysis and the effectiveness of the mitigation techniques applied to bipolar HVDC systems.

1.3 Thesis Objectives

Power system harmonic analysis is not a new topic. A considerable amount of time and effort has been spent analysing the various components that form a power system so that appropriate harmonic models can be developed. This thesis investigation was carried out at the Centre of Power System Laboratory at Cape Peninsula University of Technology. The key objective was to provide a working structure for a bipolar HVDC system that combines all the important aspects of steady-state harmonic analysis; analyse the harmonic impact

created by HVDC when it interacts with an HVAC network, and to evaluate the effectiveness of the mitigation techniques used to alleviate the harmonic effect.
As the power system is continually changing, its modelling requires multiple snapshots of fixed operating points. To ensure that the engineer's task mimics the real world system, specifications should attempt to reflect the state of the physical system as closely as possible, with as few simplifications as possible.

Firstly, an integrated HVAC/HVDC system is modelled on a computer and a load flow analysis is conducted to prove that the modelling is correct at the fundamental frequency of the system.

Once this procedure is achieved, the secondary objective is then to investigate the effect of harmonic distortion. Here harmonic analysis is conducted. These results are usually evaluated against harmonic limits provided by standards ensuring compliance with internationally recognised recommendations and this usually means the equipment can be operated safely and reliably. The study of harmonics in a bipolar HVDC is not common and it is for this reason that this investigation was conducted and to contribute to the knowledge in this advanced field in power systems. In an integrated HVAC/HVDC system harmonics are found at both ends of HVDC systems. Bipolar systems operate in a bi-directional manner, thus at each end of the HVDC system there are rectifiers and inverters (non-linear devices).

1.4 Project Motivation

The project motivation shows that there is a need for research to be conducted in the field of harmonics produced from large size rectifiers and inverters, especially when bipolar HVDC system are integrated into existing HVAC system.
This research is to identify and explain the mitigation techniques used with bipolar HVDC systems in terms of international standards on harmonic distortion. The research questions that need to be answered by this research thesis are as follows:

- How does a bipolar HVDC system work when integrated to a HVAC network using a computer model?
- What harmonic mitigation techniques are typically applied to bi-polar HVDC systems and how do they operate?
- How successful (or effective) are these mitigation techniques under various operating conditions?

In order to answer these questions, certain objectives have to be set in order to lay the right theoretical foundations, create valid simulation models and cases studies.

Once this is done, the key questions can be answered and conclusions and recommendations can be formulated. This gives rise to the following objectives:

- Explore LCC HVDC theory and specifically bi-polar LCC HVDC theory
- Explain harmonic theory
- Show how power system harmonics are related to sequence analysis
- Explain network resonance studies
- Identify and explain mitigation techniques, such as filters and transformer connections
- Choose a software analysis tool for modelling of a bi-polar HVDC system and explain how the model and sub-models are developed and analysed
- Explain harmonic analysis in the frequency domain
- Elucidate on scenarios to be investigated through simulation case studies that include effective mitigation techniques (for example: filters, selecting an appropriate rectifier and inverters angles, and transformer connections star to star and star to delta)
- Explain IEEE 519 harmonic analysis standards techniques.
- If recommendations can be made, test recommended solutions where applicable and practical
- Identify unanswered or new questions and recommend future work

1.5 Document Overview

1.5.1 Chapter 2 – Theory of HVDC Transmission Network

This chapter examines the different fields that have relevance to the thesis topic as set out in the objectives and combines relevant inputs from published journals, books, conference proceedings, and other references. These inputs are used as guidance for the specific topic and refer to previous research, but are also evaluated against one another and against the findings of this research thesis for validity and applicability.

First, background information is given on the theory of LCC HVDC for which the research is performed in order to understand the parameters within which the analysed scheme operates. Next, an overview is given of HVDC schemes and its control with focus on a bipolar HVDC scheme and the typical composition of such a scheme. The unique features of the analysed scheme are discussed here in detail.

Subsequently, the foundation of power system harmonics, resonance and sensitivity are laid before continuing into bipolar HVDC theory. This is followed by AC/DC harmonic interaction theory, after which modelling and simulation techniques to implement these theories are discussed.

1.5.2 Chapter 3 – Harmonic Analysis Methods

This chapter builds on the foundations laid in the previous chapter on the combination of relevant sources and further explores the different fields of power system harmonic sequence components, harmonics generation and AC/DC harmonic interaction. The purpose of this is to go into more detail and give new perspectives, relationships and understanding of existing theories, illustrate some theories and to set the scene for the next chapter.

1.5.3 Chapter 4 – Effectiveness of Harmonic Mitigation Technique in Bipolar HVDC System

This chapter covers the different mitigation techniques used in this thesis which can reduce the impact of harmonics on a bipolar HVDC network. It starts with transformer connections by elaborating on their configurations and the impact they have on reducing harmonics into HVAC network. Thereafter, other mitigation techniques such as filters and rectifier and inverter switching angles are included. The capturing of these techniques and the development of a process, using indices is included to evaluate their effectiveness. These make up the contributions of this work.

1.5.4 Chapter 5 – HVDC Network Modelling, Case studies and Results Analysis

This is a more practical chapter on how the relevant power system components can be modelled using DIgSILENT PowerFactory software and what tools can be used to analyse the data generated.

The purpose of the case studies are to prove the theories presented earlier and that the simulation models demonstrate the effectiveness of the mitigate techniques. Each case background and methodology is presented. Case study one presents effectiveness of filters. Case studies two and three are about effectiveness of rectifier transformer reactance and switching angles respectively. It presents the impact that transformer connections in star to star and star to delta have on reducing harmonics on AC side, as well the switching angles of rectifiers and inverters as mitigation techniques.

1.5.5 Chapter 6 – Results and conclusions

The most important results and findings throughout the thesis are summarised and a short discussion of each is presented to put it in context and show why these results are significant or valuable to the industry.

1.5.6 Appendices

Appendices give the specialised details and are provided for completeness.

1.6 List of Publications (See Appendix A)

● M J. Matabaro and G. Atkinson-Hope: "*Optimization of Loss Reduction through a converted HVAC Transmission Line into HVDC Model in DIgSILENT Software*", *SAUPEC* 2014 Conference in University of Kwazulu Natal, Durban, South Africa, 30 January 2014- 31 January 2014.

● M J. Matabaro and G. Atkinson-Hope: "*Efficiency of an Alternating Current Transmission Line Converted into a Direct Current System*", *ICUE* 2013 Conference at Newlands, Cape Town, South Africa, 19 August 2013- 21 August 2013, pp: 311-316.
http://eepublishers.co.za/article/icue-020-11-efficiency-of-an-alternating-current-transmission-line-converted-into-a-direct-current-system.html

● M J. Matabaro, W.C. Stemmet and G. Atkinson-Hope: "*Converting Conventional High Voltage Alternating Current Transmission lines into a Direct Current Transmission System*", *SAUPEC* 2013 Conference in North – West University, Potchefstroom, South Africa, 31 January 2013- 01 February 2013, pp: 139-142.

Chapter Two:

2 Theory of HVDC Transmission Network

This chapter looks at the theory of Bipolar HVDC (BPHVDC) converters and the harmonics they generate. First, background information is given on the theory of LCC HVDC in order to understand its operating scheme. Thereafter, the theory on AC/DC harmonic interaction is given, which reviews how harmonics are generated by BPHVDC rectifiers and inverters. The theory of operation of bipolar HVDC system is also reviewed in this chapter.

2.1 Literature study

This chapter reviews the theory fields that are relevant to this research topic as set out in the project motivation and combines relevant inputs from published journals, books, conference proceedings and other references. These inputs are used as guidance on the specific topic with regards to previous research, but are also evaluated against one another and against the findings of this research thesis for validity and applicability.

Firstly, background information is given on the theory of a Line Commutated Converter (LCC) BPHVDC system in order to understand the operation within which the scheme operates. Secondly, a review is given on the fundamentals of power system harmonics and their relations to sequence components. Thirdly, harmonic resonance is reviewed. Lastly, the interaction of the BPHVDC system with an existing HVAC grid and its influence on AC grid strength is also reviewed.

2.1 Basic Structure of HVDC Interconnection

The following is a brief description of a typical BPHVDC configuration and its control strategies. Figure 2.1 shows a BPHVDC system fed from a generating source G1 interconnected to a grid. The BPHVDC scheme comprises of various essential pieces of equipment and their role and or functions are introduced here.

2.1.1 Converters

A converter performs the energy conversion from AC to DC (rectifier) and DC to AC (inverter) (Arrillaga & Watson, 2003). It usually has a 12-pulse arrangement, in which two 6-pulse bridges are connected in series on the DC side, as depicted in Figure 2.1. The switching of the thyristor valves is done through a converter control system. The rectifier is the converter in which power flows from AC to DC, and the inverter is the converter in which power flows from DC to AC.

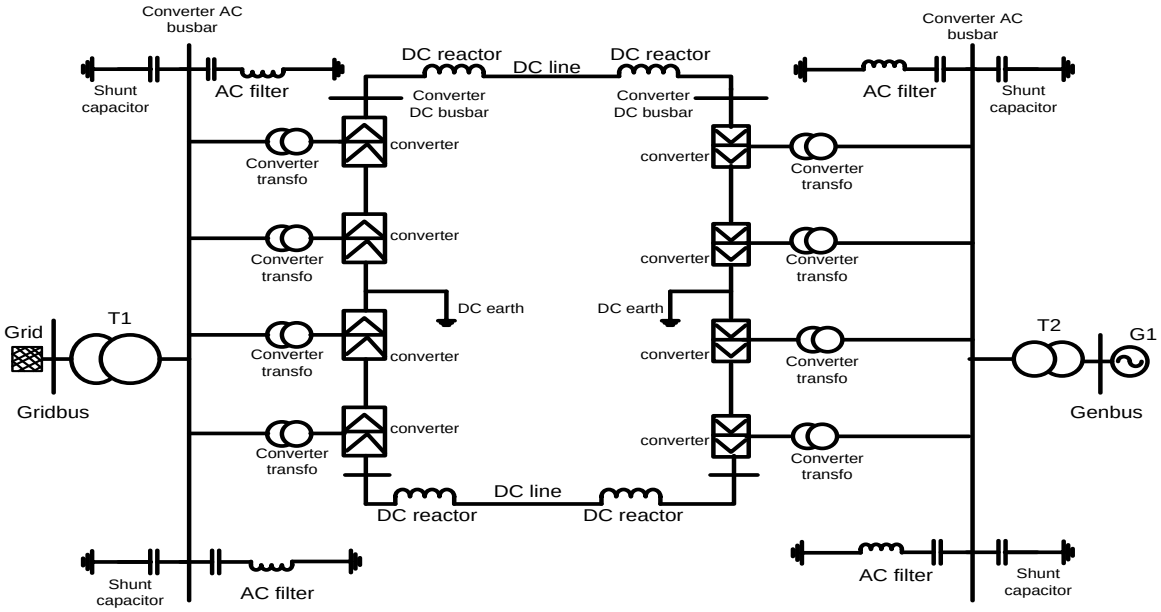

Figure 2. 1: One line diagram of a two terminal (Bipolar) HVDC system

2.1.2 Converter Transformers

Normally, the converters are connected to the HVAC system via transformers (called converter transformers). The most important function of these transformers is to transform the voltage of the HVAC system to a suitable level to obtain the rated DC voltage for the converter. The 12-pulse bridge usually has two converter transformers, a star-star transformer and star-delta transformer. These converter transformers have these configurations so that when operated in combination they provide an important harmonic mitigation technique used with BPHVDC scheme and is described in detail later in the thesis in chapter four.

2.1.3 Harmonic Filters

Converter operation generates harmonic currents and voltages on the HVAC and HVDC sides, respectively. Harmonic filters are needed on both HVAC and HVDC sides of converters in order to prevent harmonics generated by the rectifier and inverter from entering into the HVAC and HVDC systems. On the HVAC side, a converter with a pulse number of "*p*" generates characteristic harmonics having the order of $np \pm 1$ (n=1, 2, 3, etc.). Filters are installed to mitigate harmonic components and to reduce voltage and current distortion below a required threshold at the points of common coupling (PCC) on both sides of the BPHVDC schemes. Typically, tuned filters and high pass filters are used as HVAC filters. On the HVDC side, the order of harmonics is np (Kundur, 1994). HVDC filters, along with HVDC reactors, reduce the harmonics flowing out into the HVDC line. These also form essential components to mitigate the effects of harmonics and their effectiveness is evaluated as part of the research objectives of this thesis.

2.1.4 Shunt Capacitors

A line commutated converter (LCC) in steady-state operation consumes reactive power of about 60% compared to the active power (or DC power) transferred (Arrillaga, 1998). The shunt capacitors installed at the converter HVAC bus in steady-state operation, help to supply the reactive power required to maintain the converter AC bus voltage. To achieve a satisfactory power factor at the fundamental frequency called displacement power factor (dpf) for the LCC HVDC converter, the shunt capacitors are normally subdivided and switched by circuit breakers as the DC power varies. Some or all of the shunt capacitors are typically configured to be part of the AC harmonic filters (Baggini, 2008).

2.1.5 DC Reactors

The HVDC reactor contributes to the smoothing of the DC current on the HVDC line and provides harmonic voltage reduction on the HVDC line. The DC reactor also contributes to the limitation of the peak current during a short-circuit fault on the DC line (Callaghan, 1989). It should be noted that the inductance of the converter transformer also contributes significantly to the reduction of this peak current during short circuit fault on the HVDC line.

2.1.6 DC Transmission Connections

A bipolar scheme has two sets of HVDC overhead transmission lines, one positive with respect to earth and other negative. The midpoint of the bipolar at each terminal is earthed via an electrode line and earth electrode. Under normal conditions power flows through the lines and a negligible current will flow to ground when the scheme becomes unbalanced (Arrillaga, 1998).

2.1.7 Three-phase bridge converter

The energy conversion from HVAC to HVDC is called rectification and the conversion from HVDC to HVAC is called inversion. A converter can operate as a rectifier or as an inverter provided that it has a controller. A valve does conduct in only one direction, from anode to cathode and nowadays these valves are solid state devices (thyristor). Presently, thyristor valves are used for LCC and have a current rating up to 2 kA, and have a large number of thyristors connected in parallel depending on the valve current rating.

2.1.8 Rectification

In a given bridge rectifier, the transfer of current from one valve to another in the same row is called commutation. The time during which the current is commutated between two rectifying elements is known as the overlap angle (μ) or commutation time. Therefore, if two valves conduct simultaneously, there is no overlap, that is no commutation delay. The time during which the starting point of commutation is delayed is called the delay angle (α). The delay angle is governed by a control setting. When the overlap angle is neglected, the average direct voltage ($V_{DCaverage}$) depends on a given delay angle(α).

The average dc voltage per cycle for a 6 pulse converter is defined as (Arrillaga, 1998):

$$V_{d-RMS} = \frac{6}{2\pi} \times V_{phmax} \times \cos\alpha \quad (2.\ 1)$$

The average dc voltage for a 12 pulse converter is defined below as:

$$V_{d-RMS} = \frac{3\sqrt{3}}{\pi} \times V_{phmax} \times \cos\alpha \quad (2.\ 2)$$

Where,

V_{do}= $\frac{3\sqrt{3}}{\pi} \times V_{phmax}$; therefore V_{d-RMS} becomes

$$V_{d-RMS} = V_{do} \times \cos\alpha \quad (2.\ 3)$$

Where:

V_{d0} = The ideal no-load direct voltage or average DC voltage when delay angle is zero and there is no delay.

E_m= The maximum value of phase-neutral alternating voltage

α = delay angle

However, if there is no delay, that is, α = 0°, the average direct voltage can be expressed as

$$V_{d-RMS} = V_{do-RMS} = \frac{3\sqrt{3}}{\pi} \times V_{ph-max} \quad (2.\ 4)$$

or:

$$V_{d-RMS} = V_{do-max} = \frac{3\sqrt{3\times 2}}{\pi} \times V_{ph} = \frac{3\sqrt{6}}{\pi} \times V_{ph}$$
$$= 2.34 \times V_{ph} \quad (2.\ 5)$$

or:

$$V_{d-RMS} = V_{do-RMS} = \frac{3\sqrt{2}}{\pi} \times U_L$$
$$= 1.35 \times U_L \quad (2.\ 6)$$

Where:

V_{ph} = rms line to neutral alternating voltage

U_L = rms line to line alternating voltage

The delay angle α can change the average direct voltage by a factor of $\cos\alpha$, this is shown in equation 2.1 and 2.2. Since α can take values from 0° to almost 180°, the average direct voltage can take values from positive V_d to negative V_d. However, the negative direct voltage V_d with positive current I_d causes the power to flow in the opposite direction. Therefore, the converter operates as an inverter rather than as a rectifier (Bathurst et al., 1998). Since the current can only flow from anode to cathode, the direction of current I_d remains the same.

The rms value for fundamental frequency of alternating current (I_L) is:

$$I_L = \frac{\sqrt{6}}{\pi} \times I_d \quad (2.\ 7)$$

When losses in the converters are neglected, the active AC power can be set equal to the DC power, therefore:

$$P_{ac} = P_{dc} \quad (2.\ 8)$$

With

$$P_{ac} = 3 \times V_{ph} \times I_L \times cos\varphi \quad (2.\ 9)$$

$$P_d = V_d \times I_d \quad (2.\ 10)$$

When equation 2.7 is substituted in equation 2.9; as well by substituting equation 2.3 and 2.5 simultaneously into equation 2.10, therefore, following equations are obtained:

$$P_{ac} = \frac{3\sqrt{6}}{\pi} \times V_{ph} \times I_d \times cos\,\varphi \quad (2.\ 11)$$

and

$$P_{dc} = \frac{3\sqrt{6}}{\pi} \times V_{ph} \times I_d \times cos\,\alpha \quad (2.\ 12)$$

When both equations 2.11 and 2.12 are substituted into equation 2.8, it becomes:

$$\cos\varphi = cos\,\alpha \quad (2.\ 13)$$

Where:

$\cos\varphi$ = is a displacement power factor (dpf).

φ = it is an angle by which fundamental frequency component of alternating line current lags line to neutral of the source voltage.

Thus, the delay angle α displaces the fundamental component of the current by an angle φ. Therefore, the converter draws reactive power from the AC system. The rectifier is said to take lagging current from the AC system, and the inverter is said either to take lagging current or to deliver leading current to the AC system. When there is an overlap angle (μ), it causes the alternating current in each phase to lag behind its voltage. Therefore, a decrease in direct voltage due to the commutation delay can be expressed as:

$$\Delta V_d = \frac{V_{do}}{2}[\cos\alpha - \cos(\alpha + \mu)] \quad (2.14)$$

ΔV_d is a reduction in average direct voltage due to commutation overlap. The associated average direct voltage can be expressed as

$$V_d = V_{do} \times \cos\alpha - \Delta V_d \quad (2.15)$$

After substituting (2.14) into (2.15), the following formula is obtained:

$$V_d = \frac{V_{do}}{2}[cos\,\alpha + cos(\alpha + \mu)] \quad (2.16)$$

This introduces an extinction angle, namely:

$$\delta = \alpha + \mu \quad (2.17)$$

In order to calculate V_d both variables (α and μ) need to be known. Alpha (α) is the given firing angle and overlap angle (μ) needs to be calculated.

When equation 2.17 is substituted into equations 2.14 and 2.16, therefore the corresponding decrease in direct voltage due to the commutation delay can be expressed as:

$$\Delta V_d = \frac{V_{do}}{2}[\cos\alpha - \cos\delta] \quad (2.18)$$

and

$$V_d = \frac{V_{do}}{2}[\cos\alpha + \cos\delta] \quad (2.19)$$

The overlap angle μ is due to the fact that the AC supply source has a transformer with inductances. Thus, the currents in it cannot change instantaneously. Therefore, the current transfer from one phase to another takes a certain time, which is known as the commutation time or overlap time (μ or ω). Under normal operation, the overlap angle is within the range of $0° < \mu < 60°$. During abnormal operation mode, the range is $60° < \mu < 120°$.

2.1.9 Inversion

In a given converter (for inverters or rectifiers), the current flow is always from anode to cathode, that is, unidirectional inside a rectifying valve or thyristor, so that the cathode remains the positive terminal.

Therefore, the current direction in the converter cannot be reversed. When it is required to operate a converter as an inverter in order to reverse the direction of power flow, the direction of the average direct voltage (V_{DC}) must be reversed. This can be obtained by using the converter control by changing the delay angle α until the average direct voltage (V_d) decreases as the delay angle α is advanced, and it becomes zero when α is 90°. With further increase in the delay angle α, the average direct voltage becomes negative. Therefore, it can be said that the rectification and inversion processes occur when $0° < \alpha < 90°$ and $90° < \alpha < 180°$, respectively (Arrillaga, 1998). If there is an overlap, the inversion process may start at a value of the delay angle that is less than 90°.

Therefore,

$$\alpha = \pi - \delta \quad (2.\ 20)$$

or

$$\alpha = \frac{1}{2}(\pi - \mu) \quad (2.\ 21)$$

Where

α = delay angle in electrical degrees

δ = extinction angle in electrical degrees

μ = overlap angle in electrical degrees

Figure 2.2 shows the relationship among angles which are used in converters. The curvature of the front of a current pulse of an inverter differs from that of a rectifier. Page 106 of Kimbark (Kimbark, 1971) has demonstrated some references which gives the relations among these various inverter angles as:

$$\beta = \pi - \alpha \quad (2.\ 22)$$

$$\gamma = \pi - \delta \quad (2.\ 23)$$

$$\mu = \delta - \alpha \quad (2.\ 24)$$

$$\mu = \beta - \gamma \quad (2.\ 25)$$

Where

$\beta =$ Inverter ignition angle in electrical degrees

$\gamma =$ Inverter extinction angle in electrical degrees

In order to provide adequate time for the operation for the appropriate valve thyristor, the minimum value of the inverter extinction angle γ_0 must be in the range of 1° to 8° . If the value of γ_0 is not adequate, the valve will start to conduct again and is called commutation failure.

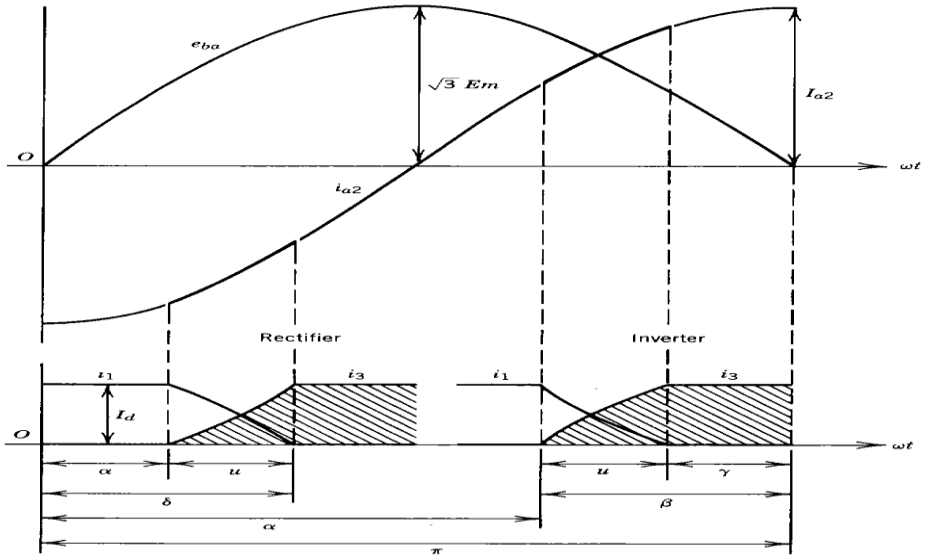

Figure 2. 2: Relations amongst Angles used in Converters **(Kundur, 1994)**

When rectifier equations are used to define an inverter operation α and δ will be substituted by $\pi - \beta$ and $\pi - \gamma$. In order to distinguish the inverter equations from the rectifier equations subscripts *i* and *r* have been used to signify the inverter and rectifier operations.

Which are expressed as:

$$I_{di} = I_r(\cos\gamma - \cos\beta) \qquad (2.\ 26)$$

For a good operation of inverters, it is preferable to operate inverters with constant extinction angle (CEA) control rather than with constant ignition angle (CIA) control (Kimbark, 1971).

The inverter does have a leading power factor, contrary to a rectifier, which has a lagging power factor. This is due to the fact that the lagging reactive power is provided to the inverter by the AC system into which the inverter is feeding current to the AC system at a leading power factor. The required additional reactive power by the inverter is provided by synchronous capacitors or by static shunt capacitors.

2.1.10 HVDC Control

The full control structure of an HVDC link is very complicated due to the interconnection of steady-state, transient and protection strategies. It is generally sufficient for steady state representation to simplify this structure down to the basic philosophy of the link operation, while maintaining the aspects important to steady-state analysis.

Typically, an HVDC link is under some form of current control, usually specified by the rectifier. This controller will have some form of integral action so that the specified setpoint is reached and can usually be approximated by a simple PI (Proportional Integral) controller. A model description from DIgSILENT of this control is found in appendix B (as shown in figures B.1 to B.3). The inverter maintains the link voltage by minimising its extinction angles, i.e. the time remaining after the end of commutation. This also has the effect of minimising the reactive power consumption of the inverter. While under ideal conditions it would be possible to minimise the extinction angle to virtually zero, this would make the inverter very vulnerable to any disturbance on the inverter or rectifier ac systems, thus resulting in a commutation failure. Most inverter controls specify a minimum angle of extinction that should be maintained during normal operation to minimise this risk. A model description from DIgSILENT of this control is found in appendix C (as shown in figures C.1 to C.3). This control strategy is referred to as constant commutation margin control or minimum gamma control, where gamma is the angle of extinction (Kimbark, 1971).

These two controls represent the basic operation of an HVDC link where the inverter acts as a voltage source and the rectifier as a current source. This form of control is illustrated by the static characteristic shown in Figure 2.3. This characteristic has been modified to improve the dynamic performance by specifying non-optimal inverter. The characteristic shows the inverter operating nominally under constant DC voltage control, but can move into either minimum gamma or proportional current control if operating conditions require. The steady-state operation can be in any of these three conditions during non-ideal system conditions, and so the full control should be represented. Improved representation can be achieved by the addition of further control blocks which specify various operating conditions for optimum

or more realistic performance. The current control can be represented by a PI control loop where the firing angles are modulated by the DC current harmonics. Other extended controls such as the converter transformer tap-changer should also be modelled. The rectifier tap-changer is used to minimise the average firing angle of the converter to reduce its reactive power consumption while still maintaining sufficient voltage to ensure firing (Kimbark, 1971). The inverter tap-changer controller is used to maximise the DC voltage which in turn, for a specified DC power transfer, will reduce the DC current and hence the real power losses. Finally a DC power controller can be used which adjusts the DC current setpoint of the current controller to obtain a specified power transfer.

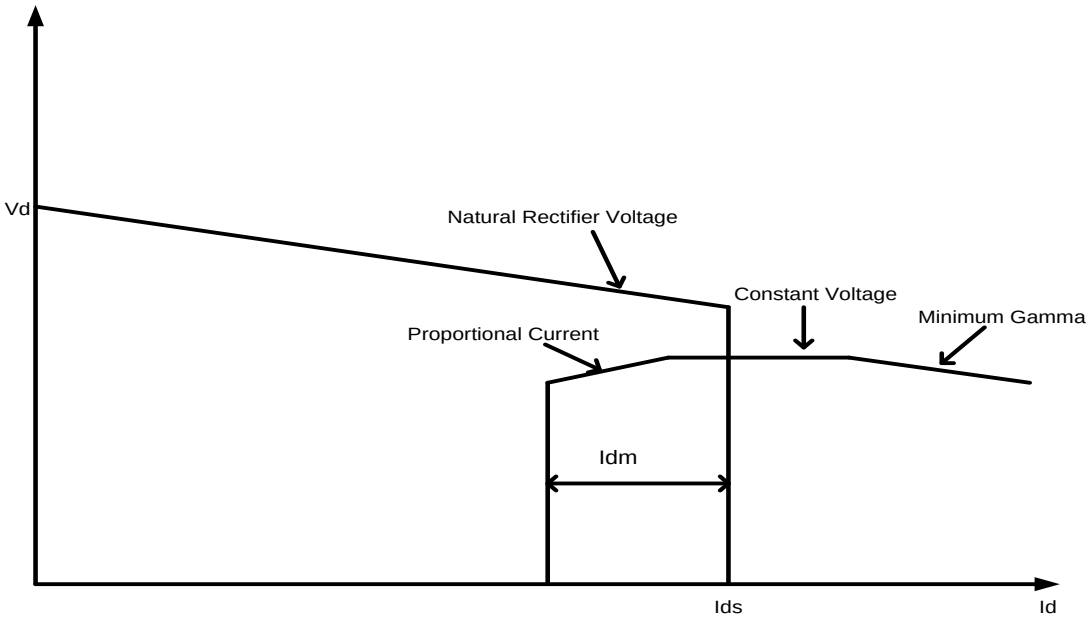

Figure 2. 3: Three Stage control Characteristic for an HVDC link

2.2 Power System Harmonic Analysis Overview

2.2.1 Fundamentals of power system harmonics

The generation of electricity by a utility is ideally required to be at a constant frequency, e.g. 50Hz or 60Hz, and to be purely sinusoidal. Even if this was the case, the sinusoidal voltage that is applied to non-linear loads cause non-sinusoidal currents to flow through these devices or loads. System impedances such as lines, transformers, etc. between generation points and loads can cause non-sinusoidal voltage drops, especially when non-sinusoidal load currents are drawn. As a result, the voltage presented to load terminals also contains components that contribute to the supply voltage not being purely sinusoidal. Even linear loads presented with non-sinusoidal voltages will then draw non-sinusoidal currents.

These non-sinusoidal components are considered quality of supply (QoS) pollution and are referred to as power system harmonics occurring as harmonic voltage and harmonic current components**.** The term “harmonics” is a very broad term and is often misused. Proper reference should be made using more descriptive and contextual terms such as “harmonic component”, “harmonic distortion”, “harmonic order”, etc.

Power system harmonic components are theoretical constructs and are normally represented as independently rotating phasors with rotational speeds of integer multiples of the fundamental frequency rotational speed with a specific phase offset in relation to the fundamental phasor. In a three-phase system harmonic components have certain phase-rotation or sequence component characteristics. Harmonic components that do not rotate at integer multiples of the fundamental frequency, called inter-harmonics, also exist in certain cases and are often observed under transient conditions. Although this concept brings forth some conflicting theoretical implications, it will not be discussed here.

According the work of Jean Baptiste Joseph Fourier (1768-1830) as first published in 1878 (Fourier, 1978), any periodic waveform can be expanded in the form of a Fourier series as follows:

$$f(t) = a_o + \sum_{n=1}^{\alpha}(a_n \cos\frac{2\pi nt}{T_o} + b_n \sin\frac{2\pi nt}{T_o}) \quad (2.\ 27)$$

Where a_o is the mean value of the periodic signal $f(t)$ over one period given by the relationship in equation 2.28.

$$a_o = \frac{1}{T_0}\int_{-T_0/2}^{T_0/2} f(t)dt \quad (2.\ 28)$$

The coefficients a_n and b_n are given by the relationships in equations 2.29 and 2.30.

$$a_n = \frac{2}{T_0}\int_{-T_0/2}^{T_0/2} f(t)cos\frac{2\pi nt}{T_0}dt\ , n = 1,2,3\ \ldots. \quad (2.\ 29)$$

And

$$b_n = \frac{2}{T_0}\int_{-T_0/2}^{T_0/2} f(t)sin\frac{2\pi nt}{T_0}dt\ , n = 1,2,3\ \ldots. \quad (2.\ 30)$$

Where T_0 symbolises the period of the waveform.

2.2.2 Characteristic harmonic orders of power systems

Due to the symmetries found in three phase power system wave shapes, the harmonics that normally occur are referred to as characteristic harmonics. In general, the symmetry properties of the wave shapes give rise to the following effects (Kundur, 1994), (Mohan et al., 1995), (Wakileh, 2001), (Arrillaga & Watson, 2003):

- Odd symmetry: $f(-t) = -f(t)$
  This results in all the a_n terms cancelling out and the Fourier series containing only sine terms.
- Even symmetry: $f(-t) = f(t)$
  This results in all the b_n terms cancelling out and the Fourier series containing only cosine terms.
- Half-wave symmetry: $-f(t) = f(t \pm \frac{T}{2})$
  This results in a cancellation of all even order harmonics and a zero DC component.

In power systems, except where non-linearity causes half-wave symmetry to be compromised, only odd harmonics are generated. Phenomena such as transformer saturation by heavy loading or inrush currents can remove half-wave symmetry that introduces lower order even harmonics (Kundur, 1994), (Mohan et al., 1995), (Wakileh, 2001), (Arrillaga & Watson, 2003), (IEEE, 2004), (Baggini, 2008), (Neves et al., 2009).

2.2.3 How Converters Cause Harmonics

The HVAC to HVDC converter (rectifiers and inverters) are a source of harmonics. This is because the rectifier and inverter are connected to the supply for a controlled period of a fundamental frequency cycle and hence the current drawn from the supply is not sinusoidal.
When seen from the AC side, a rectifier and inverter can be considered as a generator of current harmonics (Figure 2.4), and from the DC side a generator of voltage harmonics (Figure 2.5) (Bathurst et al., 1998).

I_h* = being the sinusoidal current at harmonic "h"

Figure 2. 4: HVDC Converters (rectifier or Inverter) represented as AC harmonic Current Source viewed from AC Side

The actual level of harmonics generated by an AC to DC rectifier and inverter are a function of the duration over which a particular phase is required to provide unidirectional current to the load. When there is more switching between phases within a cycle, the harmonic distortion is lower in both the AC line current and the DC terminal voltage.

V_h* = being the sinusoidal voltage at harmonic "h"

Figure 2. 5: AC to DC Converter (Rectifier or Inverter) Represented as AC Harmonic Voltage Source on AC Side

2.3 Principles of resonance and sensitivity

2.3.1 Conditions for resonance

For a true resonance condition to occur, two conditions need to be fulfilled, namely the generation of a certain harmonic order and a sensitivity to that specific harmonic order due to a series or parallel resonance point. The damping of the system will determine if the resonance condition will remain damped or grow out of control while excited. The damping is normally determined by the resistive components in the resonant circuit.

The movement of resonance points due to contingencies, system configurations, operating regimes and the operating points of dynamic devices also plays an important role in the harmonic analysis of a power system (Kundur, 1994), (IEEE, 1997), (Wakileh, 2001), (Rens, 2005), (Baggini, 2008).

2.3.2 Series resonance

A series resonance condition occurs in a series RLC circuit when the circuit impedance is at a minimum when their inductive and capacitive reactance cancels out each other. A small excitation voltage then results in large currents (Wakileh, 2001), (Arrillaga & Watson, 2003). For a series RLC circuit, the total circuit impedance is given by:

$$Z = R + j(X_L - X_C) \quad (2.\ 31)$$

Where R is the resistance, X_L the inductive reactance and X_C the capacitive reactance of the circuit being used. The impedance $|Z|$ is at a minimum when $X_L = X_C$

Using the following relationships for X_L and X_C :

$$X_L = 2\pi f L \quad (2.\ 32)$$

$$X_C = \frac{1}{2\pi f C} \quad (2.\ 33)$$

Where: L is the inductance, C is the capacitance, f the circuit frequency and using the relationship in equations 2.32 and 2.33.

In equation 2.31 yields that $|Z|$ is at a minimum when inductive reactance is equal to the capacitive reactance when Z = R. This is being shown in equation 2.34.

$$2\pi f_r L = \frac{1}{2\pi f_r C} \quad (2.\ 34)$$

The resonant frequency of the RLC circuit is thus given by equation 2.35.

$$f_r = \frac{1}{2\pi\sqrt{LC}} \quad (2.\ 35)$$

It can also be shown that the resonant harmonic h_r is given by equation 2.36.

$$h_r = \sqrt{\frac{X_C}{X_L}} \quad (2.\ 36)$$

2.3.3 Parallel resonance

A parallel resonance condition occurs in a parallel RLC circuit when the oscillating LC part of the circuit is such that the inductive and capacitive reactances summate to zero and the total parallel circuit impedance is at a maximum. A small excitation current thus results in large voltage (Wakileh, 2001), (Arrillaga & Watson, 2003). For a parallel RLC circuit and using the relationships (2.32) and (2.33), the total circuit impedance is given by equation 2.37.

$$Z = \left[\frac{1}{R} + j\left(\frac{1}{X_L} - \frac{1}{X_C}\right)\right]^{-1} = \left[\frac{1}{R} + j\left(\frac{1}{2\pi fL} - 2\pi fC\right)\right]^{-1} \quad (2.37)$$

It can be shown that | Z | is at a maximum when $X_L = X_C$.
Using the relationships from (2.32) and (2.33), it yields that | Z |is at a maximum when

$$2\pi f_r L = \frac{1}{2\pi f_r C} \quad (2.38)$$

The resonant frequency f_r of the RLC circuit is thus given by

$$f_r = \frac{1}{2\pi\sqrt{LC}} \quad (2.39)$$

It can also be shown that the resonant harmonic h_r is given by

$$h_r = \sqrt{\frac{X_C}{X_L}} \quad (2.40)$$

2.4 Strength of Power System

2.4.1 System Interaction and Influence of AC Strength on HVAC to HVDC System

The performance of various components in a power system depends on the strength of the system. The strength of the system reflects its sensitivity of the system voltage to various disturbances in the system. In a strong system, disturbances caused, for example, by a change in the power of a load, do not cause any significant change in the voltage and angle in the power system. However, in a weak system even a small disturbance can cause so large deviations in the voltages that the operation of the system is jeopardized. The short

circuit level or equivalent impedance at a bus is a good measure of the strength of the system at that particular point (CIGRE and IEEE, 1993).

HVDC converters based on line-commutated converters (HVDC-LCC) can be seen as loads connected to the AC network with special characteristics such as voltage and angle dependence. They may offer controllability due to the possibility to control the firing instants of the valves. The strength of an HVAC system connected to an HVDC converter is often described in terms of the Effective Short-Circuit Ratio (ESCR) (CIGRE and IEEE, 1993). In general, system planners were using an ESCR of 2.5 as the lower limit for considering interconnection of systems by HVDC (Krishnayya & Reeve, July 1986). However, advanced control techniques have made it possible to successfully operate DC links located at terminals with ESCRs less than the limit of 2.5. If this occurs, the import capacity of the LCC connections has to be reduced (Statnett, 2013). This import capacity was not implemented into this research. As an example, the Itaipu HVDC transmission link in Brazil has been designed to operate under certain system conditions having ESCR of 1.7 (Baggini, 2008).

2.4.2 Short circuit level and short circuit ratio

The Short Circuit Level (SCL) of the AC system is a measure of the current that can be delivered into a solid three-phase fault at a particular bus in an HVAC system, with assumed nominal voltage (Statnett, 2013). This relationship is presented in equation 2.41.

$$SCL = \frac{E^2_{ac}}{Z_{th}} \tag{2. 41}$$

Where:
E_{ac} is the commutation AC bus voltage at the point where converters are connected and Z_{th} is the thevenin equivalent impedance of the HVAC system.

The Short Circuit Ratio (SCR), which is an expression of the relationship between the SCL of the HVAC system bus and the quantity of HVDC scheme power, can further be calculated as in equation 2.42.

$$SCR = \frac{SCL\ (MVA)}{P_{DC}\ (MW)} = \frac{E^2_{ac}}{P_{DC} \times Z_{th}} \tag{2. 42}$$

Where SCL is the short circuit level and P_{DC} is the DC operating power. A strong HVAC system is defined to have an SCR greater than 3, while a weak AC system is defined to have a SCR between 2 and 3 (Arrillaga & Wood, 1995). If the SCR becomes less than 2, commutation failure in the thyristors may occur frequently.

Chapter Three:

3 Harmonic Analysis Methods

This chapter introduces general theory that will be relied upon in subsequent chapters. It starts with a description of harmonics types found in BPHVDC and how it could be analysed. Converters transformers configurations are described for mitigating harmonics when a BPHVDC is being modelled in the frequency domain. The chapter ends by presenting guidelines as set by IEEE 519 for utilities when harmonics are being mitigated.

3.1 Introduction

HVDC converters behave as a source of harmonic currents of orders (*np±1*) on the AC side, and harmonic voltages of orders (*np*) on the HVDC side, with p equal to the pulse number of the converter, and ''*n''* an integer.

The DC voltage waveform produced by an ideal bipolar HVDC converter contains an AC ripple superimposed over a mean DC value, produced by the switching action of the converter valve. Switching occurs at every 60° interval in a six-pulse converter, and every 30° in a twelve-pulse converter as described in figure 3.3 which is for a six pulse converter. This composite voltage waveform is made up of purely sinusoidal segments for ideal conditions.

Power system harmonics come from a variety of sources, the dominant ones within transmission networks being large power converters such as those used for bipolar HVDC links and large industrial processes. The harmonics generated by these devices can be divided into three categories:

- Integer harmonics; are integer multiples of the power frequency.
- Inter-harmonics; period and integer multiples of some base frequency, they normally result from cross-modulation of the integer harmonics of two systems with different power frequencies.
- Non-integer harmonics; are the frequencies that do not fit either of the above two categories. They are not integer multiples of a base frequency and may not even be periodic.

The last two categories usually come from back-to-back HVDC links (periodic), cyclo-converters (periodic) and arc-furnaces (non-periodic) and are significantly more complex to model. They are not considered in this thesis.

The work in this thesis is concentrated only on integer harmonics as this is where the majority of concern is.

The large power converters produce mainly characteristic harmonics which are present during operation under ideal conditions and most of the early work revolved around these harmonics. Classical equations have been derived to obtain average firing angles, commutation durations, DC side voltages and harmonic magnitudes (Kimbark, 1971) (Arrillaga, 1998). However, few of the harmonic problems reported occur under ideal system operation, and so this form of analysis is very limited for harmonic purposes.

The linearity of synchronous machines and power transformers is very dependent upon their power-flow operating point. Both of these devices can normally be approximated as passive harmonic impedances, but these harmonic impedances often change with the system operating point.

Transmission asymmetries lead to a negative sequence fundamental component in the terminal busbar voltages and due to the frequency coupling behaviour of converters, this will lead to the generation of non-characteristic harmonics. Thus the AC transmission system must be represented in three-phase so that these effects be fully represented.

Also with increased public resistance to new transmission lines being built, the need for shared AC-DC right-of-ways will increase. The mutual coupling between these lines will result in both non-characteristic harmonic generation and converter transformer saturation problems. There are various solutions that minimise these effects, but analysis programs are required to accurately represent the systems, these are not included in this thesis as it not part of this research work.

3.2 Existing Harmonic Analysis Methods

Harmonic analysis methods can be fitted into three categories: time domain, direct frequency harmonic analysis and iterative techniques.

3.2.1 Time domain methods

Time domain modelling typically involves the numerical integration of system differential equations. Various methods are available for the creation of these differential equations and

their integration (Dommel, April 1969) (Gole et al., June 1983.). Time domain representation is the most extensively used method for power system modelling.

Although its primary function is for dynamic analysis, it is often used for steady-state analysis due to user's familiarity with it. Harmonic analysis with a time domain package involves simulation in the steady state and then the use of the Fourier transform.
Due to the combination of both long (inductances and capacitances) and short (device switching times), time constants within a system, small time steps and long simulation times are required for accurate steady-states. Due to this computational expense, methods for accelerating convergence to steady-state using boundary problem analysis have been developed (Aprille & Trick, January 1972.).

A significant problem is the time domain modelling of the frequency dependency of transmission lines, but a variety of methods have been developed which provide a reasonably accurate representation (Manitoba, 1988). Other methods use RLC branches calculated by numerical analysis to provide simple equivalents of large networks (Watson, 1987).

A time domain modelling does have the advantage that the same system developed for transient studies can be used for harmonics; a further advantage is the accurate representation of control systems. This is, however, due to the fact that time domain simulation has been around longer than frequency domain approaches. Modern frequency domain tools can also give good representation of realistic controllers (Bathurst et al., 1998).

3.2.2 Direct Frequency Domain Harmonic Analysis

Most commercial harmonic analysis packages use a direct frequency domain analysis using either single or three-phase representation (Densem et al., February 1984). The analysis consists of performing a loadflow to determine the system operating conditions and then calculating harmonic injections using simplified non-linear models. Then using the following nodal equation the system harmonic voltages are solved directly.

$$I_{node} = Y_{sys} \times V_{node} \qquad (3.\ 1)$$

This method does not permit the incorporation of the effect of harmonic voltages on the non-linear devices or the transfer of harmonics across HVDC links.

To maintain simplicity a variety of linearized converter models have been developed for analysing harmonic interaction with control systems (Dickmander et al., January 1994) (Arrillaga & Wood, 1995) and for the transfer of harmonics across DC links (Sadek et al., 1992) (Yacamini & Hu, November 1993). However, the accuracy of these methods is limited by the approximations made within the device linearization and the use of fixed operating points.

3.2.3 Iterative Harmonic Analysis

When a non-linear device injects a harmonic current into a non-infinite linear AC system busbar, a harmonic voltage of that same frequency is produced. If the non-linear device is sensitive to harmonic voltages, the injected harmonic current will change. This then requires an iterative solution to solve the system for accurate harmonic solution. Two basic iterative methods are used in power system iterative harmonic analysis (IHA): Fixed Point Iteration (using Gauss-Seidel) and the Newton Raphson method.

The simplest and previously most predominant iterative technique has been the Fixed Point Iteration. The current injections of a non-linear device (I_{NLinj}) are calculated from the system nodal voltages ($V_{node-inj}$) when Fixed Point Iteration is used.

Then using these currents and the system admittance matrix (Y_{sys}), new nodal voltages ($V_{node-inj+1}$) are calculated which are then used to re-calculate the non-linear device current injections. This iterative method is shown as follows:

$$I_{NL-inj} = f(V_{node-inj}) \tag{3. 2}$$

$$V_{node-inj+1} = \left|Y_{sys}\right|^{-1} \times I_{NL-inj} \tag{3. 3}$$

This method has been reported to have poor convergence for highly distorted or resonant systems (Callaghan, 1989). Better convergence has been obtained by using the Newton Raphson method for adjusting the solution variables.

3.3 HVDC Network Specification

It is import to develop a detailed procedure for harmonic analysis; this will specify the important aspects of HVDC harmonic modelling within power systems. The specifications

should detail the possible device and network configurations, operating point definitions and incorporate all important mechanisms of harmonic generation.

3.4 Non-linear Harmonic Generating Components

3.4.1 Active sources

Components such as large AC to DC converters and saturated transformers couple between frequencies and are generally non-linear harmonic generating components at their operating points. The busbars that they are connected to are represented in full harmonic form within the solution. Generally the non-linear devices require a control variable as well.

3.4.2 Passive Sources

To approximate small non-linear devices or background harmonic levels, passive harmonic sources can be specified. These can be either current or voltage sources and are held constant during the full harmonic solution. Simplified non-linear device models can be used to minimise the effort required to calculate these constant injections. These would be active at the power frequency during the loadflow solution but the resultant harmonic injections would be constant (Acha & Madriga, 2001).

3.5 Power Frequency Loadflow Components

The majority of power system loads and generators are operated within their linear regions. Their operating point specifications are normally in terms of loadflow conditions of power and voltage magnitude. A three phase loadflow should represent the harmonic frequencies; the linear components are represented by equivalent impedances which are calculated from pre-determined equations based upon some basic load or generator information. It is important that the connection of these loads (star-ground, delta, etc.) is properly represented as this will have a significant impact on the zero sequence and inter-phase impedances (Acha & Madriga, 2001) (Arrillaga & Wood, 1995).

3.6 Passive System Components

The significant part of the system representation is in the form of passive components that are not affected by the Loadflow operating point. They are represented within the solution as

shunt impedances or equivalent π –models. These can be generally calculated in any particular method and couple between phases and busbars, but not frequencies.

For simplicity the transformers and filters have their impedances calculated internally using pre-specified equations while the transmission line data is supplied externally.
Transformers and filters can be affected by system conditions if certain external control equations are specified. An automatic tap changer will affect the transformer impedance and a reactive power controller may switch out a filter bank. In these cases, the harmonic impedance of the system will change and such control actions are only performed during an initial Loadflow to minimise computational effort (Arrillaga & Wood, 1995) (Chen & Lie, 2012) (Harnefors, 2007).

3.7 Operating Point Controllers

System controls are an important part of the operating point specification. These can be either simple controls that are used to govern the power generated by the slack busbar or more complex ones that modulate converter firing angles from measured DC currents. The modelling of these controls should be as realistic as possible so as to simplify effort in system representation.

3.8 Characteristic and Non-Characteristic Harmonics

A converter is a highly nonlinear harmonic source; it will generate lots of harmonics at the AC and DC side when running. Having p as its pulse number, the converter mainly generate $n = kp$ (k is a positive integer) order harmonics at its DC side; while $n = kp \pm 1$ (k is a positive integer) order harmonics at its AC side, as explained earlier. Harmonic frequencies in the power grid are a frequent cause of power quality problems. Harmonic components should be reduced as much as possible, failure to do so could lead to low system efficiency, poor power factor, increased loss and reactive power components from the AC side and also on the equipment present in the system and interference on the telecommunication lines.

There are two types of harmonics in electrical power systems, namely current and voltage harmonics, which are distortions to current and voltage waves, respectively. On the basis of generation, there are two types of harmonics namely characteristic and non-characteristic.

As said previously, the characteristic harmonics are those harmonics generated by the commutation of converters (rectifier or inverters) DC voltage of a converter, and can be

expressed in terms of the pulse number of the converter; for example, for a six-pulse converter, the harmonic order can be expressed as 6*n*, where *n* is an integer and, in general, the expression would be pn, where p is the pulse number. All other harmonics not defined by such an expression are traditionally termed as non-characteristic harmonics. Non-characteristic harmonics usually are relatively small. This research is limited to characteristic harmonics because the characteristic harmonics are much greater than the non-characteristic harmonic.

The following assumptions are made for this research investigation when analysing the characteristic harmonics of converters:

- The AC voltage is a perfectly balanced sinusoidal function; it has no harmonic components;
- DC current is constant and ripple free, and there is a very large smoothing reactor;
- Converter valves have a constant firing angle (α), and are fired in the same interval from the fundamental period;
- The commutation reactances are equal in each phase, and the commutation angles are equal too.

  The research investigation is carried out by analysing the harmonic current at the AC side of converter transformers, and at the AC buses where they are connected.

3.9 Harmonics on the Output Side of the Converter

The output voltage waveform (on the converter DC side) contains even harmonics of the input frequency, and the Fourier expansion is expressed by:

$$E_{do} = E_{dc} + b_2 \sin(2\omega t) + a_2 \cos(2\omega t) + b_4 sin(4\omega t) + b_4 cos(4\omega t) + \cdots \quad (3.\ 4)$$

Where:

b_m and a_m (m = 2,4,6,8,…..) are given by:

$$a_m = \frac{2E_{max}}{\pi}\left[\frac{\cos(m+1)\times\alpha}{m+1} - \frac{\cos(m-1)\times\alpha}{m-1}\right] \quad (3.\ 5)$$

$$b_m = \frac{2E_{max}}{\pi}\left[\frac{\sin(m+1)\times\alpha}{m+1} - \frac{\sin(m-1)\times\alpha}{m-1}\right] \quad (3.\ 6)$$

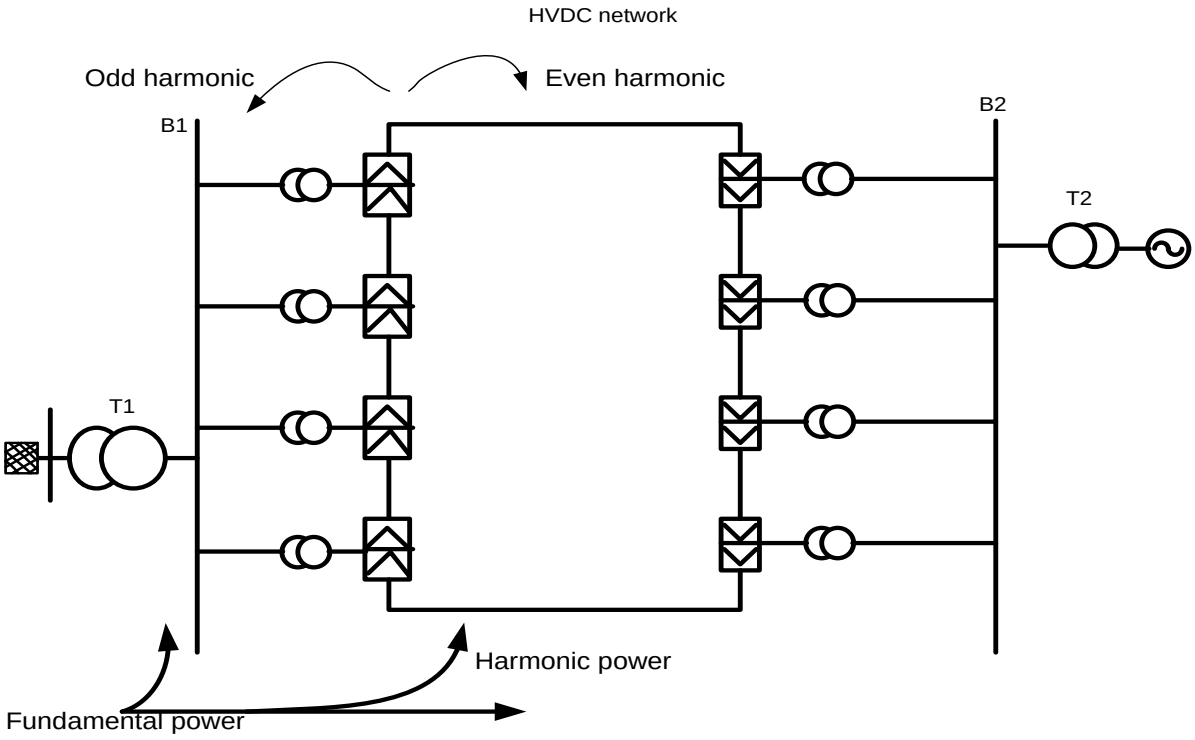

Figure 3. 1: Representation of a Bipolar Converter as a Source of Harmonic Generation

Equations 3.5 and 3.6 show that a converter can be considered as a harmonic current source when seeing from the AC side, while it is a harmonic voltage source on the DC side. The even voltage harmonics get fed into the DC bus and the odd current harmonics go into the supply source. The harmonics fed into the supply system propagate into the power system. The harmonics fed to the DC bus circuit have an adverse effect on the DC line, but are, generally, localized to the line to which these connect. There is harmonic power associated with harmonic currents, which is a function of relative system impedances and load side impedance. Figure 3.1 shows this action of the converter (Kimbark, 1971).

3.10 Three-Phase Bridge Circuit

A three-phase bridge has two forms: half-controlled, and fully controlled. A three-phase full-wave converter consists of six thyristor switches. The output DC voltage is controlled by varying the firing angle α. With a large output reactor the output DC current is continuous and the input current is a rectangular pulse of $2\pi/3$ duration and amplitude I_{dc} . The average DC voltage is:

$$E_{dc} = 2\left[\frac{3}{2\pi}\int_{\frac{-\pi}{3}+\alpha}^{\frac{\pi}{3}+\alpha} E_m \cos(\omega t)d\omega t\right] = \frac{3\sqrt{3}}{\pi}E_m \cos(\alpha) \quad (3.\ 7)$$

At α= 90°, the output voltage is zero. For 0° < α < 90°, E_{dc} is positive and power flows will be from rectifier to the inverter. For 90° < α < 180°, E_{dc} is negative and the converter operates in the inversion mode. The power factor is lagging for rectifier operation and leading for inverter operation. Under these conditions, the phase currents consist of periodic positive rectangular pulses of width $\omega c = 2\pi/p$.
Where: p is the period.

The corresponding Fourier series for the positive current pulses is:

$$F_p = \frac{2}{\pi}\begin{bmatrix} \frac{\omega}{4}+\sin\left(\frac{\omega}{2}\right)\cos(\omega t)+\frac{1}{2}\sin\left(\frac{2\omega}{2}\right)\cos(2\omega t) \\ +\frac{1}{3}sin\left(\frac{3\omega}{2}\right)cos(3\omega t)+\frac{1}{4}sin\left(\frac{4\omega}{2}\right)cos(4\omega t)+\cdots \end{bmatrix} \quad (3.\ 8)$$

An ideal *p*-phase, two-way converter produces positive and negative current pulses. Applying equations to the negative group gives the following Fourier series:

$$F_n = \frac{2}{\pi}\begin{bmatrix} \frac{-\omega}{4}+\sin\left(\frac{\omega}{2}\right)\cos(\omega t)-\frac{1}{2}\sin\left(\frac{2\omega}{2}\right)\cos(2\omega t) \\ +\frac{1}{3}sin\left(\frac{3\omega}{2}\right)cos(3\omega t)-\frac{1}{4}sin\left(\frac{4\omega}{2}\right)cos(4\omega t)+\cdots \end{bmatrix} \quad (3.\ 9)$$

The phase current of the two-way configuration consists of alternate positive and negative pulses such that $F(\omega t + \pi) = -F(wt)$.

Its Fourier series is obtained by summing the last two equations 3.8 and 3.9.

$$F = F_p + F_n = \frac{4}{\pi}\begin{bmatrix} \sin\left(\frac{\omega}{2}\right)\cos(\omega t)+\frac{1}{3}\sin\left(\frac{3\omega}{2}\right)\cos(3\omega t) \\ +\frac{1}{5}sin\left(\frac{5\omega}{2}\right)cos(5\omega t)+\cdots \end{bmatrix} \quad (3.\ 10)$$

From equation 3.10, it is noticed that the DC component and even order harmonics have been eliminated. For the square wave of $\omega = \pi$ which on substituting into equation 3.10 produces an equation 3.11, which does have a waveform in the frequency domain.

$$F(\omega t) = \frac{4}{\pi}\begin{bmatrix} cos(\omega t)-\frac{1}{3}cos(3\omega t)+ \\ +\frac{1}{5}cos(5\omega t)-\frac{1}{7}\cos(7\omega t)+\cdots \end{bmatrix} \quad (3.\ 11)$$

In which harmonics of orders n = 1, 5, 9, etc. are of positive sequence, while those of order n = 3, 7, 11, etc. are of negative sequence.

3.11 Effects of Converter Transformers Connections

3.11.1 Basic six-pulse configuration (with star-star transformer connection)

Six-pulse rectification, and inversion, is obtained from three-phase two-way configurations. Substituting $\omega = 2\pi/3$ in the general equation and inserting the actual DC current I_{dc}, the frequency domain representation of the AC current in phase "a" as an example, is

$$i_a(t) = \frac{2\sqrt{3}}{\pi} I_{dc} \begin{bmatrix} cos(\omega t) - \frac{1}{5} cos(5\omega t) + \frac{1}{7}\cos(7\omega t) \\ -\frac{1}{11} cos(11\omega t) + \frac{1}{13}\cos(13\omega t) - \cdots + \cdots \end{bmatrix} \quad (3.\ 12)$$

Some useful observations can now be made from last equation:

i) The absence of the triplen harmonics.

ii) The presence of odd harmonics of orders $6k \pm 1$ for integer values of k.

iii) Those harmonics of orders $6k + 1$ are of positive sequence and those harmonics of orders $6k - 1$ are of negative sequence.

3.11.2 Basic six-pulse configuration (with the effect of a delta-star transformer connection)

If either the primary or secondary three-phase windings of the converter transformer are connected in delta, the AC side current waveforms consist of the instantaneous differences between two rectangular secondary currents 120° apart. The time-domain representation of a six-pulse output voltage waveform is shown in Figure 3.2. The Fourier series of this waveform can be easily obtained from the general equation by superimposing the results of two component pulses of widths π and $\pi/3$, respectively. Moreover, to maintain the same primary and secondary voltages as for the star-star connection, a factor of $\sqrt{3}$ is introduced in the transformer ratio. The resulting Fourier series for the primary side current in phase "a" is:

$$i_a(t) = \frac{2\sqrt{3}}{\pi} I_{dc} \begin{bmatrix} cos(\omega t) + \frac{1}{5} cos(5\omega t) - \frac{1}{7} cos(7\omega t) \\ -\frac{1}{11} cos(11\omega t) + \frac{1}{13} cos(13\omega t) \ldots \end{bmatrix} \quad (3.\ 13)$$

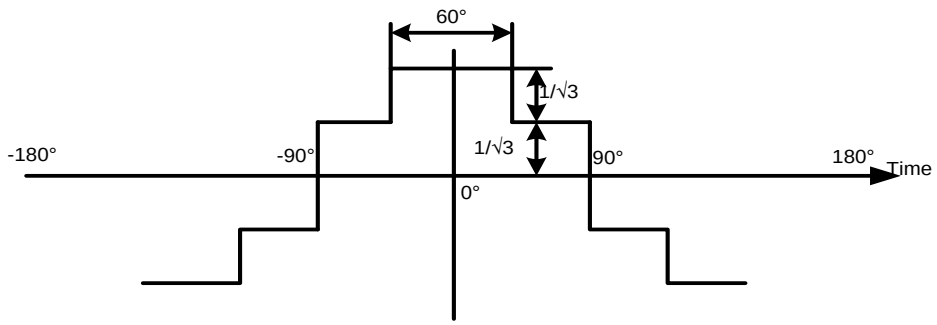

Figure 3. 2: Time-domain Representation of a Six-pulse Output Voltage Waveform

This series only differs from that of a star-star connected transformers equation 3.12 by the sign of harmonic orders $6k \pm 1$ for odd values of k, i.e. the 5th, 7th, 17th, 19th, etc..., (Allard & Forrest, 2004).

3.11.3 Twelve-pulse related harmonics

Twelve-pulse configurations as used in bipolar HVDC system consist of two six-pulse groups fed from two sets of three-phase transformers in parallel, with their fundamental voltages equal and phase shifted by 30°. A common 12-pulse configuration is shown in figure 3.3. Moreover, to maintain 12-pulse operation, the two six-pulse groups must operate with the same control angle and therefore the fundamental frequency currents on the AC side of the two transformers are in phase. The resultant AC current is given by the sum of the two Fourier series of the star-star and delta-star transformers equations 3.12 and 3.13, respectively, which results in equation 3.14.

$$(i_a)_{12} = 2\left(\frac{2\sqrt{3}}{\pi}\right) \times I_{dc} \times \begin{bmatrix} cos(\omega t) - \frac{1}{11} cos(11\omega t) + \frac{1}{13}\cos(13\omega t) \\ -\frac{1}{23} cos(23\omega t) + \frac{1}{25}\cos(25\omega t) \ldots \end{bmatrix} \quad (3.\ 14)$$

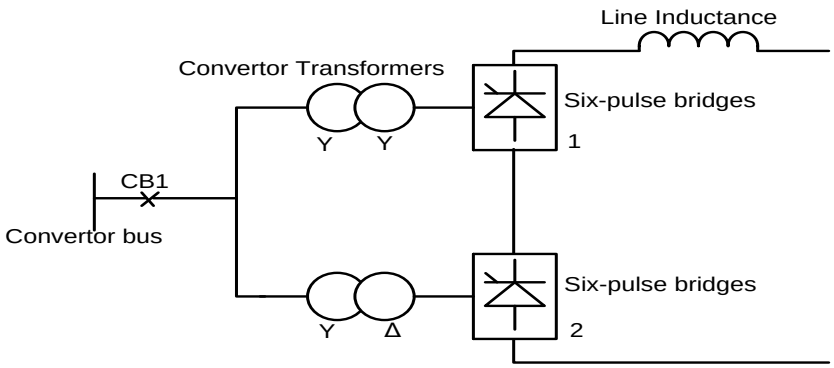

Figure 3. 3: Twelve-pulse Converter Configuration Y-Y and Y-D transformers

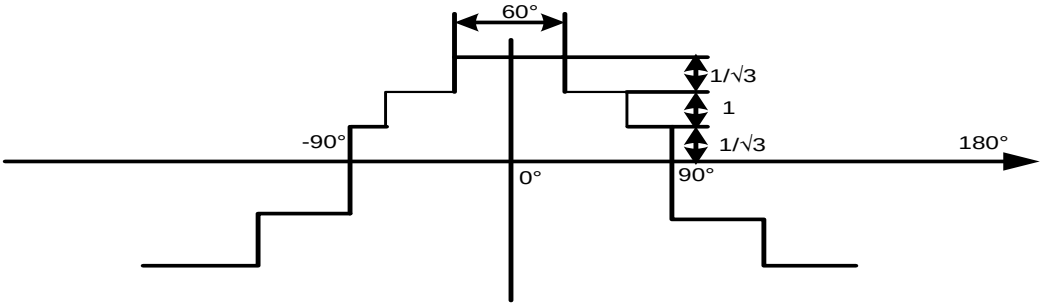

Figure 3. 4: Time-domain Representation of a twelve-pulse Phase Current

This series of equation 3.14 only contains harmonics of order $12k \pm 1$. The harmonic currents of orders $6k \pm 1$, with k odd values 5, 7, 17, 19, etc., circulate between the two converter transformers but do not penetrate the AC network. The time-domain representation of the 12-pulse waveform is shown in Figure 3.4.

As the use of two transformers with a 30° phase-shift produces 12-pulse operation, the addition of further appropriately shifted transformers in parallel provides the basis for increasing pulse configurations. For instance, 24-pulse operation is achieved by means of four transformers with 15° phase-shifts, and 48-pulse operation requires eight transformers with 7.5° phase shifts. Although theoretically possible, pulse numbers above 48 are rarely justified due to the practical levels of distortion found in the supply voltage waveforms, which can have as much influence on the voltage crossings as the theoretical phase-shifts.

Similar to the case of the 12-pulse connection, the alternative phase-shifts involved in higher pulse configurations require the use of appropriate factors in the parallel transformer ratios to achieve common fundamental frequency voltages on their primary and secondary sides. The theoretical harmonic currents are related to the pulse number (p) by the general

expression $pk \pm 1$, and their magnitudes decrease in inverse proportion to the harmonic order. Generally harmonics above the 49th can be neglected as their amplitude is too small.

3.12 Guidelines for Equipment Application and Harmonic Control

Power system problems that were associated with harmonics began to be of general concern in the 1970s, when two independent developments took place. The first was the oil embargo, which led to price increases in electricity and the move to save energy. Industrial power consumers and utilities began to apply power factor improvement capacitors. Capacitors reduce MVA demand from the utility grid systems by supplying the reactive power portion of the load locally. As a result, losses are reduced in the industrial plant and the utility network.

The second involved the coming of power electronics devices made of diodes, thyristors, etc. when converter rectifiers and inverters were developed; harmonic mitigation techniques had to be employed. The increase in use of these power electronic devices and of power factor corrector capacitor banks could create a problem like amplification in current due to resonance. Because of these problems, analytical techniques and guidelines for equipment application has been developed, called IEEE 519 standard. American standards regarding harmonics have been laid out by the IEEE in the 519 Standard: "*IEEE Recommended Practices and Requirements for Harmonic Control in Electric Power Systems"*.

The purpose of IEEE 519 is to recommend limits on harmonic distortion according to two distinct criteria, namely:

- There is a limitation on the amount of harmonic current that a consumer can inject into a utility network.
- A limitation is placed on the level of harmonic voltage that a utility can supply to a consumer.

3.12.1 Guidelines for Individual Customers

The primary limit on individual customers is the amount of harmonic current that they can inject into the utility network. The relative size of the load with respect to the source is defined as the short circuit ratio (SCR), at the point of common coupling (PCC), which is where the consumer's load connects to other loads in the power system. The consumer's size is defined by the total fundamental frequency current in the load I_L, which includes all

linear and nonlinear loads. The size of the supply system is defined by the level of short circuit current (I_{SC}), at the PCC. These two currents define the SCR:

$$SCR = \frac{short\ circuit\ MVA}{load\ MW} = \frac{I_{sc}}{I_L} \quad (3.\ 15)$$

Table 3.1 identifies harmonic distortion levels and its relationship to SCR. All of the current distortion values are in terms of relative maximum demand load current. The total distortion is in terms of total demand distortion (TDD) instead of the more common THD term.

Table 3.1 shows current limits for individual harmonic components as well as harmonic distortion. For example a consumer with a SCR less than 50 has a recommended limit of 2.5% for TDD, while for individual odd harmonic components with orders less than 11, the limit on each is 2%.

Table 3. 1: IEEE 519 current distortion limits. For conditions lasting more than one hour (shorter periods increase limit by 50%)

Harmonic current limits for Non-Linear Load at the Point of Common Coupling with other Loads, for voltages >161kV						
Maximum odd harmonic Current Distortion in % of Fundendamental Harmonic Order						
Isc/IL	HD= IH/I1					TDD
	<11	<17	17<23	23<35	35	
<50	2.0	1.0	0.75	0.30	0.15	2.50
*50	3.0	1.5	1.15	0.45	0.22	3.75
Even harmonics are limited to 25% of the odd harmonic limits above: * All Power Generation equipment are limited to these values of current distortion, regardless of their actual Isc/IL where: Isc = Maximum short circuit current at Point of Common Coupling ISL= Maximum Demand Load Current (Fundamental Frequency) at Point of Common Coupling TDD= Total Demand Distortion (RSS) in % of Maximum Demand						

It is important to note that the individual harmonic current components do not add up directly so that all characteristic harmonics cannot be at their individual maximum limit without exceeding the TDD.

3.12.2 Guidelines for Utilities

The second set of criteria established by IEEE 519 is for voltage distortion limits. This governs the amount of voltage distortion that is acceptable in the utility supply voltage at the PCC with a consumer. The harmonic voltage limits recommended are based on levels that are low enough to ensure that consumers' equipment will operate satisfactorily. Table 3.2 lists the harmonic voltage distortion limits from IEEE 519.

Table 3. 2: Voltage distortion limits from IEEE 519. For conditions lasting more than one hour (shorter periods increase limit by 50%)

Bus Voltage at PCC	Individual Voltage Distortion (%)	Total Voltage Distotion THD(%)
Below 69kV	3.0	5.0
69kV to 137.9kV	1.5	2.5
138kV and above	1.0	1.5
Note: High Voltage system can have up to 2% THD where the cause is an High Voltage DC (HVDC) terminal, that will be attenuate by the time it is tapped by the user.		

Similarly to current, limits for voltages are imposed on individual components and on total distortion from all harmonic voltages combined (THD). What is different in this table, however, is that three different limits are shown. They represent three voltage classes, below 69kV up to 69 kV, 69 to 137.8 kV, and equal to or greater than 138 kV. Note that the limits decrease as voltage increases, the same as for current limits. The total voltage distortion is calculated using equation 3.16.

$$THD_v = \frac{\sqrt{\sum_{h\neq 1} {U_h}^2}}{U_1} \qquad (3.\ 16)$$

This total harmonic distortion is obtained from formula 3.16. Power system is comprises of impedances but once there is harmonic distortion in the system they will change because, they are frequency dependant. Therefore, harmonic impedances of the power system interact with harmonic currents resulting in the generation of harmonic voltages. According to IEEE 519 the harmonic distortion limits reduce as the system voltage increases. The individual harmonic distortion is determined using formula 3.17, which is the ratio of individual voltage harmonic distortion over the fundamental voltage.

$$U_{harm\ distortion} = \frac{U_h}{U_1} \qquad (3.\ 17)$$

Table 3.2 is for odd harmonic limits. The generation of even harmonics is more restricted since the resulting DC offset can cause saturation in motors and transformers. Negative sequence current can cause heating in generators.

Individual even harmonic voltage is limited to 25% of the odd harmonic limits, the same limit as currents. Often utility feeders supply more than one consumer. The voltage distortion limits shown in the table should not be exceeded as long as all consumers conform to the current injection limits. Any consumer who degrades the voltage at the PCC should take steps to correct the problem. Therefore, a PCC is a bus where the secondary side of the utility transformer is connected to and similarly, varieties of consumers as well.

Chapter Four:

4 Effectiveness of Harmonic Mitigation Techniques on a Bipolar HVDC System

This chapter presents a developed flowchart that shows how to assess the effectiveness of the AC harmonic mitigation techniques typically used on a bipolar HVDC system using new evaluation indices. It involves the design of a system that utilizes a special configuration of converter transformers, filters and a control system to control the converter switching angle. Knowing that converters do need reactive power for their proper operation, a selection of a proper switching angle will go a long way to prevent a high reactive power from being consumed by the rectifier and inverter converters under normal conditions. The selection of a delay angle within the range of 7° to 15° normally ensures an effective system operation, which will minimize harmonic perturbation.

4.1 Harmonic Analysis in HVDC Bipolar Systems

The semiconductor devices in a HVDC converter station operate as non-linear loads causing current harmonics to be generated. They are mainly characteristic harmonic currents and are injected into the HVAC power system when the HVDC system is running even though the supply voltage waveform on AC side is virtually a sinusoidal wave at fundamental frequency.

Harmonic components should be reduced as much as possible as their presence can lead to low system efficiency, a poor power factor and affect the reactive power delivered from the HVAC system. To reduce these effects, design techniques need to be used to mitigate harmonic distortion. This chapter reviews the designs of the various mitigations techniques that are used and which can effectively reduce these harmonics below admissible internationally recognised limits provided by standards.

4.2 Bipolar HVDC Network

The model of a bipolar HVDC is shown in figure 4.1 with different blocks (A, B, C, D and E) showing the main parts constituting a typical bipolar HVDC network. Blocks A being filters on the AC side. Blocks B are converter transformers on the rectifier and inverter sides. Blocks C and E are rectifiers and inverters, respectively. Block D is the control system. Calculated parameters for this BPHVDC are found in appendix B (in table B.1) and appendix C (in table C.1).

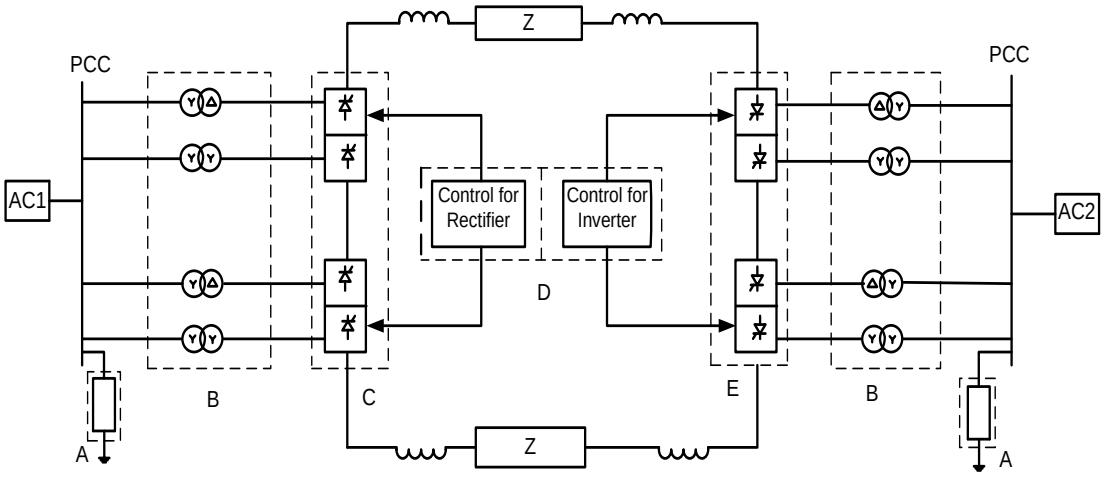

Figure 4. 1: Bipolar HVDC system

4.3 Harmonic Mitigating Technique using a special Converter Transformer Configurations (Block B)

Harmonics within a power system are defined as the variation of the voltage or current as an integer multiple of the fundamental frequency (ALSTOM, 2010). Excessive current harmonics result in voltage distortion, additional losses, overheating, and harmonic interference, and must therefore be limited. The 12 pulse LCC converter operates as a source of current harmonics on the AC side, and as a source of voltage harmonics on the DC side. The presence of harmonic distortion is an issue for power quality and can have serious consequences on connected equipment. By designing a system using a special converter transformer configuration the impact of harmonics on the HVAC network can be substantially reduced (Block B).

4.3.1 Power system harmonic sequence components

In order to explain the harmonic interaction phenomena introduced by Current Source Converter (CSC) schemes, it is important to introduce the concept of harmonic sequence components.

On the basis of inspection, (Wakileh, 2001) describes the individual harmonic components of balanced three phase power systems to be entirely of positive, negative, or zero sequences by using, for example, the Fourier representation of phase voltages:

$$V_a(t) = V_1 cos(\omega_0 t) + V_2 cos(2\omega_0 t) + V_3 cos(3\omega_0 t) + \cdots \quad (4.\ 1)$$

$$V_b(t) = V_1 cos(\omega_0 t - 120^\circ) + V_2 cos(2\omega_0 t - 240^\circ) + V_3 cos(3\omega_0 t - 360^\circ) + \cdots$$
$$= V_1 cos(\omega_0 t - 120^\circ) + V_2 cos(2\omega_0 t + 120^\circ) + V_3 cos(3\omega_0 t) + \cdots; \quad (4.\ 2)$$

$$V_c(t) = V_1 cos(\omega_0 t + 120^\circ) + V_2 cos(2\omega_0 t + 240^\circ) + V_3 cos(3\omega_0 t + 360^\circ) + \cdots$$
$$= V_1 \cos(\omega_0 t + 120^\circ) + V_2 \cos(2\omega_0 t - 120^\circ) + V_3 \cos(3\omega_0 t) + \cdots; \quad (4.\ 3)$$

It can be seen from the phase rotation of these quantities that the 1st, 4th, 7th, etc., harmonic orders are positive phase sequence (a, b, c), the 2nd, 5th, 8th, etc. harmonic orders are negative phase sequence (a, c, b) and the 3rd, 6th, 9th, etc. harmonic orders are zero phase sequence harmonic orders (Arrillaga & Watson, 2003). It is also accepted that zero sequence harmonics disappear in line voltages and that triplen harmonics cannot flow into a delta connection or if there is an absence of a ground connection (Wakileh, 2001).

4.3.2 Functions of the HVDC Converter Transformer

The converter transformers (Block B) transform the voltage of the AC busbar to the required entry voltage of the converter. The 12 pulse converter requires two 3 phase systems which are spaced apart from each other by 30° or 150° (electrical degrees). This is achieved by installing a transformer on each network side using the vector groups Yy0 and Yd5. At the same time, they ensure the voltage insulation necessary in order to make it possible to connect converter bridges in series on the DC side, as is necessary for HVDC technology. The transformer main insulation, therefore, is stressed by both the AC voltage and the direct voltage (DC) potential between valve-side winding and ground. The converter transformers are equipped with on-load tap-changers in order to provide the correct valve voltage (Siemens, 2011). The power rating is obtained using the formulas below:

$$S_{Transfo\ Rec(6-pulse)} = \sqrt{2} \times I_{dN-Rec} \times U_{sec-Rec} \quad (4.\ 4)$$

$$S_{Transfo\ Inv(6-pulse)} = \sqrt{2} \times I_{dN-Inv} \times U_{Sec-Inv} \quad (4.\ 5)$$

Where:

I_{dNRec} = Nominal DC current of rectifier.

U_{SecRec} = Transformer voltage valve side (rectifier).

I_{dNInv} = Nominal DC current

U_{SecInv} = Transformer voltage valve side (Inverter).

Figure 4. 2: A typical HVDC system converter transformer **(Siemens, 2011)**

4.3.3 Twelve Pulse Group and Converter Transformer

HVDC converters are usually built as 12-pulse circuits. This is a serial connection of two fully controlled 6 pulse converter bridges and the design technique used to help reduce the effects of harmonics, is to use two 3 phase systems which are spaced apart from each other by 30° electrical degrees. The effect of phase difference is to cancel out the 6 pulse harmonics on the AC and DC side. This coupling connection is shown in figure 4.3 as presented above in Block B of figure 4.1.

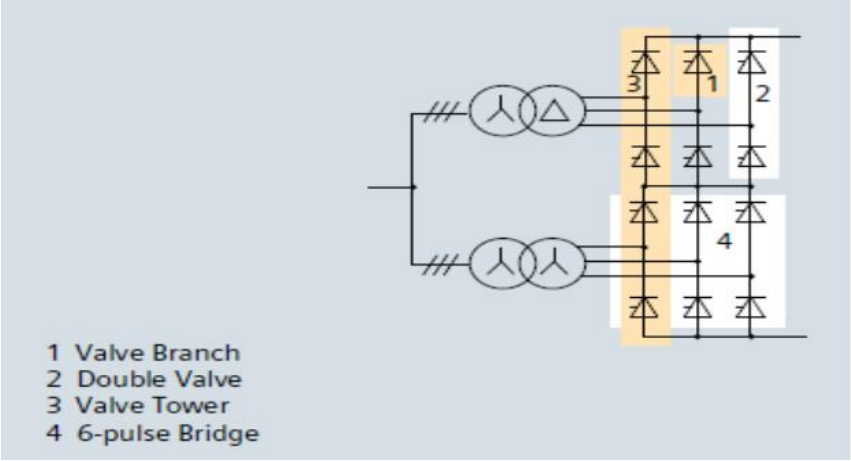

Figure 4. 3: Arrangement of the valve branches in a 12 pulse bridge **(Siemens, 2011)**

The two 6 pulse bridges that make up the 12 pulse converter are connected to a Y-Y and a Y-Δ transformer, respectively. As a result, the AC voltage supplied to each bridge has a 30° phase shift, as illustrated in Figure 4.4. Each bridge has a ripple component that is six times the fundamental frequency, and so by connecting the bridges in series, the DC side ripple component is reduced when operating as a 12-pulse system.

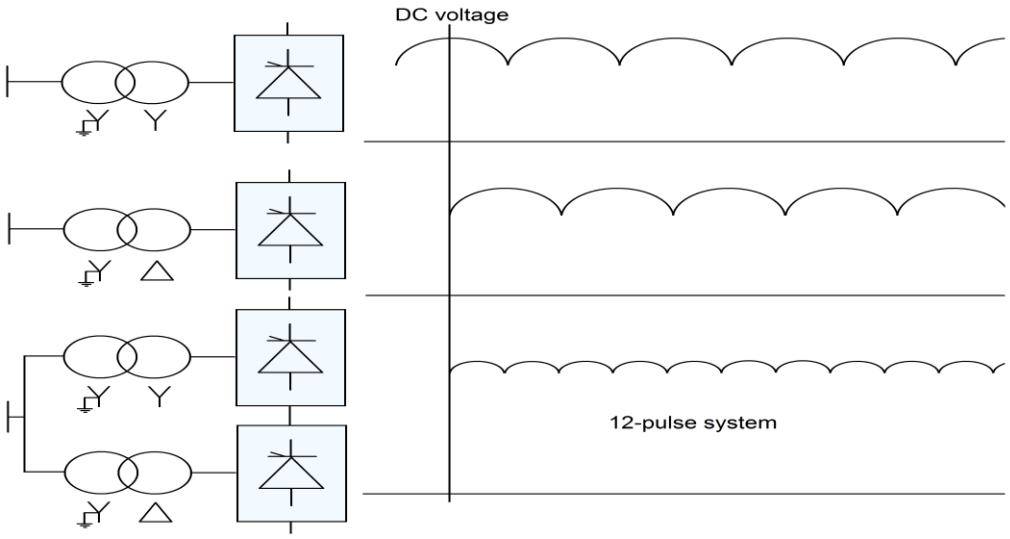

Figure 4. 4: DC voltage waveform with harmonic disturbance **(Kim et al., 2009)**

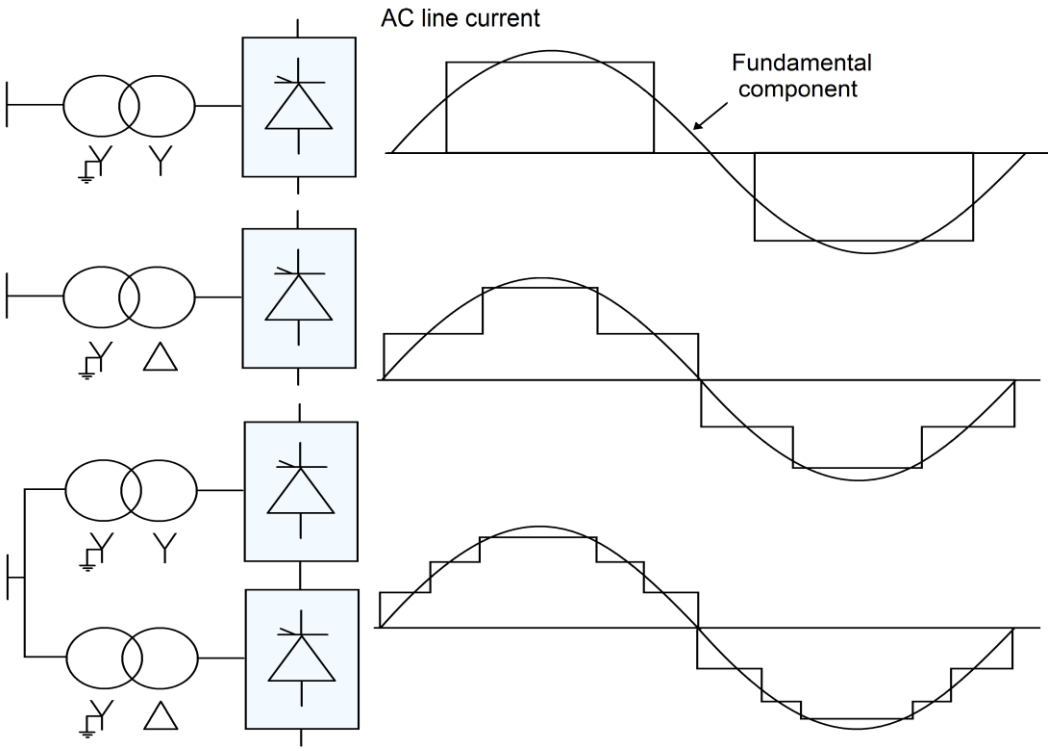

Figure 4. 5: AC current waveform with harmonic disturbance **(Kim et al., 2009)**

Figure 4.5 illustrates the AC phase current supplied to the converter by the HVAC network. The current has fundamental and harmonic components in its waveform. Individually, the waveform of the Y-Y connected transformer is rectangular, while a more stepwise waveform is obtained for the Y-Δ transformer. When combined, the design technique used results in a resultant waveform that approaches a sine wave, demonstrating the reduction of harmonic components.

4.3.4 Mitigation Effectiveness of Converter transformers

The total AC current of the 12 pulse converter is thus the sum of the two 6 pulse currents (Kim et al., 2009). Characteristic harmonics are related to the pulse number (*p*) of the converters, and are of the order of *pk* ± 1 for the AC side and in the order of *pk* for the DC side, where *k* is any integer. There is elimination in harmonics lower than the 11^{th} and 12^{th} harmonics when converter transformers are connected in star delta (Y-Δ) and star to star (Y-Y) connection on AC side. This technique is effective as it eliminates harmonics of lesser than 11^{th} harmonic. It thus results in harmonics on the AC side in the order of 11^{th}, 13^{th}, 23^{rd}, 25^{th} so on, and harmonics in the order of 12^{th}, 24^{th}, etc. on the DC side (ALSTOM, 2010). The effectiveness of these transformers will be demonstrated in case studies.

4.3.5 Evaluation Index to Assess Effectiveness of Converter Transformer Design Technique

Analytic expressions are introduced to describe the best way to assess the effectiveness of the converter transformer mitigation technique and this is done by looking at the change in $\%THDV_{AC-primRect}$ or $\%THDV_{AC-primInv}$ indices, when varied them.

With "*prim*" being the primary side of the converter transformer. These limits apply at PCC which is a common bus for rectifier and inverter on the AC side; for a rectifier on the AC1 side and AC2 side on the inverter side at the AC buses. This will show how the PCC on the AC bus voltages have been operating. Formulas 4.6 and 4.8 are introduced for this purpose. Their admissible indices in per unit voltage are given by equation 4.7 and 4.9, respectively.

$$\%THDV_{AC-primRect} = \frac{\sqrt{\sum {U_h}^2}}{U_1} \times 100\% \qquad (4.\ 6)$$

Where "*h"* are BPHVDC PCC characteristics, namely h= 1st, 11th, 13th, 23rd, 25th, etc.
Within the $U_{(1)}$ range:

$$0.95U_{(1)AC-primRect} \leq 1.0U_{(1)AC-primRect} \geq 1.05U_{(1)AC-primRect} \quad (4.\ 7)$$

Where $U_{(1)AC-primRect}$ is a fundamental frequency of the AC voltages at PCC on the rectifier sides, in kV.

Similarly,

$$\%THDV_{AC-primInv} = \frac{\sqrt{\sum {U_h}^2}}{U_1} \times 100\% \quad (4.\ 8)$$

Where "*h"* are BPHVDC PCC characteristics, namely h = 1st, 11th, 13th, 23rd, 25th, etc.

Within the range:

$$0.95U_{(1)AC-primInv} \leq 1.0U_{(1)AC-primInv} \geq 1.05U_{(1)AC-primInv} \quad (4.\ 9)$$

Where $U_{(1)AC-primInv}$ is a fundamental of the AC voltages at PCC on the inverter side, in kV.

The PCC voltage $U_{(1)AC-primRect/inv}$ can vary over the range of 0.95 and 1.05 and still be admissible. This is when BPHVDC is operating as per figure 4.1 that is when power is transferred from AC1 side to AC2 side. If power transfer is changed the formulas are still applicable.

It shows that any rectifier or inverter with lesser than 0.95 or higher 1.05 per unit voltage level will be a violation to these equations 4.7 and 4.9. Thereafter, these $\%THD_V$ at PCC results, are to be compared to IEEE 519 standard to analyse how effective they are as mitigation techniques over the defined operating range.

4.4 Harmonic Mitigation Techniques with Filters

4.4.1 AC Harmonic Filter

An AC harmonic filter reduces the amplitude of one or more fixed frequency harmonic currents and voltages. Generally, they consist of one or more L-C tuned circuits. R-L-C filters circuits constitute a special type of damped harmonic filters, where “R” influences the damping effect. These filters, in addition to filtering the harmonic currents or voltages, can also reduce either overshoot or rate of rise of a transient current or voltage.
By definition, a filter (F) is a function of several parameters (Acha & Madriga, 2001) as shown in equation 4.10 below:

$$F = f[Z_s;\ X_t;\ I_h;\ C_f;\ P_d;\ Q_t] \quad (4.\ 10)$$

Where:
Z_s = system impedance
X_t = converter transformer reactance
I_h = harmonic current at harmonic h
C_f = filter capacitor
Q_t = total reactive power demanded of converter
P_d = active power transmitted by converter

The design and role of the AC harmonic filter (Block A) is an integral and important part of BPHVDC converter station operation. The AC filter constitutes about 15% (Manitoba, 1988) of the total cost of the converter station. The AC harmonic filter at a BPHVDC converter station, as shown in figure 4.6, is another design technique and serves to reduce the generated level of AC harmonics which are injected into the HVAC system by block B converter transformers. In addition its capacitors assist in providing the reactive power required by the converter on both sides of the BPHVDC system.

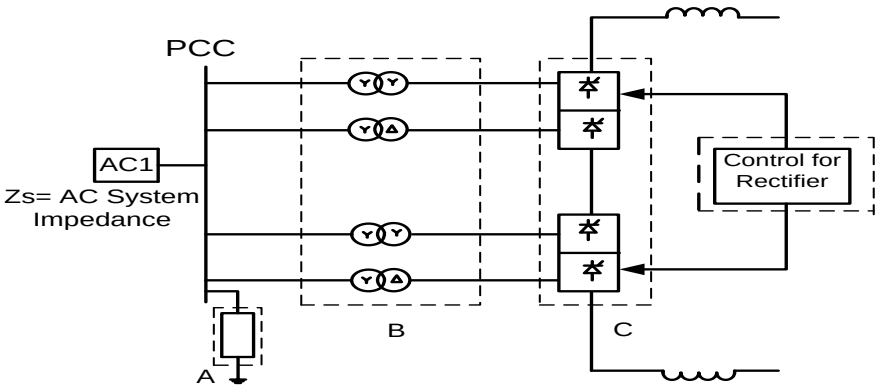

Figure 4. 6 : AC filter shown in block "A"

Figure 4. 7: A typical AC harmonic filtering system **(ALSTOM, 2010)**

The filters are designed with branches and each filter branch can have one to three tuning frequencies. Figure 4.8 shows different harmonic filter types with their impedance frequency characteristics.

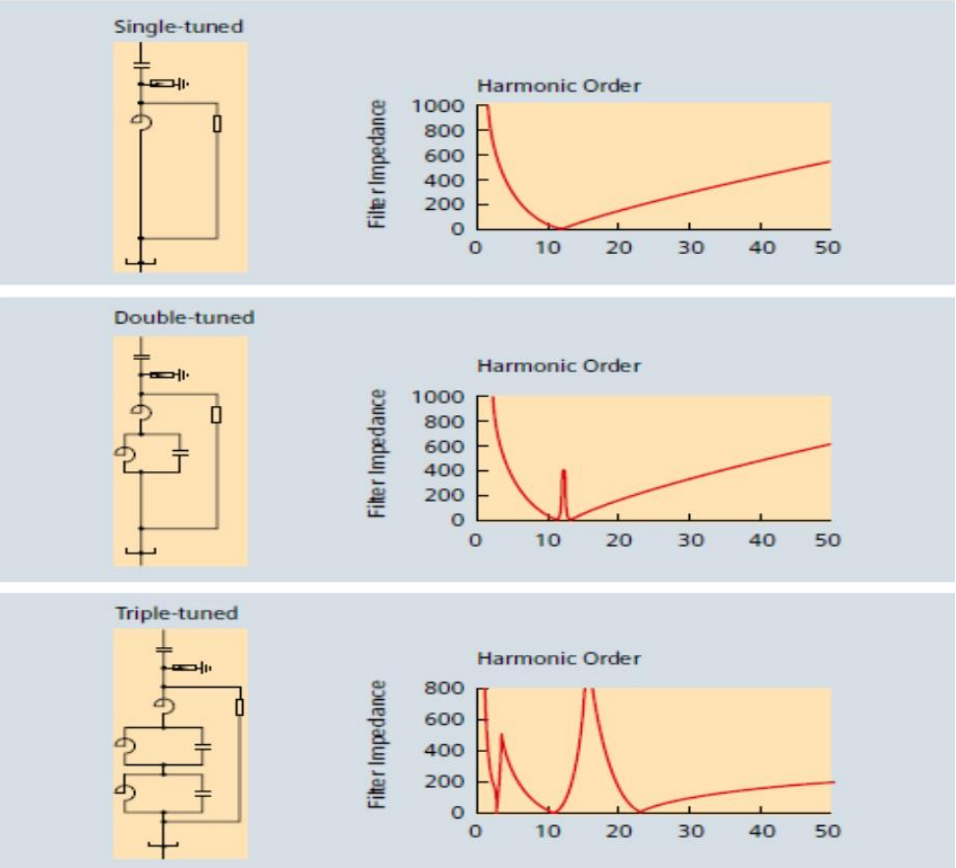

Figure 4. 8: Different harmonic filters types **(ALSTOM, 2010)**

4.4.2 Effectiveness of Mitigating Harmonics using Filters

When rectifiers and inverters are in operation, this will result in both the generation of AC current harmonics and the absorption of reactive power. In order to limit the impact of these AC harmonic currents and absorbed reactive power, the rectifier and inverter have shunt connected switchable AC harmonic filters as shown in Figure 4.6 in “block A”, which are directly connected to the rectifier and inverter buses on either side.

Tuned filters or band-pass filters are utilized to mitigate harmonic frequencies. These filters are used in order to remove the 11th and 13th harmonics. High-pass filters offer low impedance over a broad band of harmonic frequencies in order to reduce harmonics to an acceptable level, which produces a damped characteristic at frequencies above the tuning frequency (ALSTOM, 2010). More information about the design of such filters which are typically used in a bipolar HVDC system is found in Appendix D. How effective these filters are will be demonstrated in case studies.

4.4.3 Evaluation Index to Assess Effectiveness of AC filters

Similar analytical expressions (formulas 4.6 and 4.8) are used to assess the effectiveness of the mitigation technique for the filters within the defined PCC range of U_1 operation. However, the $\%THD$ change in this case is evaluated using formulas 4.6 and 4.8. It serves to assess how effective these filters are in mitigating AC harmonics at the measured PCC AC bus when looking at their $\%THDV_{ac-primRec}$ or $\%THDV_{ac-primInv}$ indices. Thereafter, these $\%THD$ results are to be compared to IEEE 519 standard to analyse how effective these mitigation techniques were.

4.5 Harmonic Mitigation Technique with Control Philosophy (Block D)

The main objectives for the implementation of a HVDC control system philosophy are for reliable energy transmission resulting in highly efficient and flexible energy flow that responds to sudden changes in demand thus contributing to network stability (Siemens, 2011).

4.5.1 Control of Power Transmission

The bipolar HVDC control system is responsible for firing the thyristor valves so that the requested power is transmitted. There is a controller on each side of the DC transmission link, and each has to fulfil different tasks. The controller on the rectifier side controls the DC current so that the requested power is achieved. The controller on the inverter side controls the DC voltage so that the rated DC voltage is achieved (figure 4.9).

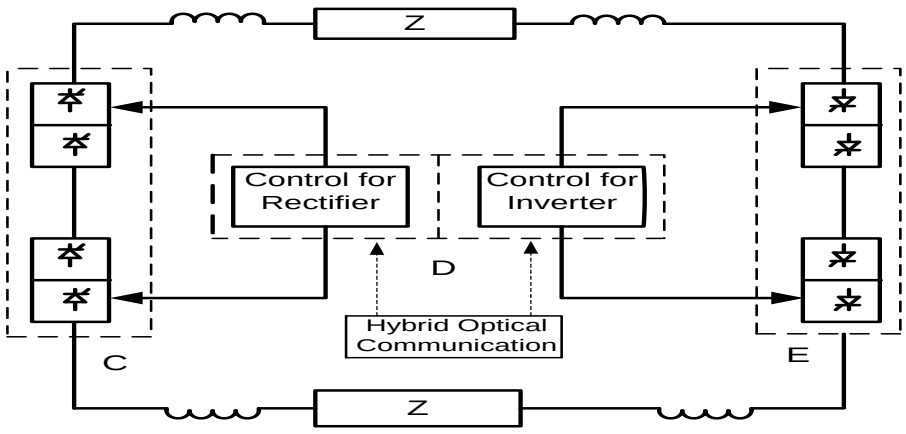

Figure 4. 9: HVDC Control scheme

4.5.2 Real and reactive power control schemes

The assumption that the harmonics do not propagate through the controller is particularly applicable to control schemes which regulate real or reactive power since these quantities are predominantly a function of fundamental frequency quantities. The limited bandwidth of metering transducers and the requirement that both harmonic voltage and current must be present at the same harmonic to generate real or reactive power, make the assumption of harmonic isolation fair in all but the most distorted systems. Given this assumption fundamental frequency real or reactive control schemes can be implemented entirely within the power flow solution.

4.5.3 Voltage and current control schemes

While voltage and current quantities are often more distorted than power quantities it is sometimes useful to make the somewhat questionable assumption that these quantities can be isolated from the harmonic solution. This is done primarily because incorporating harmonic propagation through the controller requires significantly more computational effort.
For phase angle control schemes, the power flow mismatches, state that the positive sequence voltage at the PCC (or current through the converter) must equate to the corresponding voltage (or current) order.

4.5.4 Determination of Control Topology for Bipolar HVDC

The selection of operational sequences of the switching devices is the prime consideration for any controlling topology on bipolar HVDC. For maximum power transfer and balanced system operation it is required to determine the exact values of delay angle, advance angle and extinction angle for both converter rectifier and inverter. The control strategy should be defined in such a way that both the converter rectifier and inverter operate at constant current mode. The extinction angle of the inverter is also maintained constant which is called constant extinction angle (CEA) mode (Roy & Amin, 2014). The control strategy is illustrated in figure 4.9 with block D. The converter characteristic is composed of two control modes which are minimum delay angle and constant current (Stan et al., 2011). The minimum delay angle is maintained within a range of 15° to 45° for firing of the switching devices at a minimum threshold voltage (Zhang et al., 2010), (Stan et al., 2011) . Similarly the inverter characteristic is composed of two modes which are minimum extinction angle and constant current.

The operating point for the DC link is defined by the crossover point of the two characteristics (Rashid, 2001). In order to avoid cross over and ensure safe operation of the HVDC link, the rectifier current is kept at a slightly higher value than the inverter current. The overlap angle of the inverter is retained within a range of 1° to 3° so that no cross over occurs between operational characteristics of the rectifier and inverter (Agneholm et al., 2008). Generally a current margin of about 10% is maintained between the rectifier and inverter current. The selection of current margin is an important consideration for the controlling topology (Rahimi et al., 2006). The current margin should be selected in such a way that the current modes of converter and inverter do not impose on each other so that harmonics cannot cause perturbation on the system. The advantage of having a large current margin is the shift of control point of the converter which increases the converter current to about 5% to 10% of its rated value as well as the decrement of converter voltage of about 7% to 10% of its rated value (Jieqiu et al., 2011). The controlling of DC current in any HVDC link is managed by either varying DC voltage or AC voltage which is termed as the voltage dependant current limit (VDCL) (Roy & Amin, 2014). In order to retain the conduction voltage of the switching devices above the threshold value, the DC current, I_d must be retained to minimum current limit of 20% to 30% of its rated value (Rashid, 2001), (Stan et al., 2011).

There is a possibility of sign change of current margin when the inverter current becomes slightly higher than the rectifier current which may cause power reversal in the HVDC link. This causes severe unbalance in the system due to effect of harmonics on the DC current (Rahimi et al., 2006).

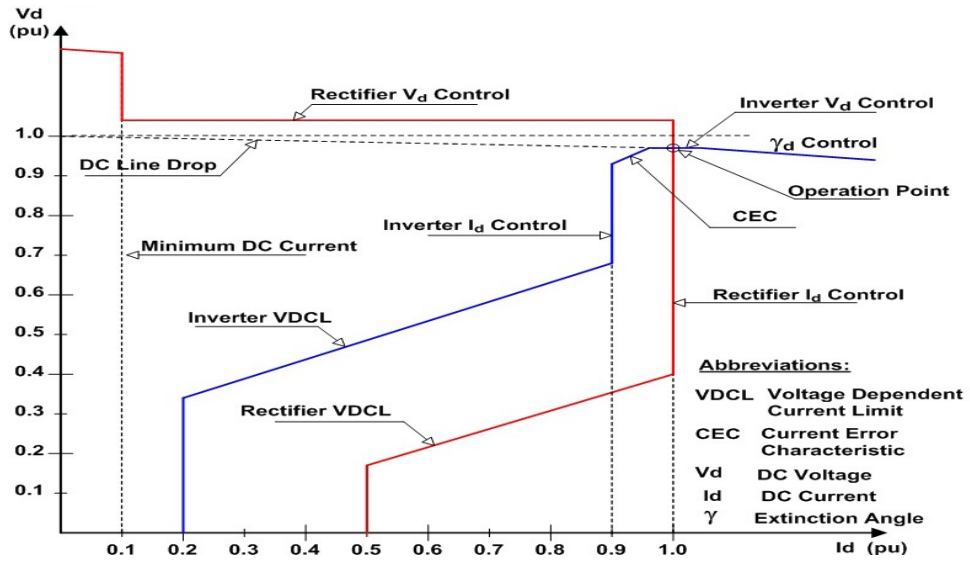

Figure 4. 10: Control characteristics of converter of HVDC link **(Kundur, 1994)**

For stable operation of the system, the delay angle and advance angle of the switching devices of both converter rectifier and inverter need to be maintained within a specified limit of 7° to 15° and 5° to 10°, respectively (Chen & Lie, 2012).

Generally the PI regulator is used for controlling the delay angle and advance angle which also controls the switching sequences of the switching devices according to the system requirement (Shuhui & Timothy, 2010).

The extinction angle of the inverter is controlled by the PI regulator so that it remains within the range of 2° to 5° (Jieqiu et al., 2011). In this way the PI regulator is used as both an alpha controller for rectifier and gamma controller for inverter. The regulator manages the optimal gain for its operation by proper selection of current control loops of both rectifier and inverter by using the minimum select block (Agneholm et al., 2008).

The minimum select block manages the exchange between fixed gain and optimal gain of operation of the regulator. The current control loops for rectifier and inverter are shown in figures 4.11 and 4.12. It is necessary to coordinate the rectifier and inverter to maintain a current margin of about 10A to 15A between the two terminals otherwise there is a risk of loss of margin and the DC voltage can be reduced significantly from the rated value (Chen & Lie, 2012). At the inverter end there are two known methods for the gamma control loop for determining the extinction angle, which are, direct and predictive methods (Rashid, 2001). The direct method tries to maintain the gamma constant irrespective of the relative change of the commutation voltage with respect to the specified minimum value (Agneholm et al., 2008). The gamma prediction method corrects the gamma by means of a feedback loop that calculates the error between the predicted value and actual value of gamma (Jieqiu et al., 2011). The waveforms for measuring gamma are shown in figure 4.13. The bipolar controller is generally located at both ends of the DC link which is being monitored and controlled by the supervisory control and data acquisition (SCADA) system (Flourentzou et al., 2009). The PI controller regulates the operational sequences of the switching device by consequent selection of the delay angle, advance angle and extinction angle so that the firing pulses of the switching devices are properly synchronized with the system voltage and current, (Rahimi et al., 2006), (Agneholm et al., 2008). The system parameters like DC and AC voltages and currents are continuously monitored by the controller for the sake of a stable system operation. The overall system operation is recorded in sequential events in the server of the SCADA for future references.

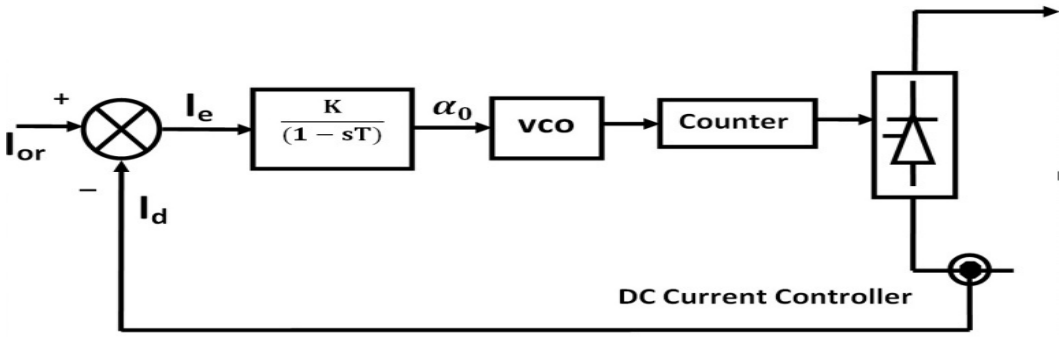

Figure 4. 11: Converter current control loop **(Acha & Madriga, 2001)**

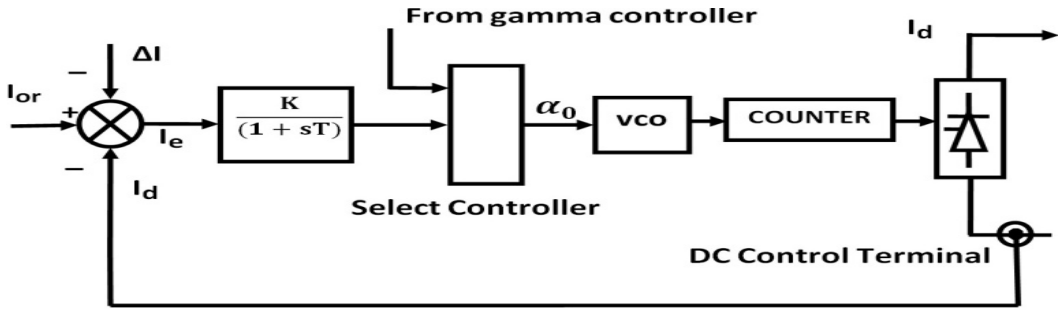

Figure 4. 12: Inverter current control loop **(Acha & Madriga, 2001)**

The DC voltage is varied by means of a converter bridge. When a converter operates as a rectifier, the power flow is from the HVAC system and being rectified to DC to be transmitted over DC power line (Zhang et al., 2010). The power flow is changed from the DC system to the AC system at the inverter end by inverting the DC voltage to AC (Rashid, 2001). However the DC current into the HVDC power line does not change its direction. It flows from the rectifier to the inverter. The operating range of an ideal converter is from 0° to 180° (Harnefors, 2007). However the operating range of a real converter is from approximately 5° to 160°. The PI controller is used for comparing actual power, P_{act} with the reference power, P_{ref} and if any difference occurs, the pre-control value is corrected by the controller (Chen & Lie, 2012).

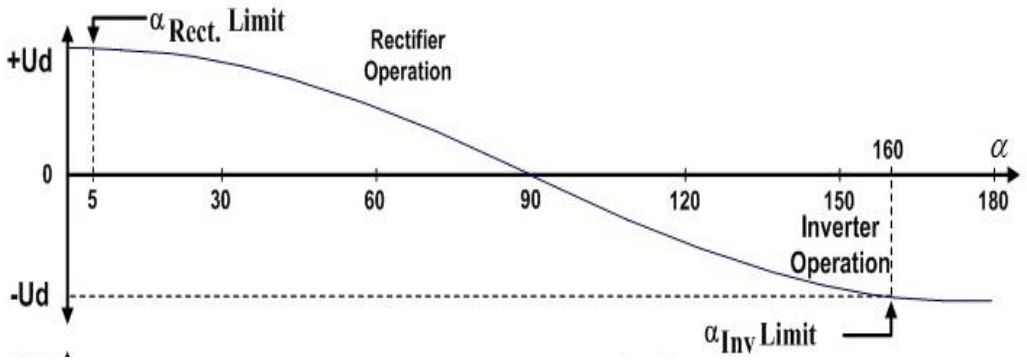

Figure 4. 13: Operating range for a real rectifier and inverter **(Mohan et al., 1995)**

The point of power control is maintained at both rectifier and inverter side for proper synchronization of voltage and current (Flourentzou et al., 2009). The PI controller measures both, the DC current and voltage from the rectifier and inverter sections for proper operation of the DC link (Prabhu & Padiyar, 2009). More details of a model control philosophy for a bipolar HVDC system are found in Appendices B and C.

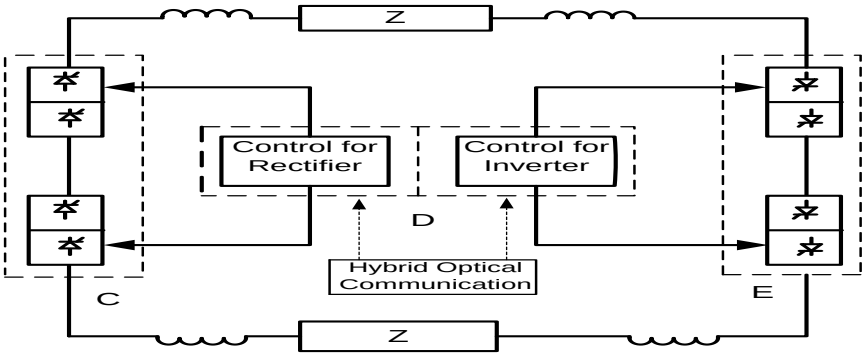

Figure 4. 14: Control topology of Bipolar HVDC link with hybrid SCADA communication

4.5.5 Effectiveness of Mitigating Harmonics with Control Philosophy

The effect of harmonics is distortion in HVAC system parameters, and it hampers the maximum power that will be transferred through the HVDC link. Rectifiers and inverters need reactive power for their proper operation, and most of the reactive power is supplied by the AC filter capacitors. A rectifier and inverter are considered as non-linear loads because of the characteristic harmonics they generate. A proper selection of a rectifier and inverter switching angle plays a major role in reducing these AC harmonics. Therefore; a selection in

switching angle within the range of 5° to 20° for rectifiers and 140° to 160° for inverters as shown in figure 4.13 will reduce the number of filters the network needs. Also, the control philosophy will help with the reduction of reactive power consumed and in addition there will be reduction in harmonic amplitudes these converters could transfer to the HVAC network. The effectiveness of these design techniques will be demonstrated in the case studies.

4.5.6 Evaluation Index to Assess Effectiveness of the control Philosophy when Switching Angle Varies

Analytic expression in formulas 4.6 and 4.8 which was used in section 4.3.5 is assessed here, when there is a change in switching angle. It serves to assess how effective the change in control angle were when selecting rectifier angle in range of 5° to 20° and inverter in a range of 145° to 160°, by looking at their $\%THDV_{ac-primRec}$ or $\%THDV_{ac-primInv}$ indices at PCC, as well as their $U_{(1)AC-primRect/inv}$ range. Thereafter, these voltage results obtained at PCC are to be compared to indices formula 4.7 or 4.9 and their $\%THDV_{ac-primRec}$ or $\%THDV_{ac-primInv}$ values under variations to IEEE 519 standard to analyse how effective these mitigation techniques are under variations.

4.5.7 Flow-chart Guideline for Evaluating the Harmonic Mitigation Techniques applied to Bipolar HVDC Systems

The main contribution of this thesis is a developed flowchart (steps 1 to 11) to guide how to evaluate the techniques used to reduce the effects of harmonics. The tool used is the DIgSILENT PowerFactory software and frequency domain modelling is applied. This tool is used to demonstrate the mitigation techniques applied and the results obtained are analysed with IEEE 519 Standard on harmonics.

A flow-chart of the developed AC harmonic mitigation technique evaluation process for a BPHVDC network is shown in figure 4.15 and its implementation will be demonstrated in chapter five.

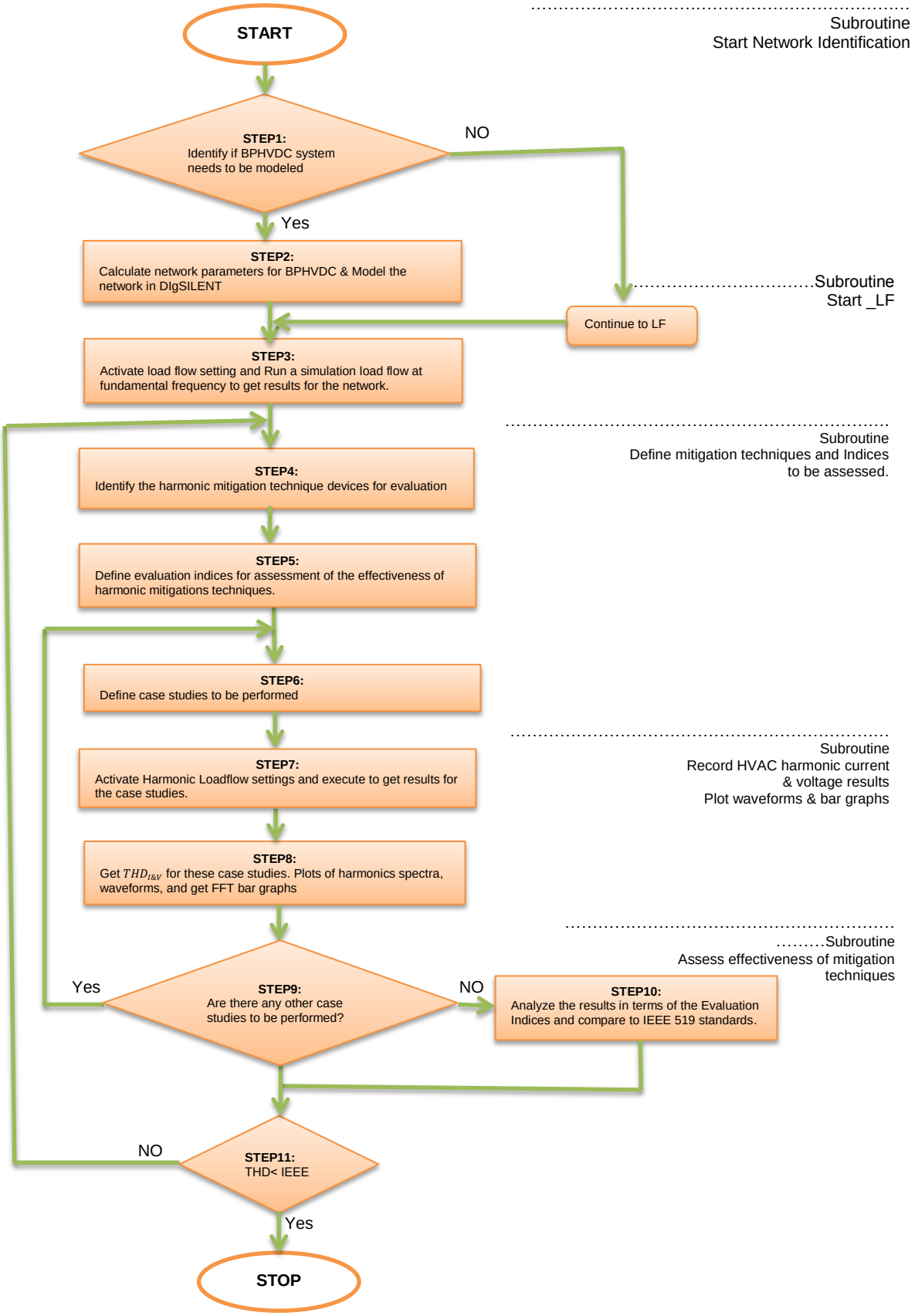

Figure 4. 15: Flow-chart of the developed algorithm for effectively mitigating AC harmonic on a BPHVDC network in frequency domain using DIgSILENT Powerfactory software

Chapter Five:

5 HVDC Network Modelling, Case studies and Results Analysis

This chapter is an implementation approach through case studies and the recordal of results, by applying the flowchart methodology developed in chapter four. It starts with a presentation on how some major components can be modelled in DIgSILENT Powerfactory. Thereafter, the processes on how to generate harmonic results are shown and how results were recorded. There have been three case studies performed to analyse the effectiveness of the mitigation techniques presented in chapter four. These case studies and their results are analysed and evaluated against an international standard regarding harmonic mitigation, as described in chapter three under section 3.12.

5.1 Bipolar HVDC Model for Performance and Rating

Figure 5.1, identifies the BPHVDC system configuration (step1 of flowchart) to be used for the case studies. On the inverter side; the AC network was modelled as a grid source. The AC source on the rectifier side has been modelled using synchronous machines in DIgSILENT configured as generator. The generator's parameters used are real and are taken from the South Africa power station, Koeberg. The calculated Short Circuit Level (SCL) and Short Circuit Ratio (SCR) of the system, as discussed in Section 2.4.2 was found to be of the value of 3.2. This is at the rectifier HVAC bus side (AC1).

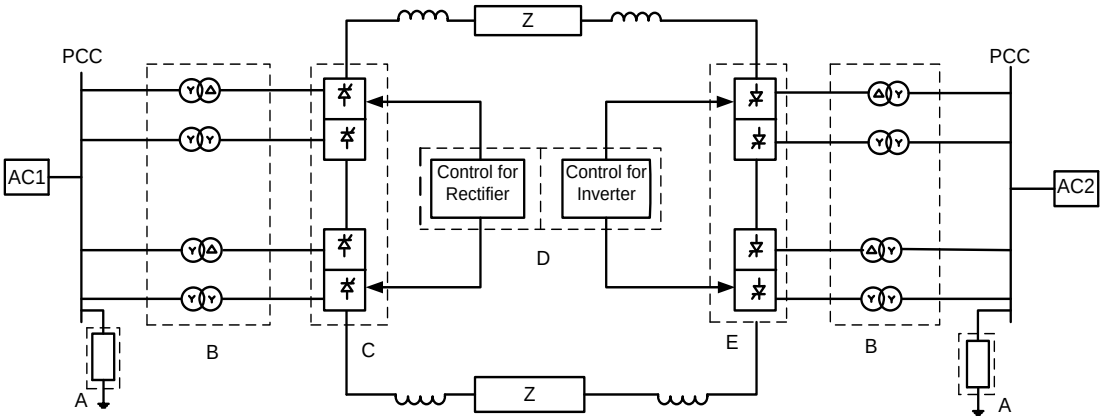

Figure 5. 1: Bipolar HVDC network showing block diagram for case studies which will be performed

The HVDC circuit model includes four parts, namely the converter with their converter transformers (in blocks B, C and E), the transmission line, AC generating source with their AC transformers (AC1 and AC2) and the AC filters (in block A). Each 12 pulse converter which is made of two 6 pulses in series with converter transformers connected in star to star and star to delta. The DC transmission line is modelled taking into account line geometry, ground resistivity and all aspects of conductor construction available in DIgSILENT.

5.1.1 Modelling of a Synchronous Machine

Each of the synchronous generators from the South Africa (S.A) power plant was modelled using the standard synchronous machine model available in the DIgSILENT. During synchronous operation, the flux produced by the stator is rotating with the same speed as the rotor. This flux is penetrating the rotor core and the resultant reluctance, this flux runs through, is a sum of the stator reluctance and rotor reluctance, see Figure 5.2 taken from (Machowski & Kacejko, 2002) and the relation between the reactance and reluctance is given by the equation 5.1 below (Matsch & Morgan, 1987) :

$$X = \omega . L = \omega . \frac{N^2}{\Re} \qquad (5.1)$$

Where:
X is the reactance in ohms (Ω)
N is number of turns
$\Re$ is the reluctance, (H^{-1}).
ω is the frequency in radians per second (rad/sec)
L is the inductance in henry (H).

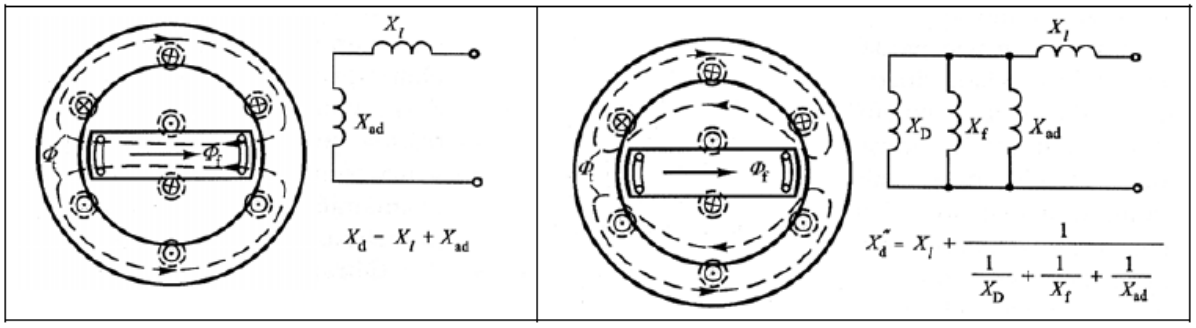

Figure 5. 2: Difference between synchronous (left) and sub-transient (right) reactance of a synchronous machine. Source: **(Machowski & Kacejko, 2002)**

where X_d is the synchronous reactance, X_{ad} is the reactance corresponding to the air gap reluctance, X_l is the leakage stator reactance, $X"_d$ is the sub-transient reactance, X_D is the reactance corresponding to the reluctance of the flux that is pushed out by the damped windings and runs through the air gap, and X_f is the reactance corresponding to the reluctance of the flux that is pushed out by the field winding and runs through the air gap.

In the sub-transient state, which occurs directly after faults (Machowski & Kacejko, 2002), the rotation of the flux is varying with respect to the rotating rotor. This varying flux induces currents in the field winding and the damper winding on the rotor. These currents in turn produce opposing fluxes that push the original flux out of the rotor, and the resultant flux in the sub-transient condition runs therefore through the high reluctance of the air gap, and the corresponding sub-transient reactance is small, as can be seen from equation 5.1.

The fluxes produced by positive or negative sequence harmonic currents in the stator are also rotating with respect to the rotor, and are therefore also pushed out of the rotor by the damper windings and the field winding. Therefore, the assumption is made that the reactance of a synchronous machine for harmonic analysis shall be the sub-transient reactance $X"_d$, or more often the average value of the direct and quadrature axis sub-transient reactances is used (Force, Jan. 1996) (Acha & Madriga, 2001), (Arrillaga & Watson, 2003) :

$$X = \frac{X"_d + X"_q}{2} \qquad (5.\ 2)$$

PowerFactory uses equation 5.2 for modelling synchronous machines (GmbH2013, n.d.).
The resistive component of synchronous machines used for harmonic analysis studies, similar to the winding resistances of a transformer, increases with frequency due to the winding eddy current losses and losses in the stator core. Therefore, the most common approach found in the literature is to use the following equation (Force, Jan. 1996), (Arrillaga et al., 1997), (Acha & Madriga, 2001):

$$R_s(f) = R_{50HZ} \times \sqrt{\frac{f}{f_1}} \qquad (5.\ 3)$$

The equivalent diagram of a synchronous machine used for fundamental frequency load-flow studies and higher frequency harmonic studies is shown in Figure 5.3.

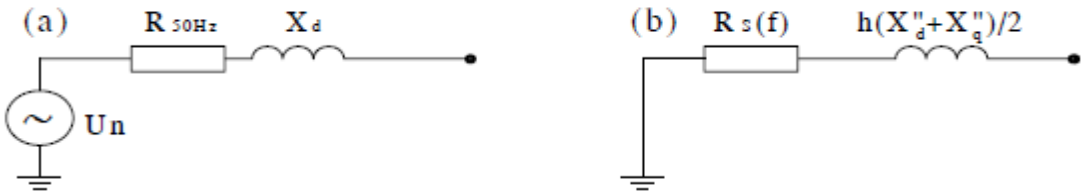

Figure 5. 3: Equivalent diagram of a synchronous generator. (a) - For a fundamental frequency load flow studies, (b) - For harmonic analysis. Assumption: The generator supplies a perfectly sinusoidal voltage **(Machowski & Kacejko, 2002)**

The frequency dependence described by equation 5.3 is implemented in PowerFactory using the *ChaPol* characteristic. Data for the model generators are shown in table 5.1.

Table 5. 1: Constants parameters used for modelling synchronous machine in DIgSILENT

Rs	XL	Xd	Xq	X'd	X"d	X"q	X2	X0	U-LL	P	Q
p.u	p.u	p.u	p.u	p.u	p.u	p.u	p.u	p.u	kV	MW	Mvars
0.0052	0.264	1.53	0.62	0.204	0.144	0.209	0.157	0.066	13.2	918	56.912

Where: R_s is stator resistance, X_L is stator leakage reactance, X_d, X_q, X'_d, X'_q, X''_d, X''_q, are synchronous, transient and subtransient reactances in d and q axes. X_2, X_0, negative and zero sequence reactance. U_{LL}- line to line AC voltage, P active power and Q is reactive power.

5.1.2 Modelling of Harmonic Converter in DIgSILENT

In the harmonic loadflow calculation of PowerFactory, HVDC rectifiers were modelled as ideal rectifiers (ideal current spectra). This was done after activating the box for ideal rectifier. Thereafter, a click in the drop down arrow next to harmonic currents box and by selecting project type, will allow assigning different harmonic orders for a selected converter. This can be selected as shown in Figure 5.4.

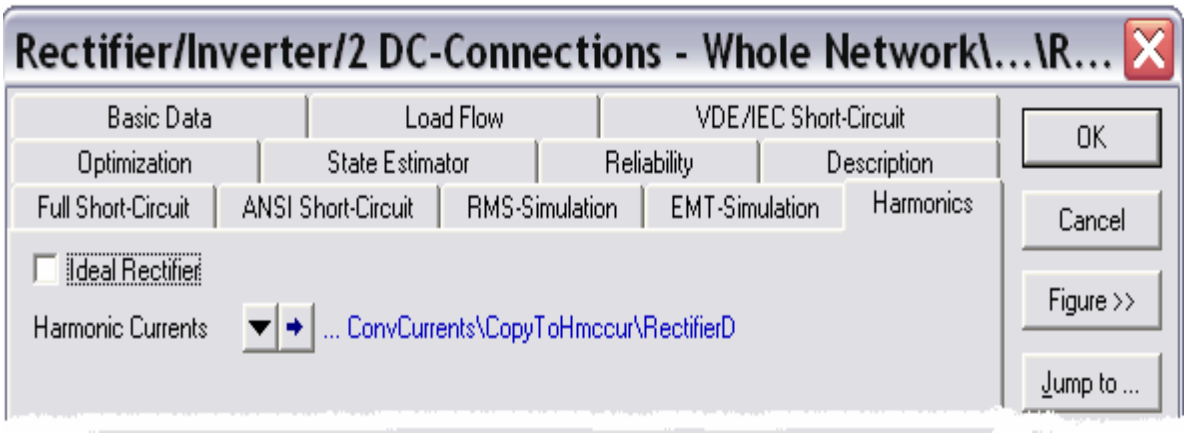

Figure 5. 4: Dialog box of Harmonic rectifier converter being modelled in DIgSILENT

5.2 Case Background and Methodology

The aim for these case studies is to investigate on how effectively the mitigation techniques presented in chapter four will reduce AC harmonics produced by the rectifiers and inverters. These harmonics are generated by HVDC converter rectifiers and inverters and are transferred to their respective HVAC side. The harmonic content analysis is then done to establish their harmonic order amplitudes and what would be the impact of the converter transformers configurations, converters switching angle and AC filters when it comes about mitigating them. It starts by implementing the step by step process as illustrated in the flowchart in figure 4.15.

The theoretical analysis presented in Chapters 2 and 3 on harmonics produced by rectifiers and inverters can then be utilised to ascertain how these harmonic orders would interact with the HVAC terminal to give rise to AC harmonic current and voltage distortion on the AC side.

In order to confirm the theoretical analysis and to evaluate the effectiveness of the mitigation technique used as described earlier, a BPHVDC network is simulated in DIgSILENT. The detailed model of this bipolar HVDC network in DIgSILENT PowerFactory is sufficient for harmonic loadflows and harmonic waveforms simulation results. These results will clarify the behaviour of this network under harmonic distortion and how it is behaving in line with the international standard set by IEEE.

To be able to monitor continuous harmonic sequence components under transient conditions that change from cycle to cycle, it was decided to only look at their FFT bar graphs. This was when determining the sequence components of a three-phase system under an unbalanced

transient condition. Figure 5.5 is a demonstration on how this study could be activated in DIgSILENT.

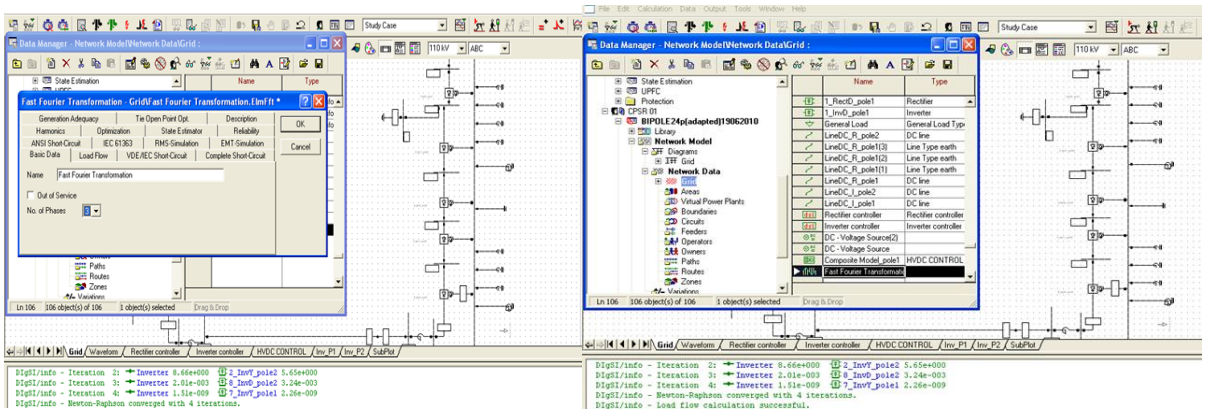

Figure 5. 5: Dialog box for performing harmonic penetration under unbalanced condition for a BPHVDC

5.3 Detailed Description of Harmonic Study in Frequency Domain Using DIgSILENT

Powerfactory has the capability of performing harmonic study using frequency domain calculations. The steps to execute these case studies are described in the following four points after a BPHVDC network is modelled in DIgSILENT:

1. Get the command HLF (Harmonic Load-Flow), select unbalanced and execute. This command in fact first runs the classical unbalanced load flow calculation, and in the second step, performs unbalanced direct harmonic calculation, and the harmonic flows and harmonic bus voltages are obtained.

2. After the HLF calculation, the calculated harmonic voltages at the HVDC bus are recorded together with the positive, negative and zero sequence values of the fundamental frequency voltage and record their total voltage harmonic distortion.

3. The software calculates their harmonic current at the star to star and star to delta converter transformer on the AC side and records their total current harmonic distortion as well.

4. Generate their current and voltage distortion waveforms and FFT bar graphs.

5.4 Case Studies

This is an implementation of the steps 6 to 9 of the flowchart developed in chapter four. It demonstrates different case studies which were used and their results which were obtained as well.

5.4.1 Case Study One: Mitigating AC harmonics by Configuring Converter Transformers in star to star and star to delta

The following BPHVDC network is investigated after being modelled in DIgSILENT PowerFactory as shown in figure 5.6. A load flow simulation was run to make sure the network is operational. Thereafter, harmonic simulation was performed.

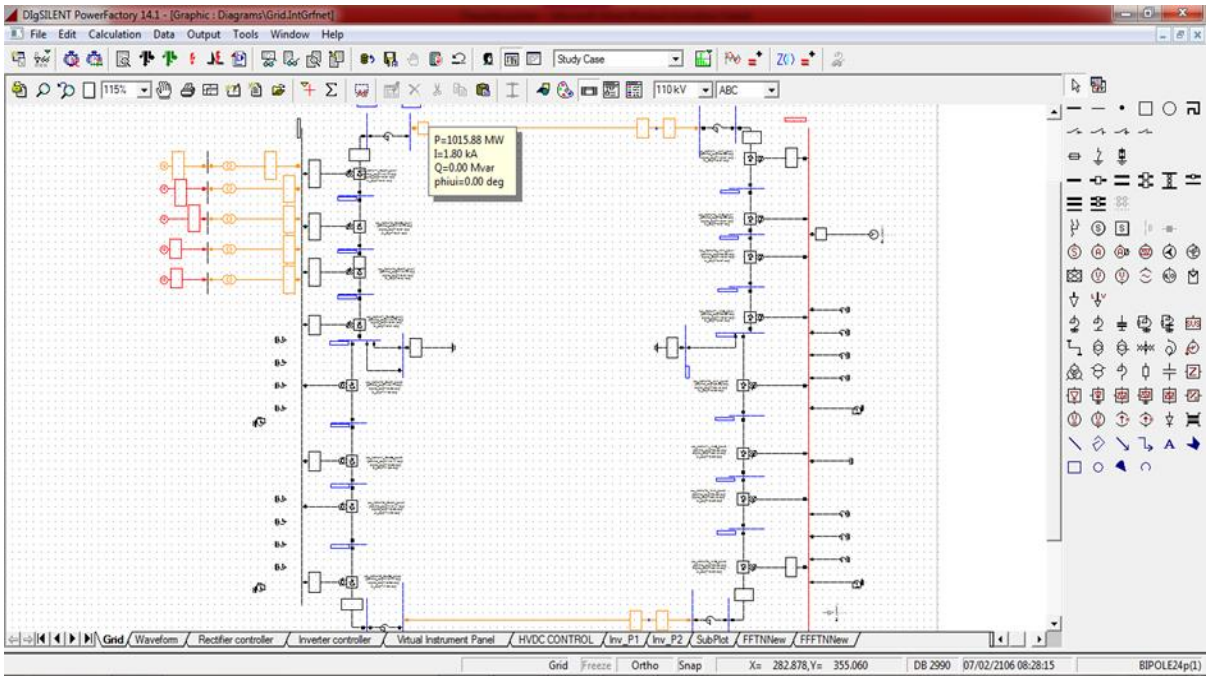

Figure 5. 6: A Bipolar HVDC network after being modelled in DIgSILENT

Harmonic cancellation by converter transformer configurations requires that the twelve pulse system and their converter transformers to be connected in star to star and star to delta in order for the 5^{th} and 7^{th} harmonics to be cancelled. The reactance for these transformers should also be identical to have these harmonics cancelled. A difference in the transformer secondary reactances will result in different commutation durations and hence operating points. The results recorded in table 5.2 are for voltage per unit, powers, current and voltages when analysing the effectiveness of the converters transformers, with no filters

being connected to the rectifier AC bus. The results are recorded from their AC side on the first two converter top transformers (Top of block B). Of the two, one of these rectifier and inverter transformers is connected in star to star and the other one is connected in star to delta.

Table 5. 2: Results on the AC side when analysing the impact of the converter transformer in mitigating AC harmonics

	Load Flow at Fundamental Frequency					Harmonic Results				
	U-L-L(kV)	U-p.u	I-(kA)	P(MW)	Q(Mvar)	U-L-L(kV)	U-p.u	TP(MW)	TQ(Mvar)	THD(%)
Converter Transfo Rectifier Side	-	-	0.73	253.97	141.02	-	-	252.52	207.54	-
Converter Transfo Inverter Side	-	-	0.59	227.86	143.44	-	-	-227.88	163.84	-
Converter Transfo Rectifier AC Bus	229.25	1.00	-	-	-	247.50	1.08	-	-	40.65
Converter Transfo Inverter AC Bus	288.87	1.05	-	-	-	276.68	1.04	-	-	55.13

From the FFT plots, it can be concluded that the converter transformers when connected in star to star and star to delta prove to be effective by eliminating harmonics below 11th and it is shown in figure 5.7, this when $U_{(1)}$ is equal to 1.08 and 1.05 at rectifier and inverter, respectively. The switching angles were 15° and 165° for rectifier and inverter, respectively.

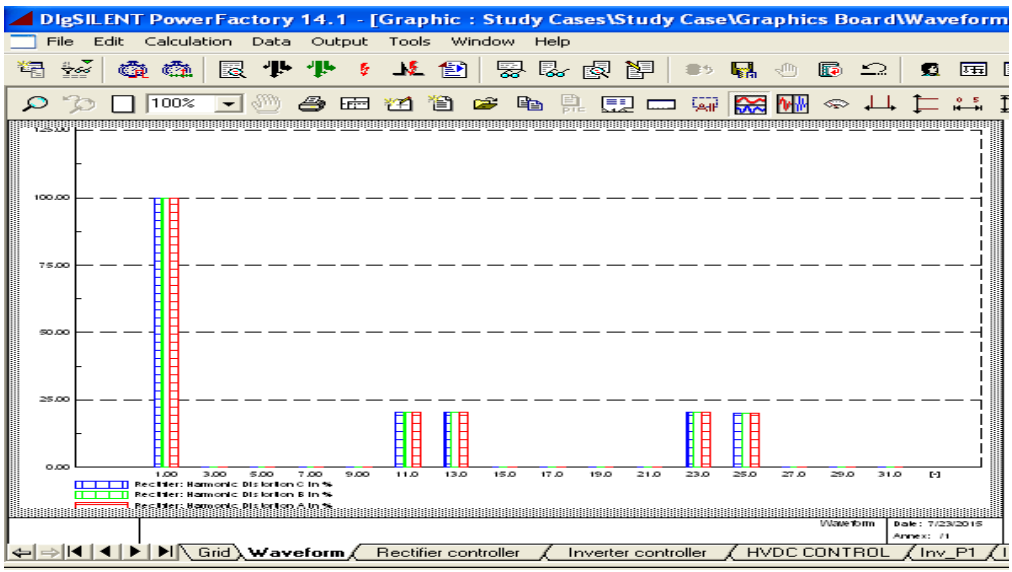

Figure 5. 7: Recorded on the HVAC bus where rectifier converter transformer are connected, when analysing the effectiveness of the converter transformers which are connected in Y-Y and Y-Δ to mitigate harmonic distortion

5.4.2 Case Study Two: AC Harmonic filter to mitigate harmonics on the AC side of converter Transformers

A waveform showing how the network behaves when no filters are connected to the rectifier AC bus side, during harmonic condition in BPHVDC network is shown in figure 5.8.

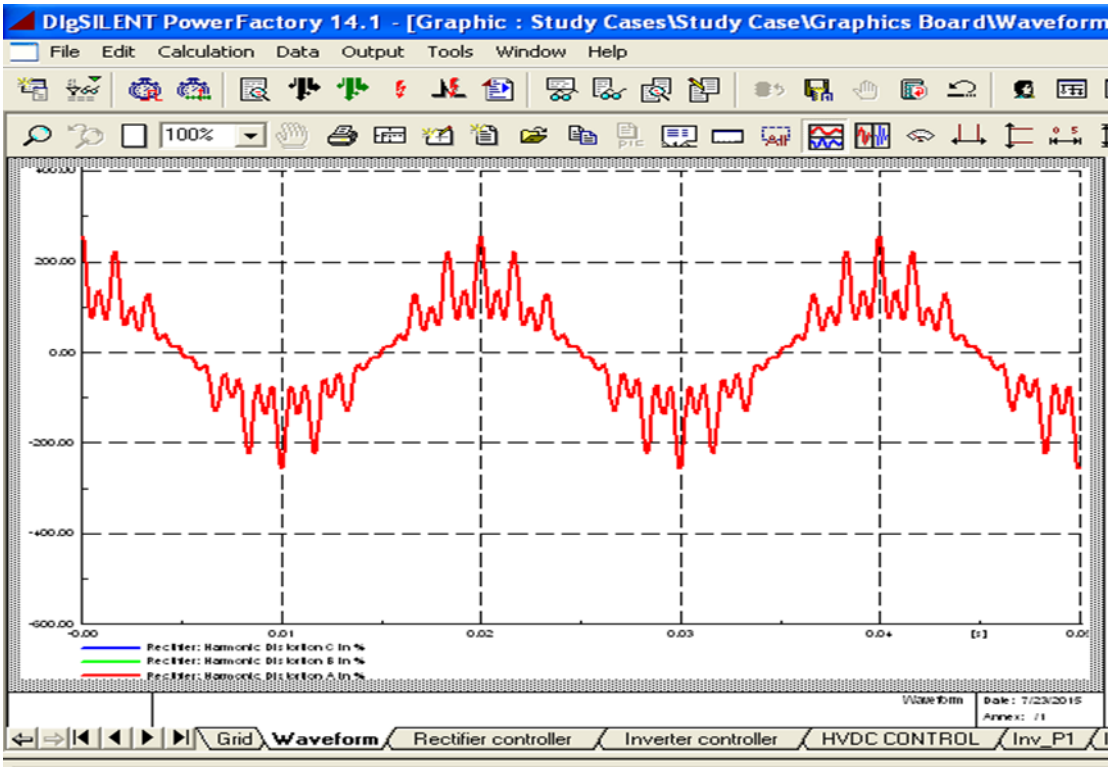

Figure 5. 8: A distorted voltage waveform recorded on the HVAC bus where the rectifier converter transformers are connected, when all filters were not connected to these HVAC busbars

After harmonic filters were inserted into the model at the HVAC bus on rectifier side to mitigate AC harmonics, it proves to be effective in mitigating harmonic distortion. There was elimination of 11th and 13th harmonics, a drop in $\%THDv$ and a reduction in 23rd and 25th harmonic amplitudes when looking at their FFT bar graph as shown in figure 5.9.

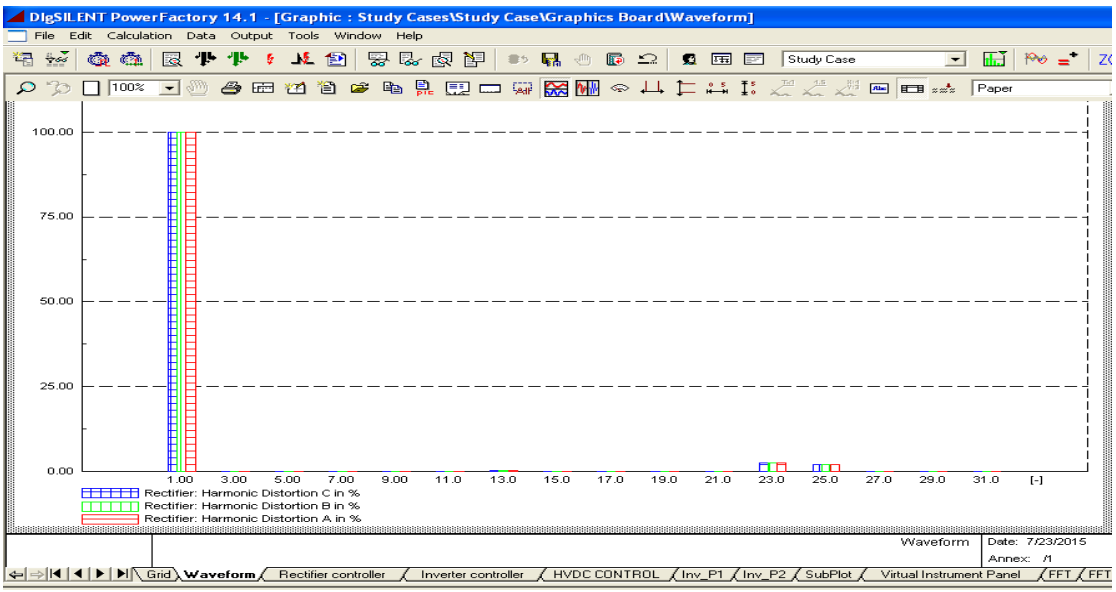

Figure 5. 9: A bargraph recorded on the HVAC busbar where rectifier's converter transformers were connected, showing an elimination of harmonic order of below 23rd order after filters were inserted to the HVAC busbars

The results recorded in Table 5.3 are obtained when doing harmonic load flow (HLF) and a reflexion of how a BPHVDC network behaves on the HVAC side under harmonic conditions.

Table 5. 3: Results on the AC side of Converter transformers with AC filters in the network

	Load Flow at Fundamental Frequency					Harmonic Results				
	U-L-L(kV)	U-p.u	I-(kA)	P(MW)	Q(Mvar)	U-L-L(kV)	U-p.u	TP(MW)	TQ(Mvar)	THD(%)
Converter Transfo Rectifier Side	-	-	0.73	253.97	146.05	-	-	253.48	170.59	-
Converter Transfo Inverter Side	-	-	0.54	227.86	131.52	-	-	-227.88	152.58	-
Converter Transfo Rectifier AC Bus	231.16	1.01	-	-	-	231.28	1.01	-	-	3.17
Converter Transfo Inverter AC Bus	282.46	1.05	-	-	-	282.47	1.03	-	-	0.60

5.4.3 Case Study 3: Harmonic Analysis with change in operating switching angle

The generation of harmonics by HVDC rectifiers and inverters which are induced to the HVAC also come from commutation action of the thyristor valves of converter rectifiers and inverters when there is a change in their switching angle. A change in converter switching angle is analysed here in this 3rd case study. Table 5.4 is a combined rectifier side results recorded during fundamental and harmonic loadflow results when all rectifiers firing (or alpha) angle were changed from 8° to 20°.

Table 5. 4: Rectifier results at PCC when a rectifier firing angle is being changed from 8° to 20°

	Load Flow Results				Harmonic Load Flow Results				
Alpha-Angle(°)	Udc(kV)	Idc(kA)	Pd(MW)	Qd(Mvar)	Uac-pcc(kV)	Irms (kA)	TP(MW)	TQ(Mvar)	%THDv
8	581.78	2.34	1361.66	0.00	230.38	0.99	2716.32	1597.12	4.20
12	577.65	2.21	1277.96	0.00	228.49	0.93	2549.60	1552.96	3.98
15	573.54	2.08	1195.82	0.00	226.64	0.88	2386.00	1501.36	3.76
20	564.86	1.82	1025.63	0.00	231.20	0.77	2046.96	1372.48	3.09

During this case study its shows a reduction in $\%THD_V$ on the AC busbar where the rectifier is connected through its converter transformer.

The change in rectifier firing angle proves to be effective in reducing total reactive powers as seen in table 5.4. This shows that AC reactive power is consumed by the rectifier. There was a huge amount of reactive power required by rectifier and inverter, which is seen in tables 5.4 and in table 5.5 and this, was when the rectifier was operating at an angle of 8°. As firing angle increases, converters (rectifier and inverter) start to draw less reactive power from the AC system. Therefore, some capacitors banks which do play a role in controlling reactive power could be disconnected as there is no need for all of them to be kept in the network. If kept they can alter the proper operation of the entire network. These capacitors banks are part of the filters.

Table 5. 5: Inverter results at PCC when a rectifier angle was changed from 8° to 20°

	Load Flow Results				Harmonic Load Flow Results				
Alpha-Angle (°)	Udc(kV)	Idc(kA)	Pd(MW)	Qd(Mvar)	Uac-pcc(kV)	Irms (kA)	TP(MW)	TQ(Mvar)	%THDv
8	506.33	2.340	1185.06	0	280.44	0.80	-2370.64	1644.88	0.94
12	506.33	2.210	1120.17	0	280.44	0.75	-2240.8	1598.48	0.87
15	506.33	2.800	1055.67	0	280.43	0.65	-2111.68	1371.36	0.71
20	506.33	1.882	919.34	0	285.56	0.57	-1838.96	1275.6	0.59

5.5 Results Analysis: Analysis of Effectiveness of Mitigation Technique Based on Cases Studies Results

This is an implementation of the steps 10 and 11 of the flowchart developed in chapter four. It assesses how effective these mitigation techniques have been, by looking at the results obtained under the case studies by assessing them against the presented indices and to the IEEE standard on harmonics as well.

5.5.1 Analysis of Harmonic Results for Case Studies

5.5.1.1 Case Study 1:

It was found that the techniques of connecting the converter transformers in star to star and star to delta proved to be effective in mitigating AC harmonics. It can be seen that there is no presence of 5^{th} and 7^{th} harmonic content in the network. It was found that the converter connection in star to star and star to delta did play a major role in cancelling out these harmonics. The only visible harmonics offenders which did remain were of the orders of 11^{th}, 13^{th}, 23^{rd} and 25^{th} so on. This could be seen on the bar graph of the figure 5.7.

5.5.1.2 Case Study 2:

The $\%THD_V$ results obtained after the insertion of a filter on the rectifier AC side bus has proven them to be effective. It was found that filters had a high effect on the dropping of the harmonic voltage and in turn on the injected harmonic current reductions as well on the rectifier AC side. This can be viewed in table 5.3. These filters used under this case study two, were tuned to the varieties of characteristics harmonics created by the converters rectifiers and inverters. All formulas used on designing each of the individual filters are in appendix D.

5.5.1.3 Case Study 3:

The BPHVDC is comprised of controllable switches and they are arranged to be periodically fired in a predetermined sequence in timed relation to alternating voltage cycle. Converters rectifiers and inverters being source of harmonics, these do occur during the switching of the thyristors. These converters do end up inducing harmonics into the AC network to which they are connected. The results obtained under this case study, by analysing them under an excel bar graph as shown in figure 5.10, show a decrease in total reactive power demand by the converters, every time there is an increase in switching angles.

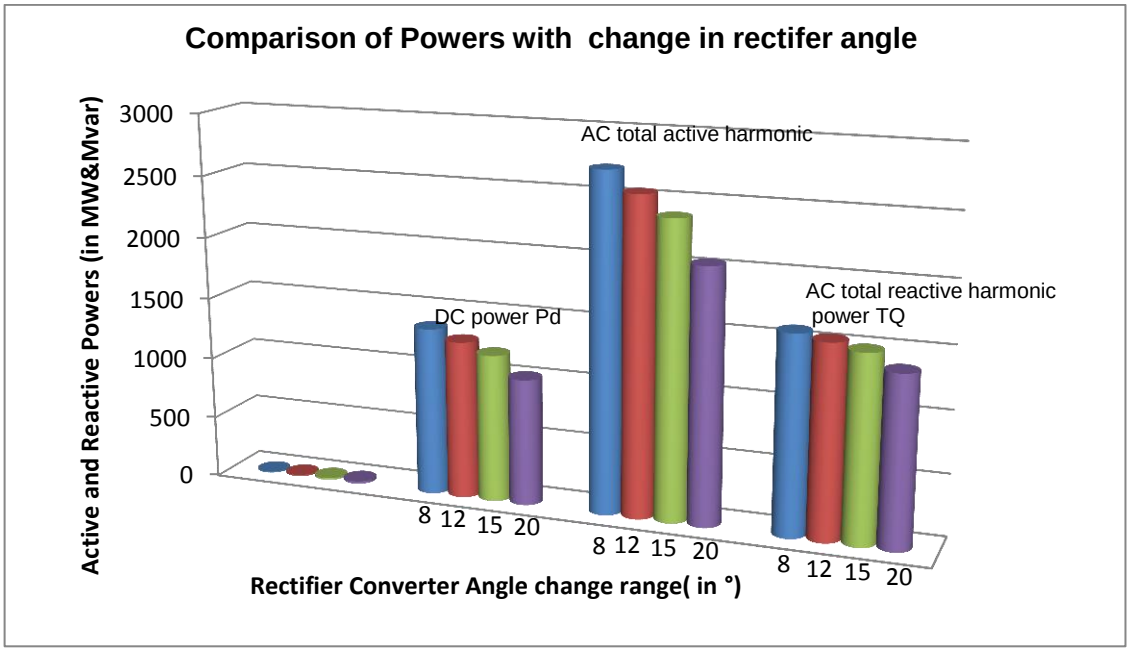

Figure 5. 10: A decrease in active and reactive powers when there was an increase in firing angle is shown in this figure

When assessing the change in rectifier firing angle on how it will have an impact in reducing harmonics induced into the AC network, it proved to be effective. There was a decrease in $\%THD_V$ on the PCC AC bus. Figure 5.11 displays the results obtained in table 5.4.

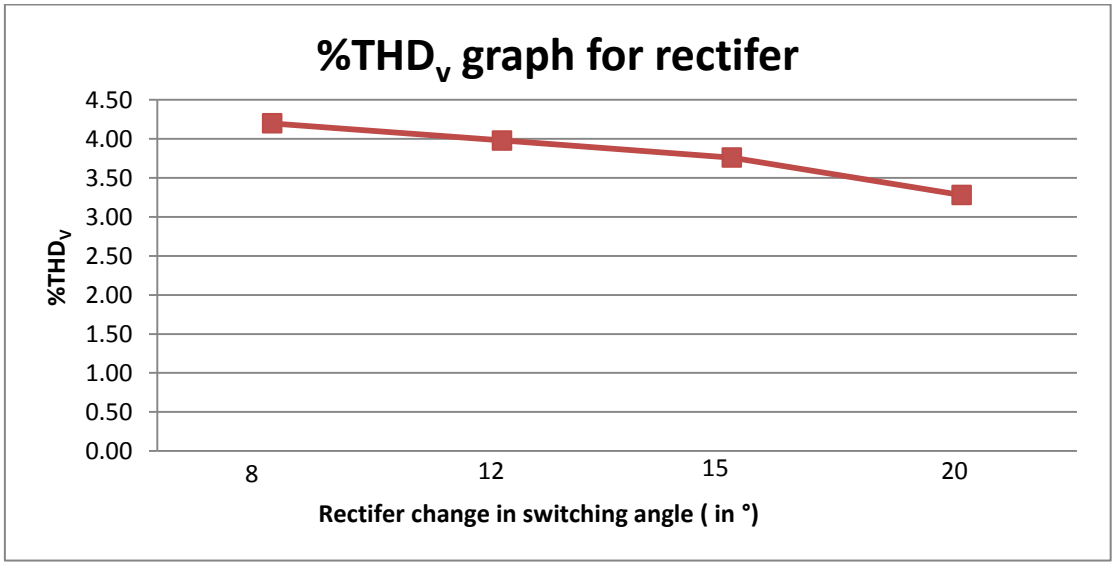

Figure 5. 11: A decrease in $\%THD_V$ as there is a decrease in switching angle on the rectifier side

5.6 Analysis of Effectiveness of Mitigation Technique Based on Indices defined

The $\%THD_V$ and per unit voltage drop results obtained for all the three case studies, are found in table 5.6 below, when assessing them with the developed indices (equations 4.6 and 4.8) and the IEEE 519 on harmonics limits, it was found that:

Case study one has a $\%THD_V$ distortion level above that recommended by IEEE 519. Even though the converter transformers are being connected in star to star and star to delta it did eliminate the harmonic orders of 5th and 7th, but the distortions are found to still be out of the range prescribed by the total harmonic distortion ($\%THD_V$) limit as stated by IEEE 519 for this network which is above 138kVAC range. It was also found to have a high per unit voltage when assessing against the developed indices (equations 4.7 and 4.9). Therefore, this mitigation technique by connecting converters transformers in star to star and star to delta needed to be supplemented with the other two mitigation techniques to be more effective when a higher harmonic order has to be mitigated.

The case studies 2 and 3 comply with voltage index limits and are within the IEEE 519 prescribed limit on total harmonic distortion at the AC bus on rectifier and inverter side. It can be said that these two mitigation techniques have been effective and their use is supported.

Table 5. 6: Summary of the three case studies for %THD$_V$ and the voltage drop in per unit (p.u)

	CASE 1	
	THDv(%)	U_{AC-RMS}(p.u)
AC Bus at Rectifier side	40.65	1.08
AC Bus at Inverter side	55.13	1.04
	CASE 2	
	THDv(%)	U_{AC-RMS}(p.u)
AC Bus at Rectifier side	3.17	1.01
AC Bus at Inverter side	0.60	1.03
	CASE 3	
	THDv(%)	U_{AC-RMS}(p.u)
AC Bus at Rectifier side	3.09	0.98
AC Bus at Inverter side	0.59	1.02

Chapter Six:

6 Results and conclusions

In this thesis, the process of mitigating AC harmonic distortion after modelling a bipolar HVDC network using the simulation software DIgSILENT PowerFactory is shown. A fundamental frequency load-flow model is used as a basis that is to be extended to harmonic studies. The model was extended for harmonic frequencies in the range from 50 Hz up to 1,55 kHz(which is 31st harmonic order).

The investigated AC harmonic mitigation techniques on a BPHVDC system have been analyzed to determine their effectiveness. There have been three case studies; the first one was on converter transformer connection. The second case study was on the introduction of AC harmonic filters and the last case study was on the selection of converter switching angles using harmonic domain calculations of PowerFactory software tool.

The main aim for this research was achieved, i.e. the BPHVDC network model was created and verified within the harmonic domain. Additionally, when assessing the total harmonic distortion for voltage and current for three mitigation techniques using case studies, and the IEEE standard on harmonics, the techniques proved to be effective even under varying switching angle conditions.

6.1 General conclusions

In conclusion, it was found that a wide range of related fields needed to be reviewed in order to lay a sound theoretical foundation for investigating harmonic interaction for a BPHVDC network. The theory in Chapters two and three and its applications thereof in Chapters four and five proved essential for investigating harmonic mitigation techniques on BPHVDC.

In Chapter one, certain key questions were raised as well as objectives to be met in order to realize the study. These objectives have been met by various discussions in the literature study in Chapter two, which discusses about HVDC theory and their control philosophy, power system harmonic principles, harmonic sequence components, AC to DC harmonic interaction, simulation techniques and simulation tools. This laid the foundation for Chapter three to further explore on harmonic analysis methods. Chapter four made these theories more practical by showing different AC harmonic mitigation techniques and how effectively they could reduce AC harmonics produced by BPHVDC rectifier and inverter. The case studies in Chapter five confirmed that the simulation results are in line with the theories presented in the previous chapters and they have been assessed and compared with IEEE recommended standards on harmonics.

In general, it can be concluded that the studies conducted show that the three mitigation techniques (converter transformers, filters and switching angles) are effective on BPHVDC systems over a range of switching angles.
Also, the flowchart and indices developed for conducting harmonic analysis and for evaluating the effectiveness of mitigation techniques are implementable and recommended for use.

Further, it can be concluded that it is possible to apply the DIgSILENT Powerfactory software tool to evaluate the mitigation techniques applied to a BPHVDC model and it allows for variations in parameters and is capable of generating meaningful results and visual outputs enhancing understanding.

The computer model of a BPHVDC system lays a foundation for applications to other BPHVDC systems and is one of the main contributions to this field.
The main results and conclusions from this research project are summarized below. The conclusions are grouped into sections, each section concerning a part of the project. Therefore a summary of the most important results are given in the next section.

6.2 Overview of Important Results

6.2.1 Harmonic Cancellation by Converters transformers Configuration

The theory and equations presented in section 3.15 show that when the 6-pulse converter configuration, is changed to a 12-pulse configuration the impact on the harmonic mitigation is altered or improved. When a 12 pulse configuration is used it eliminates in the AC line the 5^{th}, 7^{th} harmonics orders $6k \pm 1$ the odd values 5, 7, 17, 19, etc, will circulate between the two converter transformers only but will not penetrate to the AC network.

6.2.2 Modelling techniques and simulations

The modelling techniques and tools presented in Section 1.5.3 and Section 1.5.4 are further discussed in Section 4.1, and are validated by the fact that the theories presented, the simulations done for each theory and the case study results all line up very closely. This shows the reliability and exactness of the simulation package used and alleviates the concerns expressed in Section 1.5.4.

6.2.3 Case study results

Although the case study results have been discussed in chapter 5, it gives a satisfying conclusion to the important role these applied AC harmonic mitigation techniques play in damping the proliferation of power system AC harmonics.

Yet the case studies show that all the mitigation techniques applied can to some extent prove their effectiveness in mitigating harmonic distortion levels and could alleviate the miss-operation of the network and all the risks which had not been identified during a design or conceptualisation process.

Such harmonic mitigation study will need to be re-done on a continual basis to cater for all future network developments. In that case, new studies need to be done to mitigate these new harmonics with the least cost implications such as operational regimes(when looking at switching of rectifiers or inverters), filter banks, gradual increase in fault level as a system develops, etc.

6.3 Specific Findings

In case study 1, it was found that when no filters were present the THD_V and U_1 values were unacceptable as both were found to be outside the acceptable ranges. This case showed that the converter transformer configurations, star to star and star to delta were effective in eliminating the 5th, 7th harmonics, which are usually the largest amplitudes.

Case study 2 shows that when there was no filter, the recorded AC voltage waveform (shown in figure 5.8) was distorted at the rectifier AC side. This means that distortion was created by harmonics and this could result in the overheating of the capacitors and generators. To counter these, AC filters were inserted in network. When a filter was inserted, the 11th and 13th were eliminated and there was also a drop in $\%THD_V$ and in U_1.

Case study 3 techniques, proved to be effective in reducing harmonic distortions. It is well known that converters consume reactive power, which can be 50 to 60% of the active power transfer. Under an abnormal moment the harmonics can cause total reactive power (TQ) to be much higher as shown in table 5.4 and 5.5. Therefore, the converter switching angle had to be selected between 5° and 20° for rectifier and 140° and 160° for inverter as presented in figure 4.13, these for an appreciable operation, which will result in maximum flexibility of power to be controlled without compromising on the safety of the equipment, and it proved to be effective in reducing $\%THD_V$ and in $U_{(1)-prim}\ (p.u)$ in this case study.

6.3.1 Future work

Based on this research investigation, the following topics could be considered for future work:

- Investigating harmonic mitigation techniques used in other types of HVDC schemes, not only LCC. For example: Back to Back, Voltage source converter systems, higher pulse number converters.
- Investigating HVDC schemes in time domain.
- Investigate other harmonic analysis software tools and doing comparative studies.
- Investigating the effectiveness of harmonic mitigation techniques under contingency, faults and stability conditions.
- Further interesting work can be done with respect to the harmonic frequency model, especially; the modelling of dynamically varying harmonics.
- Investigating the effect of standing waves on HVDC lines and their reliability to the harmonic distortion.

6.4 Recommendations and final conclusion

Although the pursuit of a deeper theoretical understanding of the mechanisms behind harmonic interaction is valid, sight should not be lost of the real life practical implications. Some aspects are very relevant and need to be taken into account. For other aspects, where the accuracy and dependability of field measurements become realistically doubtful and where the level of relative harmonic quantities become too small and insignificant to be meaningful, a reality check may be required. Yet, the point where theoretically interesting and practically relevant become mutually exclusive is not always so clear especially given the great variations in fault level and network characteristics encountered in transmission systems all over the world.

In conclusion, it can be said that power systems harmonic analysis and the search for solutions and mitigations is not always simple and straightforward and is by some considered not only a science, but also an art where at the end, years of experience in the field backed by a solid theoretical foundation is the best teacher.

Chapter Seven:

7 References

Acha, E. & Madriga, M., 2001. Power Systems Harmonics: Computer Modeling and Analysis.

Agneholm, E., Du, C. & Olsson, G., 2008. Comparison of different frequency controllers for a VSC-HVDC supplied system. *IEEE Trans.on Power Delivery*, 4, p.2224–2232.

Allard, J.A.C. & Forrest, B., 2004. Thermal problems caused by harmonic frequency leakage fluxes in three-phase, three-winding converter transformers. In *IEEE Transactions on Power Delivery*., 2004. IEEE.

ALSTOM, 2010. Connecting to the future, Alstom Grid. *ALSTOM HVDC*.

Aprille, T.J. & Trick, T.N., January 1972. Steady-state Analysis of non-linearCircuits with Periodic Inputs. *Proceedings of the IEEE*, 60(1), pp.108-14.

Arrillaga, J., 1998. *High Voltage Direct Current Transmission*. 2nd ed. London, United Kingdom: The Institution of Electrical Engineers.

Arrillaga, J. et al., 1997. Power System Harmonic Analysis.

Arrillaga, J. & Watson, N.R., 2003. *Power System Harmonics*. 2nd ed. England: John Wiley & Sons.

Arrillaga, A.R. & Wood, J., 1995. Composite Resonance; a Circuit Approach to the Waveform Distortion Dynamics of an HVDC Converter. *IEEE Transactions on Power Delivery*.

Baggini, A., 2008. *Handbook of Power Quality*. Chichester in United Kingdom: John Wiley & Sons.

Baggini, A., 2008. *Handbook of Power Quality*. Chichester: John Wiley & Sons.

Bathurst, G.N., Smith, B.C., Watson, N.R. & Arrillaga, J., 1998. A modular approach to the solution of the three-phase harmonic power-flow. In *Proceedings of the 8th ICHQP Conference*., 1998.

Bronzeado, E.D. & Jaeger, H., June 2011. ISBN 978-2-85873-158-9 *Review of Disturbance Emission Assessment Techniques*. Cigre Working Group C4.109.

Callaghan, C.D., 1999. *Three phase integrated load and harmonic flows*. PhD thesis. Christchurch, New Zealand, August 1999: University of Canterbury, Department of Electrical and Electronic Engineering, University of Canterbury.

Chen, Z. & Lie, Y., 2012. A Flexible Power Control Method of VSC-HVDC Link for the Enhancement of Effective Short-Circuit Ratio in a Hybrid Multi-Infeed HVDC System. *IEEE Trans. on Power Systems*, 28(2), p.1568 – 1581.

CIGRE and IEEE, I., 1993. IEEE Standard Department *Guide for planning DC links Terminating at AC Locations having Low Short Circuit Capacities*. IEEE report. New York: IEEE.

Densem, T.J., Bodger, P.S. & Arrillaga, J., February 1984. Three Phase Transmission System Modelling for Harmonic Penetration. *IEEE Transactions on Power Apparatus and Systems*, 103, pp.310-17.

Dickmander, D.L., Lee, S.Y., Desilets, G.L. & Granger, M., January 1994. AC/DC Harmonic Interactions in the Presence of GIC for the Quebec-New England Phase II HVDC Transmission. *IEEE Transactions on Power Delivery*, 9(1), pp.68-78.

DIgSILENT, 2004. *DIgSILENT Technical Information*. Gomaringen, Germany.

Dommel, H.W., April 1969. Digital Computer Simulation of Electromagnetic Transients in Single and Multiphase Networks. *IEEE Transactions on Power Apparatus and Systems*, 88(4), pp.388-99.

Flourentzou, N., Agelidis, V.G. & Demetriades, G.D., 2009. VSC-based HVDC Power Transmission Systems: An Overview. *IEEE Trans. Power Electronic*, 24(3), p.592–602.

Force, T., Jan. 1996. Modeling and simulation of the propagation of harmonics in electric power networks. I. Concepts, models, and simulation techniques, II. Sample systems and examples. *IEEE Transactions on Power Delivery*, 11(1), pp.452 – 465; 466 - 474.

Fortescue, C.L., 1918. Method of Symmetrical Co-ordinates Applied to the Solution of Polyphase Networks. *Transactions of the American Institute of Electrical Engineers*, 37(2), pp.1027 - 1140.

Fourier, J., 1978. *The analytical theory of heat*. Cambridge: Cambridge University Press.

GmbH2013, D., n.d. *Dynamic Simulation with PowerFactory*. [Online] Available at: http://www.irena.org/DocumentDownloads/events/2014/March/Palau/04_stabilityhandling.pdf .

Gole, D., Menzies, A. & Woodford, R., June 1983. Digital simulation of DC Links and AC Machines. *IEEE Transactions on Power Apparatus and Systems*, 102(6), pp.1616-23.

Harnefors, L., 2007. Modeling of three-phase dynamic systems using complex transfer functions and transfer matrices. *IEEE Trans. Ind. Electron*, 54(4), p.2239–2248.

IEEE, 1997. *IEEE Interharmonic Task Force, "InterHarmonic in Power Systems"*.

IEEE, 2004. *IEEE Recommended Practice for Industrial and Commercial Power Systems Analysis*. New York USA.

Jieqiu, B., Gao, Z., Yu, L. & Meng, C., 2011. Research on dynamic model and decoupling control strategy of VSC-HVDC system. *International Conference on Electrical Machines and Systems*, pp.1-4; 20-23.

Kimbark, W., 1971. *Direct Current Transmission*. First ed. New York: John Wiley & Sons.

Kim, C.K. et al., 2009. *HVDC Transmission for Power Conversion Application in Power Systems*. Asia: John Wiley& Sons.

Krishnayya, P.C.S. & Reeve, J., July 1986. PWRD-1 *Report of a panel discussion sponsored by the Working Group on interaction with Low Short Circuit Ratio AC System*. IEEE Transaction on Power Delivery. New York: IEEE DC Transmission Subcommittee.

Kundur, P., 1994. *Power Stability and Control*. United State of America: The EPRI Power System Engineering Series.

Machowski, P. & Kacejko, J., 2002. Faults in electrical power systems (in Polish). *WNT*.

Manitoba, 1988. PSCAD/EMTDC V3 users manual. *Manitoba HVDC Research Center, Winnipeg, Canada*.

Matsch, L. & Morgan, D., 1987. *Electromagnetic and electromechanical machines*.

Mohan, N., Underland, T.M. & and Robbins, W.P., 1995. *Power Electronics, Converters, Applications, and Design*. 2nd ed. United State of America: John Wiley & Sons.Inc.

Neves, F. et al., 2009. A Space Vector Discrete Fourier Transformer for Detecting Harmonic Sequence Components of Three-Phase Signals. In *35th Annual Conference of IEEE Industrial Electronics*. Porto, 2009. IEEE.

Prabhu, N. & Padiyar, K.R., 2009. Investigation of subsynchronous resonance with VSC-based HVDC transmission systems. *IEEE Transmission Power Delivery*, 24(1), p.433–440.

Rahimi, E. et al., 2006. Commutation Failure in Single and Multi Infeed HVDC Systems. *IEE International Conference on AC and DC PowerTransmission*, 8(8), pp.182-86.

Rashid, M.H., 2001. *Power Electronics Handbook*. 3rd ed. California, USA: A Harcourt Science and Technology Company.

Rens, A.P., 2005. *Validation of Popular Non-Sinusoidal Power Theories for the Analysis and Management of Modern Power SYstems*. PhD dissertation. Potchefstroom, SouthAfrica: North West University.

Roy, R.B. & Amin, M.D., 2014. A Paper of Determination of Controlling Characteristics of the Monopolar HVDC System. *International Journal of Hybrid Information Technology*, 3, pp.105 - 120.

Sadek, P., Christl, K. & Luzelberger, N., 1992. AC/DC Harmonic Interaction in HVDC Systems. *IEEE International Conference on Harmonics in Power Systems*, pp.196-201.

Shuhui, L. & Timothy, H.A., 2010. Control of HVDC Light System using Conventional and Direct current vector control approaches. *IEEE Trans.On Power Electronics*, 25(12), pp.512-16.

Siemens, 2011. *High Voltage Direct Current Transmission Proven Technology for Power Exchange*. [Online] Available at: www.siemens.com/energy/hvdc.

Smith, B.C., Watson, N.R. & Arrillaga, J., 1997. Analysis of the HVDC inverter in the harmonic domain. In *Proceedings of the 7th EPE-Conference*., 1997.

Smith, B.C., Watson, N.R., Wood, A.R. & Arrillaga, J., 1996. Newton solution for the steady-state interaction of AC/DC systems. In *IEE Proceeding, Generation, Transmission, Distribution*., 1996.

Smith, B.C., Watson, N.R., Wood, A.R. & Arrillaga, J., October 1997. A SequenceComponents Model of the AC to DC Converter in the Harmonic Domain. *EEE Transactions on Power Delivery*, 12(4), pp.1736 - 1743.

Stan, A.I., Stroe, D.I. & Silva, R.D., 2011. Control strategies for VSC based HVDC transmission system. *in Proceedings of the 2011 IEEE International Symposium on Industrial Electronics (ISIE)*, pp.1387-92.

Statnett, 2013. Skagerrak Fourth Connecting renewables with new technology between Norway and Denmark. *Promotional brochure*, September.

Wakileh, G.J., 2001. *Power Systems Harmonic, Fundamentals, Analysis and Filter Desig*. Germany: Springer.

Wan-jun, Z., 1985. *HVDC Engineering Technology*. Beijing in China: China Power Press.

Watson, N.R., 1987. *Frequency Dependent AC System Equivalents for Harmonic Studies and Transient Converter Simulation*. Christchurch, New Zealand: PhD thesis, Department of Electrical and Electronic Engineering University of Canterbury.

Yacamini, L. & Hu, R., November 1993. Calculation of Harmonics and Interharmonics in HVDC Schemes with Low DC Side Impedance. *IEEE Proceedings*, 140(6), pp.469-76.

Z.Yang, 2012. Harmonic Impedance Measurement for an Island Microgrid Using Current Injection. In *IEEE 7th Power Electronic and Motion Control Conference- ECCE*. Beijing, 2012.

Zhang, L., Harnefors, L., Nee & H.P., 2010. *Modeling and control of VSC HVDC links connected to island systems*. Society General Meeting. Minneapolis, USA: IEEE Power and Energy.

Zhi-dao, X. & Zan-xun, S., 1985. *HVDC Banch of Power Teaching and Research Group of Zhejiang Unversity*. Beijing in China: Electric Power Press Water Resources and Electric Power Press.

8 Appendices

8.1 Appendix A: Selection of publication with their abstract

Selected publications with their abstracts:

Paper A

M J. Matabaro and G. Atkinson-Hope: "*Optimization of Loss Reduction through a converted HVAC Transmission Line into HVDC Model in DIgSILENT Software*", *SAUPEC* 2014 Conference in University of Kwazulu Natal, Durban, South Africa, 30 January 2014- 31 January 2014.

Abstract: Losses are an important parameter of consideration for mitigation and thereby enhancing the Available Transfer Capability of Power Systems. Loss mitigation is a two stage process the first stage is the Planning phase and the second stage is the Operational phase. This paper discusses briefly the Planning phase activities. The various methods of mitigating the losses in the Operational phase have been presented in this paper with emphasis on one technique whereby a converted existing HVAC transmission line has to carry direct current (DC). The contribution of this paper is the combination of HVAC and converted DC transmission line working in parallel to monitor their operations. These results obtained through decision making factors will demonstrate that a combination of HVAC and converted DC transmission line could be a solution enhancing power transfer. The method is tested with an HVAC working parallel with a converted DC transmission line modelled in DIgSILENT and validated. Results have been presented and analysed in this paper.

Key Words: Current carrying capacity; HVDC; Power transfer capacity; DIgSILENT

Appendix A: Continued

Paper B

M J. Matabaro and G. Atkinson-Hope: "*Efficiency of an Alternating Current Transmission Line Converted into a Direct Current System*", *ICUE* 2013 Conference at Newlands, Cape Town, South Africa, 19 August 2013- 21 August 2013, pp: 311-316.
http://eepublishers.co.za/article/icue-020-11-efficiency-of-an-alternating-current-transmission-line-converted-into-a-direct-current-system.html

Abstract: The concept of energy efficiency could perhaps be summed up as "doing more with less". This means more power is being transmitted over a long transmission line with fewer losses. There is a special interest in the amount of energy being lost over a line. When looking at how electric power is produced at a remote area, where power generation is built, and has to be transmitted over a long distance through transmission lines to the location of power demand is the challenge. It is thus essential to look at how energy could be transmitted as efficiently as possible. High voltage alternating current (HVAC) has been used for many years as the means of transmitting bulk energy. However, HVAC lines incur increased losses as the distance becomes longer. This research investigates how energy could be transported with minimum losses when an existing HVAC transmission line is converted into a HVDC transmission system and the end users still receive AC as the DC is inverted to AC. To evaluate the effectiveness of this methodology, a number of scenarios have been conducted as case studies. The results show that an existing HVAC transmission line when converted to DC is found to improve the energy efficiency while still meeting consumer demand.

Keywords: Current carrying capacity, HVDC, Power transfer capacity, DIgSILENT

Appendix A: Continued

Paper C

M J. Matabaro, W.C. Stemmet and G. Atkinson-Hope: "*Converting Convention High Voltage Alternating Current Transmission lines into a Direct Current Transmission System*", *SAUPEC* 2013 Conference in North – West University, Potchefstroom, South Africa, 31 January 2013 to 01 February 2013, pp: 139-142.

Abstract: Over the last few decades economic growth and industrialization have led to a rapidly rising demand for electric power in many countries. One effect of this increase in demand is that the power transmission systems are nearing a point where they will be unable to meet supply needs. Therefore a need thus arises to consider transmission line alternatives that could substantially increase the power transfer capability of existing high voltage alternating current (HVAC) transmission lines. One alternative is to use high voltage direct current (HVDC) transmission systems as a direct replacement, thus eliminating the need for any major new tower constructions. The existing conductors and tower structures has to be used. This paper will demonstrate how the power transfer capability of an existing HVAC transmission line could be maximized by feeding this line with HVDC. The power transfer capability of HVAC lines is limited by the reactive power needed by the line. However, when HVDC is applied, the only loss on the line is due to the resistance of the conductors, thus it is expected that more power will be transferred across the line compared to a HVAC system. In this investigation a methodology will be developed showing how to convert a HVAC line to a HVDC line. To prove the effectiveness of this methodology, a number of scenarios were investigated as case studies. The research will conclude with findings as to the suitability of converting an existing HVAC line into a HVDC fed system from which increased HVAC can be drawn and supplied at the load end.

Keywords: HVDC, Power Transfer Capability, Creepage Distance, Thermal Capacity, Static Var Compensator, Synchronous Condensers, Short Circuit Ratio

8.2 Appendix B: Calculation for rectifier parameters and rectifier control philosophy

Rectifier Parameters Calculation

Conductor type:
2xDinosaur 50
Nominal voltage: 400kV and Nominal current: 1.704kA
Number of subconductors: 2
Bundle spacing: 0.38m
DC resistance: 0.0437Ω/km
GMR (equivalent radius): 14.54312mm
Outer diameter: 35.94mm
Maximum sag per phase conductors: 13.1m
Maximum sag per ground wires: 11.8m
Earth resistivity: 700Ω

Total DC power for single DC power line: 1182MW
Total DC power for both DC bipolar power line: 1182x2 = 2364MW
Power rating per single valve: $\frac{P_t}{8} = \frac{2364}{8} \approx 296MW$

$V_{DC\ at\ rectifier\ btwn\ DC\ lines} = \frac{2364000000}{1704} = 1387323.94366V \approx 1387.324kV$

$V_{DC\ btwn\ each\ converter} = \frac{1387323.94366}{8} = 173415.49296V$

The firing angle was selected at 15° to determine the voltage on the AC side

$V_{ac3\sim L-L} = \frac{V_{DC}}{1.35\times\cos\alpha}$

$V_{ac3\sim L-L} = \frac{173415.49296}{1.35\times\cos 15°} = 132987.35494kV \approx 133kV$

As there is no standard AC voltage of 133kV, therefore, this research network was modelled using an AC voltage of 132kV, which is a standard voltage.
This voltage is the one which is found on the AC high voltage side of the rectifier converter transformer.

Appendix B: Continued

Determining here power for single converter transformer

LV side transformer which is the DC side:

P_{DC}: 296MW

Q_{DC}: 0MVar

HV side for the converter transformer is connected to the AC voltage:

The powers in a transformer are equal in both (HV and LV) windings.

$P_{AC} = P_{DC}$: 296MW

$Q_{AC} = P_{AC}$ x tanα = 296xtan15° = 79.31296MVar

S = 296+79.31296j = 306.44175∠15°MVA

$Z_{base} = \frac{U^2{}_{AC}}{S_{base}} = \frac{132000^2}{306441750} = 56.8591\Omega$

$X_{comp.p.u}$ = 0.14p.u (this is obtained from transformer nameplate)

$X_{comp.actual} = X_{comp\ p.u} x Z_{base}$ = 0.14x56.8591Ω = 7.9603Ω

$I_{DC} = [\cos\alpha - \cos(\alpha+\mu) \times \frac{U_{conv.Transfo-HVAC-side}}{\sqrt{2}\times X_{comp.actual}}$

$\cos(\alpha+\mu) = cos\,\alpha - \frac{I_{DC}\times\sqrt{2}\times X_{comp.actual}}{U_{conv.Transfo-HVAC-side}}$

$\cos(\alpha+\mu) = cos\ 15° - \frac{1704\times\sqrt{2}\times 7.9603}{132000}$

$<=> \cos(\alpha+\mu) = 0.8206 <=> \alpha+\mu = \cos^{-1}(0.8206) <=> \alpha+\mu = 34.8551°$

$<=> \mu$ = 34.8551°-15° = 19.8551°

$\mu = \delta + \alpha$

$\delta = \mu - \alpha$

$\delta = 19.8551° - 15° = 4.8551°$

α: Rectifier delay or switching angle in electrical degree

δ: Rectifier extinction (or switching off) angle in electrical degree

Here below are a summary of the calculated single (or one) rectifier ratings in a table:

Table B. 1: Table of rectifier parameters

$U_{DC-LVside}(kV)$	$U_{AC-HVside}(kV)$	I_{DC}(kA)	$P_{DC}(MW)$	$\alpha(°)$	$\mu(°)$
173.42	132	1.704	296	15	19.8551

The grid AC does supply the rectifier transformer. This grid had these ratings for it AC transformer:

S : 1200MVA

U_{HV} : 400kV

U_{LV} : 132kV

Short circuit voltage uk : 14.55%

Appendix B: Continued

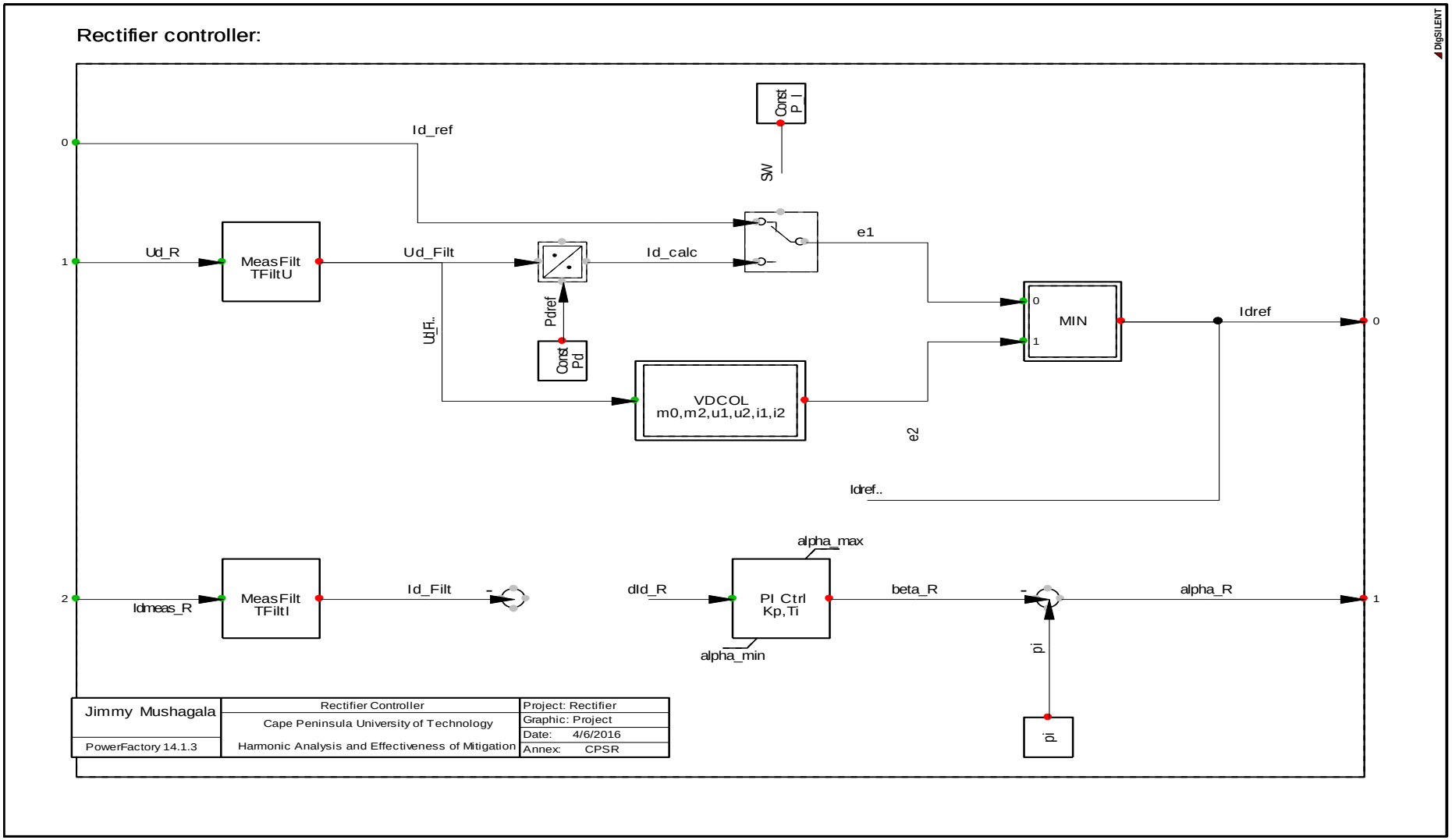

Figure B. 1: Rectifier controller block diagram as model in DIgSILENT

Appendix B: Continued

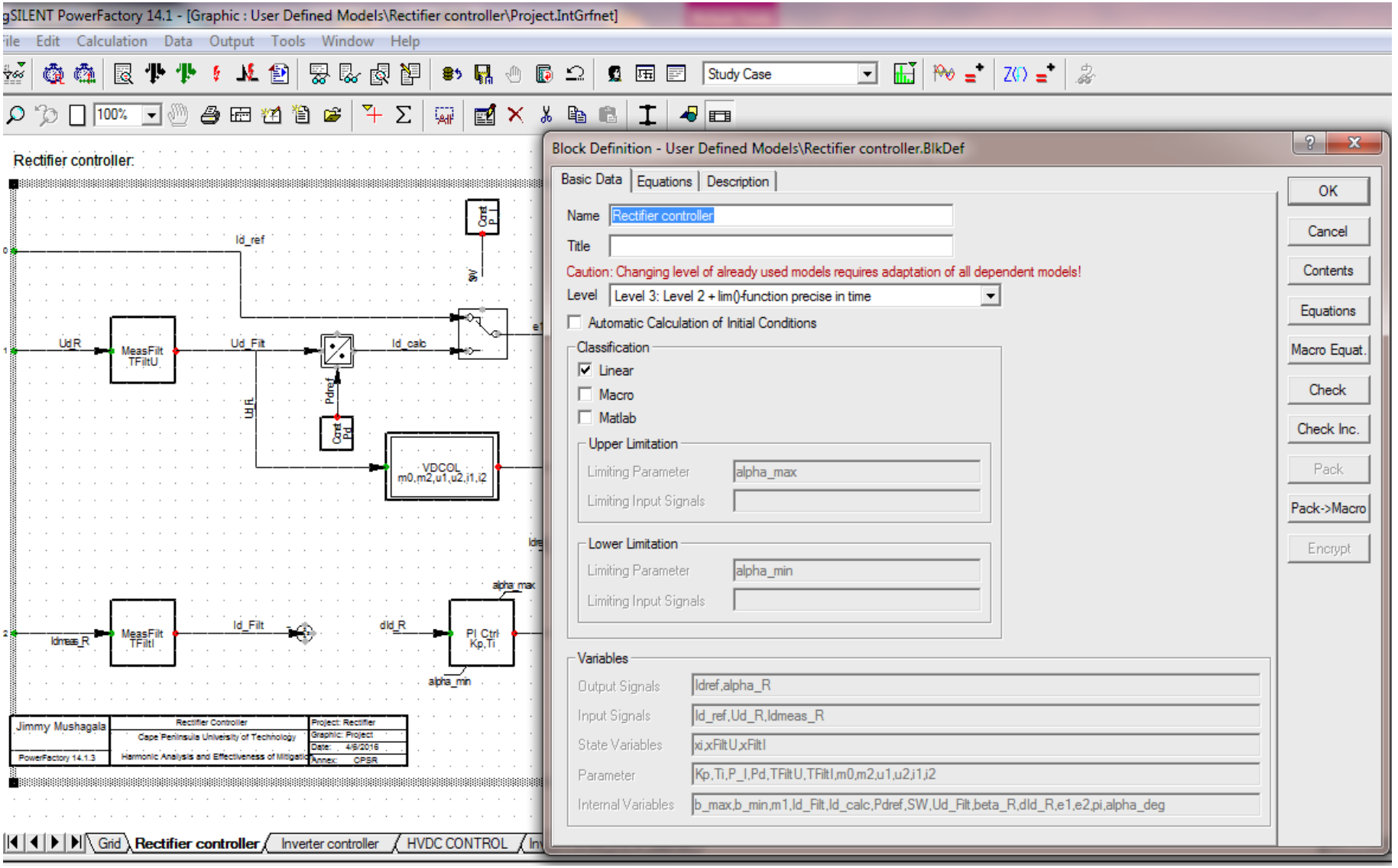

Figure B. 2: Rectifier controller block diagram with parameters description

Appendix B: Continued

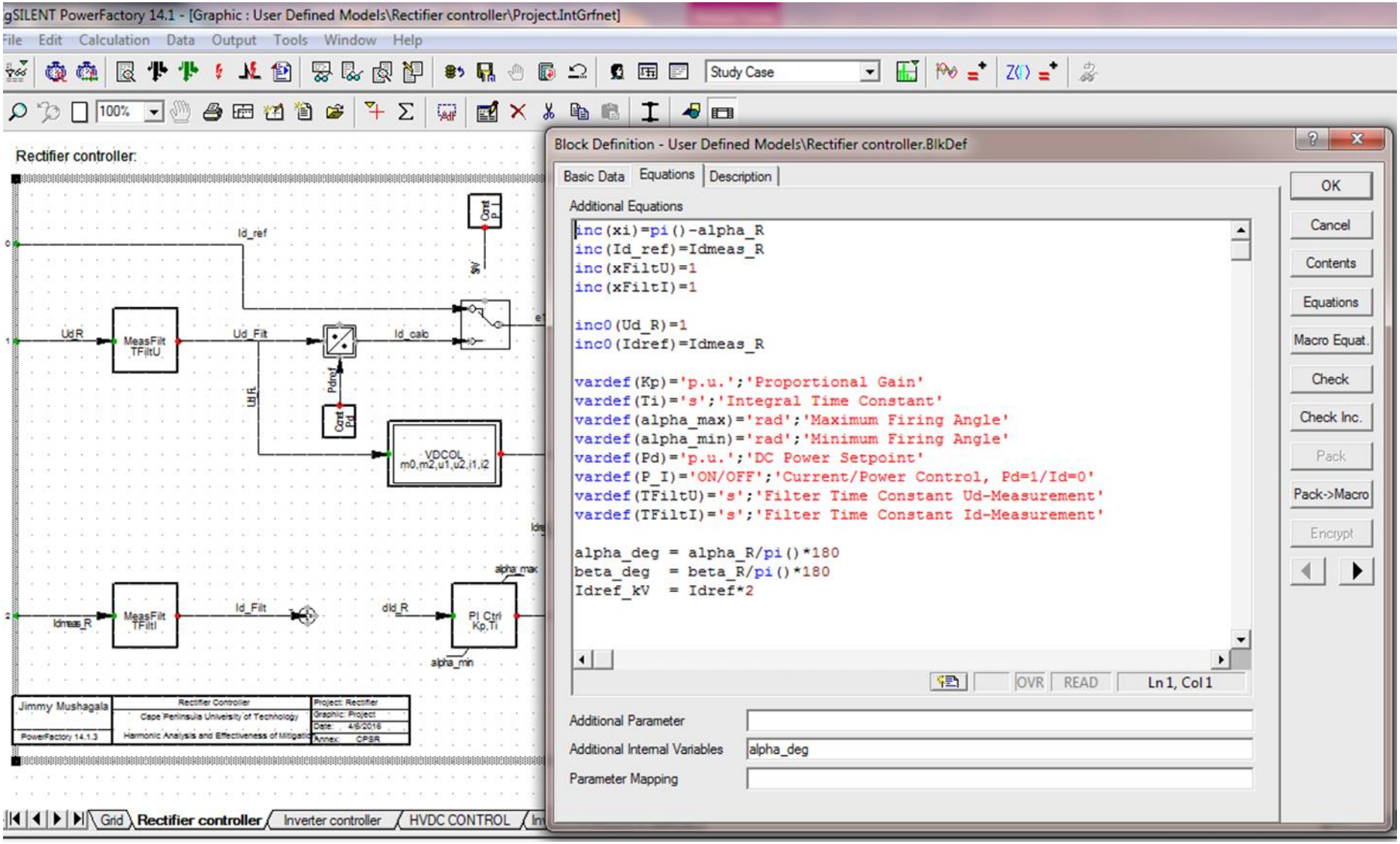

Figure B. 3: Rectifier controller block diagram with equation descriptions

8.3 Appendix C: Calculation for inverter parameters and rectifier control philosophy

Inverter Parameters Calculation

$I_{DC} = \frac{V_{DC-Rec} - V_{DC-Inv}}{R_{tot}} <=> V_{DC-Inv} = V_{DC-Rec} - (I_{DC} \times R_{tot})$

Total length of the line is 1200km

Therefore the total line resistance will be:

R_{tot} = 0.0437x1200= 52.44Ω

V_{DC-Inv} = 1387323.94366 - (1704x52.44) = 1297966.18366V ≈ 1298kV$_{DC}$

$V_{DC\ btwn\ each\ converter} = \frac{1297966.18366}{8}$ = 162245.77296V

The firing angle was selected at 15° to determine the voltage on the AC side

$V_{ac3\sim L-L} = \frac{V_{DC}}{1.35 \times \cos\alpha}$

$V_{ac3\sim L-L} = \frac{162245.77296}{1.35 \times \cos 15°}$ = 124421.61786kV ≈ 125kV

Determining power for single converter transformer on the inverter side

LV side of the transformer which is the DC side had these power ratings:

$P_{DC\ inv} = U_{DC} x I_{DC}$ = 162245.77296x1704 = 276.467MW

P_{DC} : 276.467MW

Q_{DC}: 0MVar

HV side for the converter transformer is connected to the AC voltage:

The powers in a transformer are equal in both (HV and LV) windings.

$P_{AC} = P_{DC}$: 276.467MW

$Q_{AC} = P_{AC}$ x tanα = 276.467xtan15° = 74.07911MVar

S = 276.467+74.07911j = 286.2197∠15°MVA

$Z_{base} = \frac{U^2_{AC}}{S_{base}} = \frac{125000^2}{286219700} = 54.591\Omega$

$X_{comp.p.u}$ = 0.14p.u (this was for the per unit reactance for the transformer)

$X_{comp.actual} = X_{comp\ p.u} x Z_{base}$ = 0.14x54.591Ω = 7.643Ω

$I_{DC} = [\cos\alpha - \cos(\alpha + \mu) \times \frac{U_{conv.Transfo-HVAC-side}}{\sqrt{2} \times X_{comp.actual}}$

$\cos(\alpha + \mu) = cos\,\alpha - \frac{I_{DC} \times \sqrt{2} \times X_{comp.actual}}{U_{conv.Transfo-HVAC-side}}$

$\cos(\alpha + \mu) = cos\ 15° - \frac{1704 \times \sqrt{2} \times 7.643}{125000}$

$<=> \cos(\alpha + \mu) = 0.81858 <=> \alpha + \mu = \cos^{-1}(0.8206) <=> \alpha + \mu = 35.057°$

$<=> \mu$ = 35.057°-15° = 20.0571°

Appendix C: Continued

$\beta = \pi - \alpha$

$\pi = 180°$

$\beta = 180° - 15° = 165°$

$\mu = \beta - \gamma$

$\gamma = \beta - \mu$

$\gamma = 15° - 20.0571° = -5.0571°$ Or $\gamma = 180° - 5.0571 = 174.9429°$

β: Inverter ignition or a "*switching ON"* angle in electrical degree

γ: Inverter extinction (or switching off) angle in electrical degree

μ: Overlap angle in electrical degree

Here below are a summary of the calculated single (or one) inverter ratings in a table:

Table C. 1: Table of Inverter Parameters

$U_{DC-LVside}(kV)$	$U_{AC-HVside}(kV)$	I_{DC}(kA)	$P_{DC}(MW)$	$\beta(°)$	$\mu(°)$
162.25	125	1.704	276.467	165	20.0571

Appendix C: Continued

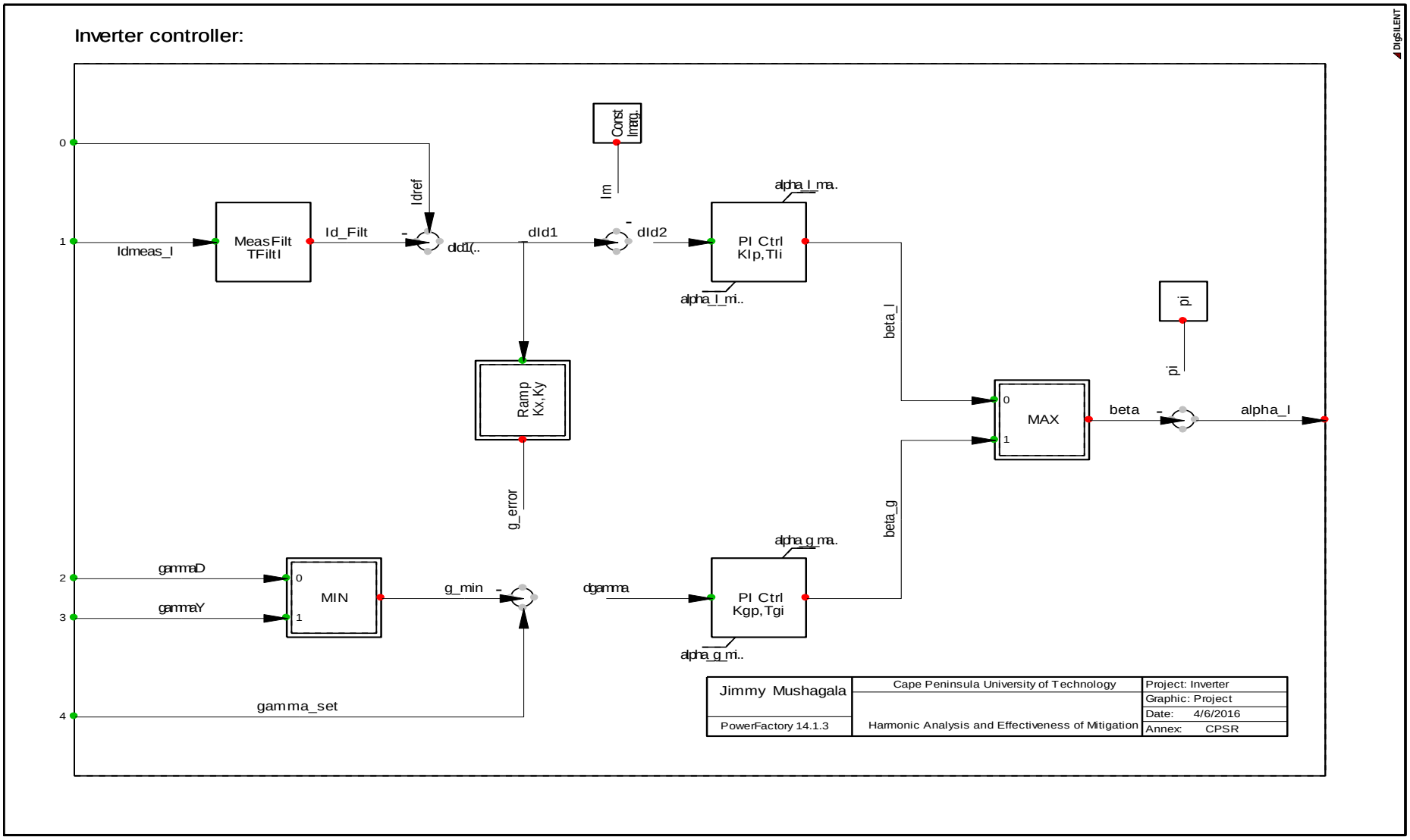

Figure C. 1: Inverter Controller Block Diagram as Model in DIgSILENT

Appendix C: Continued

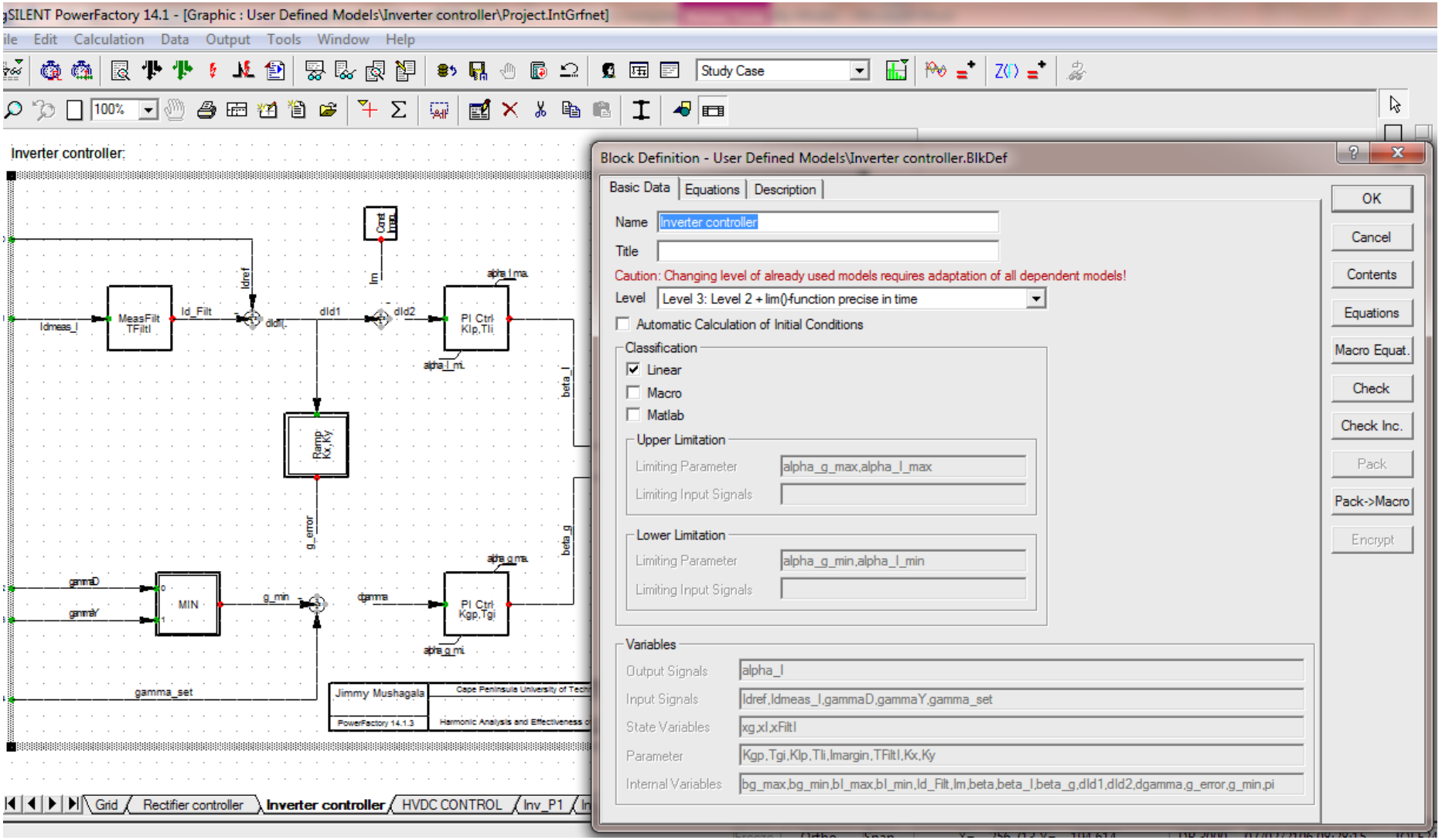

Figure C. 2: Rectifier Controller Block Diagram with Parameters Descriptions

Appendix C: Continued

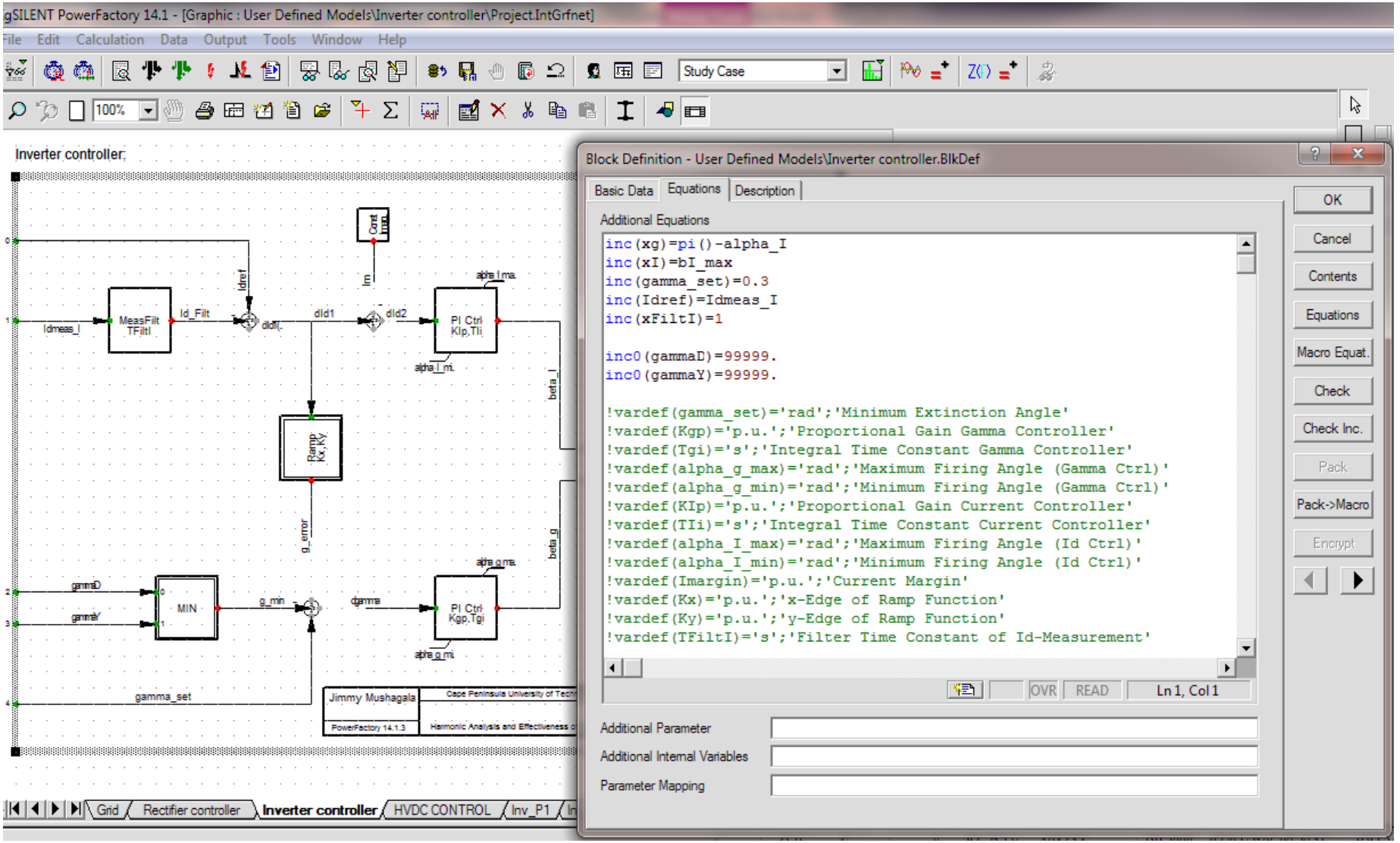

Figure C. 3: Inverter Controller Block Diagram with Equation Description

8.4 Appendix D: Filters calculations and design

Filter Calculations

The below formulas were used when designing each individuals filters on the rectifiers and inverters side.

$S_T = P_T + Q_T$ (kVA)

$Q_{comp} = P \times [tan\varphi_{new} - tan\varphi_{old}]$ $(kVAr)$

$Q_{filter} = \frac{{h_o}^2}{{h_o}^2-1} \times Q_{compensation}$ $(kVAr)$

$X_{filter} or X_{effective} = \frac{KV(U)^2 \times 1000}{Q_{filter}[kVAr]}$ (Ω)

$X_{cap\ of\ filter} = \frac{{h_o}^2}{{h_o}^2-1} \times X_{filter}$ (Ω)

$h_o = f_{@CHO} - \frac{f_{@CHO} \times PMV}{100}$ $(U-N/A)$

$h_o = \frac{f_o}{f_F}$ (H_z)

$X_{filter} or X_{effective} = X_{cap\ of\ filter} - X_{L\ of\ filter}$ (Ω)

$Q_{for\ cap\ of\ filter} = \frac{KV(U)^2 \times 1000}{X_{cap\ of\ filter}[\Omega]}$ $(kVAr)$

$L_{for\ filter} = \frac{X_{L\ of\ filter}}{2 \times \pi \times f_{@fundamental\ (50Hz)}}$ (mH)

$C_{for\ filter} = \frac{1}{2 \times \pi \times f_{@fundamental(50Hz)} \times X_{cap\ of\ filter}}$ (μF)

$f_{resonant} (or\ f_{@particular\ harmonic\ order}) = \frac{1}{2 \times \pi \times \sqrt{L \times C}}$ or $= h \times f_{@fund(50Hz)}$ (H_Z)

$X_n = \sqrt{X_{cap\ of\ filter} \times X_{L\ of\ filter}}$ (Ω)

$R_{band\ pass} = \frac{X_n}{Q_{factor}}$ (Ω)

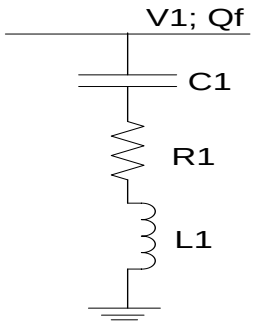

Figure D. 1: Band Pass Filter

Appendix D: Continued

$$R_{high\ pass} = X_n \times Q_{factor} \quad (\Omega)$$

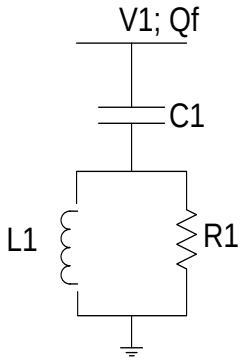

Figure D. 2: Second Order High Pass Filter

h_o = Tuned Harmonic Order

f_o = Tuned harmonic frequency

f_F = Fundamental Frequency

f_{CHO} = Frequency for characteristic harmonic order

$U - N/A$ = Unit Not Available

PMV = Percent Maximum Value. This value is selected between 5% to 15% value.

Range for Q_{factor} are:

20 to 150 for Band Pass filter

0.5 to 5 for 2nd order High Pass Filter

Appendix D: Continued

C-Type High Pass Filter

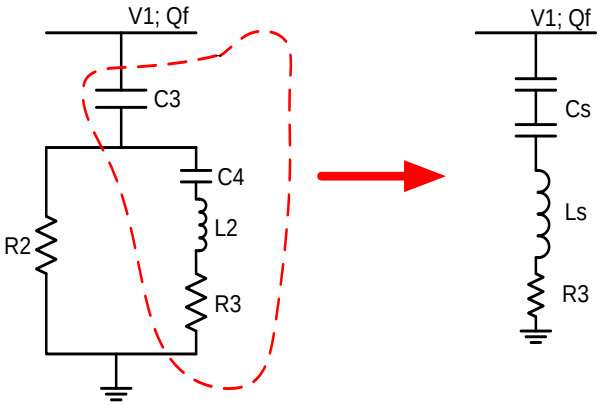

Figure D. 3: C-Type High Pass Filter

STEP1: Find C3 for the filter

$$X_{c3} = \frac{U^2{}_1}{Q_f} \quad (\Omega)$$

$$C_3 = \frac{1}{2\pi f_F X_{c3}} \quad (\mu F)$$

STEP2: Find L_s for the filter

$$L_s = \frac{V^2{}_1}{(h^2{}_o - 1) \times \omega_F \times Q_F}$$

$$\omega_F = 2\pi f_F$$

$$L_s = L_2$$

STEP3: Find C_s for the filter

$$C_s = \frac{(h^2{}_o - 1) \times Q_F}{h^2{}_o \times \omega_F \times V^2{}_1}$$

STEP4: Find R3 for the filter

$$R3 = \frac{\omega_F \times L_s}{q_s}$$

STEP5: Find C4 for the filter

$$C4 = \left(\frac{1}{C_s} - \frac{1}{C_3}\right)^{-1}$$

Appendix D: Continued

STEP6: Find R2 for the filter

$$R2 = \frac{q_C \times V^2{}_1}{h_o \times Q_F}$$

STEP7: Frequency response of the filter

$$Z_C(\omega) = -j(\omega \times C_3)^{-1} + \left[\frac{1}{R_2} + \frac{1}{R_3 + j.\omega.L_2 - j \times (\omega \times C_4)^{-1}}\right]^{-1}$$

8.5 Appendix D: A Bipolar HVDC network being Model in DIgSILENT

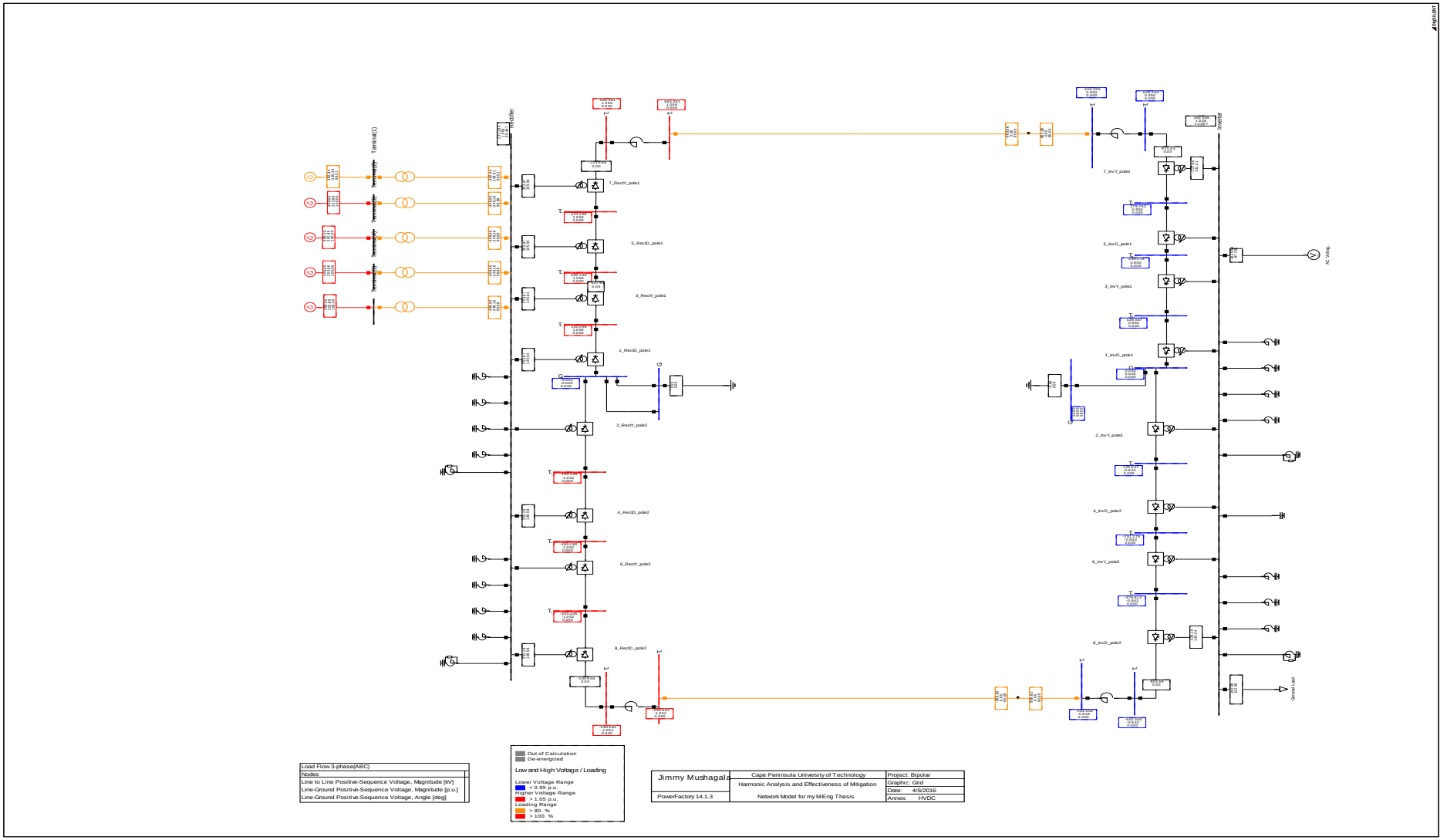

Figure D. 4: BPHVDC network being modelled in DIgSILENT